Sebastian Georg Klein

Vom Fachbereich VI
(Raum- und Umweltwissenschaften)
der Universität Trier
zur Erlangung des akademischen Grades
Doktor der Naturwissenschaften (Dr. rer. nat.)
genehmigte Dissertation

Model development to evaluate the effects of environmental particles on the lung

Betreuende: Univ.-Prof. Dr. rer. nat. Brunhilde Blömeke &
Dr. env. sci. Arno C. Gutleb

Berichterstattende: 1. Univ.-Prof. Dr. rer. nat. Brunhilde Blömeke
2. Dr. rer. nat. Reinhard Bierl
3. Dr. env. sci. Arno C. Gutleb

Datum der wissenschaftlichen Aussprache: 25.05.2016
Erscheinungsort und -jahr: Trier, 2016

Für meine lieben Eltern und Großeltern

“Dust is harmful”

LEONARDO DA VINCI
(1452-1519)

TABLE OF CONTENTS

List of abbreviations

AAPH	2,2'-azobis-2-methyl-propanimidamide-dihydrochloride
ALI	Air-liquid-interface
AM	Alveolar macrophage
AT-I	Alveolar type I
AT-II	Alveolar type II
B[a]P	Benzo[a]pyrene
CLSM	Confocal laser scanning microscopy
DAPI	4',6'-diamidino-2-phenylindole
DCFH-DA	dichlorodihydrofluorescein diacetate
DCs	Dendritic cells
DEPM	Diesel exhaust particulate matter
eNOS	Endothelial nitric oxide synthase
GM-CSF	Granulocyte macrophage colony-stimulating factor
GST1	Glutathione S-transferase
HMOX1	Heme oxygenase 1
ICAM-1	Intercellular adhesion molecule 1
IL-6	Interleukin 6
iNOS	Inducible nitric oxide synthase
LPS	Lipopolysaccharides
MAPK	Mitogen-activated protein kinase
NF_kB	Nuclear factor kappa B
NIST	National Institute for Standards and Technology
NPs	Nanoparticles
NQO1	NAD(P)H dehydrogenase (quinone 1)
Nrf2	Nuclear factor (erythroid-derived 2)-like 2,
PM	Particulate matter
PM_1	Particulate matter with aerodynamic diameter < 1 µm
PM_{10}	Particulate matter with aerodynamic diameter < 10 µm

PMA	Phorbol-12-myristat-13-acetat
QCM	Quartz crystal microbalance
ROS	Reactive oxygen species
SOD1	Superoxide dismutase 1
TCDD	2,3,7,8-tetrachlorodibenzo-*p*-dioxin
TEER	Transepithelial electrical resistance
UFPs	Ultrafine particles
VCAM1	Vascular cell adhesion molecule 1

PEER REVIEWED PUBLICATIONS BASED ON THE RESULTS OF THIS PHD WORK

Klein, S. G., Cambier, S.[#], Hennen, J.[#], Legay, S.[#], Serchi, T.[#], Nelissen, I., Krein, A., Blömeke, B., & Gutleb, A. C. (2016)**:** Endothelial responses of the alveolar barrier *in vitro* in a realistic dose-controlled exposure to diesel exhaust particulate matter. Submitted for publication to *Particle and fibre toxicology*

[#]contributed equally in alphabetical order

Klein, S. G., Serchi, T., Hoffmann, L., Blömeke, B., & Gutleb, A. C. (2013). An improved 3D tetraculture system mimicking the cellular organization at the alveolar barrier to study the potential toxic effects of particles on the lung. *Particle and fibre toxicology*, *10*(1), 31. ***(IF=9.18)***

Serchi, T., **Klein, S. G.,** Jehanno, A., Legay, S., Contal, S., Hennen, J., Gutleb, A.C., Hoffmann, L. and Blömeke, B. (2013). A 4D lung multi-culture system which mimicking alveolar cellular organization to study the toxic potential of airborne particles. *Toxicology Letters*, *221*, S183. ***(IF=3.145)***

Klein, S. G., Hennen, J., Serchi, T., Blömeke, B., & Gutleb, A. C. (2011). Potential of coculture *in vitro* models to study inflammatory and sensitizing effects of particles on the lung. *Toxicology In Vitro*, 25(8), 1516-1534.[1] ***(IF=2.65)***

[1] Featured in the **Sciencedirect Top 25 List of Most Downloaded Articles** ranked 11th on the Top 25 for Toxicology In Vitro – January to December 2012

ABSTRACT

Exposure to fine and ultra-fine environmental particles is still a problem of concern in many industrialized parts of the world and the intensified use of nanotechnology may further increase exposure to small particles. Since many years air pollution is recognized as a critical problem in western countries, which led to rigorous regulation of air quality and the introduction of strict guidelines. However, the upper thresholds for particulates in ambient air recommended by the world health organization are often exceeded several times in newly industrialized countries. Such high levels of air pollution have the potential to induce adverse effects on human health. The response triggered by air pollutants is not limited to local effects of the respiratory system but is often systemic, resulting in endothelial dysfunction or atherosclerotic malady. The link between air pollution and cardiovascular disease is now accepted by the scientific community but the underlying mechanisms responsible for the pro-atherogenic potential still need to be unraveled in detail. Based on the results from *in vivo* and *in vitro* studies the production of reactive oxygen species due to exposure to particles is the most important mechanism to explain the observed adverse effects. However, the doses that were applied in many *in vivo* and *in vitro* studies are far beyond the range of what humans are exposed to and there is the need for more realistic exposure studies. Complex *in vitro* coculture systems may be valuable tools to study particle-induced processes and to extrapolate effects of particles on the lung.

One of the objectives of this PhD thesis was the establishment and further improvement of a complex coculture system initially described by Alfaro-Moreno et al. [1]. The system is composed of an alveolar type-II cell line (A549), differentiated macrophage-like cells (THP-1), mast cells (HMC-1) and endothelial cells (EA.hy 926), seeded in a 3D-orientation on a microporous membrane to mimic the cell response of the alveolar surface *in vitro* in conjunction with native aerosol exposure (Vitrocell™ chamber).

The tetraculture system was carefully characterized to ensure its performance and repeatability of results. The spatial distribution of the cells in the tetraculture was analyzed

by confocal laser scanning microscopy (CLSM), showing a confluent layer of endothelial and epithelial cells on both sides of the Transwell™. Macrophage-like cells and mast cells can be found on top of the epithelial cells. The latter cells formed colonies under submerged conditions, which disappeared at the air-liquid-interface (ALI). The Vitrocell™ aerosol exposure system was not significantly influencing the viability. Using this system, cells were exposed to an aerosol of 50 nm SiO_2-Rhodamine nanoparticles (NPs) in PBS. The distribution of the NPs in the tetraculture after exposure was evaluated by CLSM. Fluorescence from internalized particles was detected in CD11b-positive THP-1 cells only. Furthermore, all cell lines were found to be able to respond to xenobiotic model compounds, such as benzo[a]pyrene (B[a]P) or 2,3,7,8-tetrachlorodibenzo-*p*-dioxin (TCDD) with the upregulation of *CYP1* mRNA.

With this tetraculture system the response of the endothelial part of the alveolar barrier was studied *in vitro* in a still realistic exposure scenario representing the conditions for a polluted situation without direct exposure of endothelial cells. After exposure to diesel exhaust particulate matter (DEPM) the expression of different anti-oxidant target genes and inflammatory genes such as *NAD(P)H dehydrogenase quinone 1* (*NQO1*), *superoxide dismutase 1* (*SOD1*) and *heme oxygenase 1* (*HMOX1*), as well as the nuclear translocation nuclear factor erythroid-derived 2 (Nrf2) was evaluated. In addition, the potential of DEPM to induce the upregulation of *CYP1A1* mRNA in the endothelium was analyzed.

DEPM exposure led not to an upregulation of the anti-oxidant or inflammatory target genes, but to clear nuclear translocation of Nrf2. The endothelial cells responded to the DEPM treatment also with the upregulation of *CYP1A1* mRNA and nuclear translocation of the aryl hydrocarbon receptor (AhR). Overall, DEPM triggered a response in the endothelial cells after indirect exposure of the tetraculture system to low doses of DEPM, underlining the sensitivity of ALI exposure systems. The use of the tetraculture together with the native aerosol exposure equipment may finally lead to a more realistic judgment regarding the hazard of new compounds and/or new nano-scaled materials in the future. For the first time,

it was possible to study the response of the endothelial cells of the alveolar barrier *in vitro* in a realistic exposure scenario avoiding direct exposure of endothelial cells to high amounts of particulates.

ABSTRAKT

Exposition gegenüber feinen und ultrafeinen Partikeln ist gegenwärtig ein ernstzunehmendes Problem in vielen industrialisierten Teilen der Welt und der verstärkte Einsatz von Nanotechnologie könnte das Risiko der Exposition gegenüber kleinen Partikeln weiter erhöhen. Seit vielen Jahren ist die Luftverschmutzung ein anerkanntes Problem in der westlichen Welt, was zu strikten Vorschriften und Regulierungen der Luftqualität geführt hat. Allerdings werden in den aufstrebenden Schwellenländern die von der Weltgesundheitsorganisation empfohlenen Grenzwerte teils um das Vielfache überschritten. Diese außerordentlich hohe Luftverschmutzung wirkt sich nachteilig auf die menschliche Gesundheit aus. Die Effekte, die die Luftschadstoffe auslösen sind dabei nicht nur lokal begrenzt, sondern wirken sich oft systemisch aus resultierend in endothelialer Dysfunktion oder auch Atherosklerosis. Der Zusammenhang zwischen Luftverschmutzung und kardiovaskulären Erkrankungen ist inzwischen von Experten allgemein akzeptiert, auch wenn die zugrundeliegenden Mechanismen noch im Detail untersucht werden müssen.

Basierend auf den Resultaten von *in vivo* und *in vitro* Studien ist die Produktion von reaktiven Sauerstoffverbindungen der wichtigste Mechanismus um die negativen Effekte zu erklären. Allerdings sind die für die Studien genutzten Partikeldosen weit über dem für den Menschen relevanten Bereich, weshalb realistischere Expositionsstudien gebraucht werden. Komplexe *in vitro* Cokultursysteme sind wertvolle Werkzeuge um die partikelinduzierten Prozesse zu studieren und die Effekte auf die menschliche Lunge zu extrapolieren.

Ein Ziel dieser Doktorarbeit war die Etablierung und weitere Verbesserung eines Cokultursystems, das ursprünglich von Alfaro-Moreno et al. beschrieben wurde [1]. Das System besteht aus alveolar Type-II Zellen (A549), differenzierten Makrophagen (THP-1), Mastzellen (HMC-1) und Endothelzellen (EA.hy 926), die in einer 3D-Anordnung auf einer Transwell™ Membran angesiedelt sind um die zelluläre Antwort der Alveolarbarriere gengenüber Aerosolen zu imitieren. Darüber hinaus wurde das System für die Verwendung nativer Aerosolexpositionstechnik (Vitrocell™-Kammer) angepasst. Das Tetrakultursystem

wurde sorgfältig charakterisiert um Leistungsfähigkeit und Reproduzierbarkeit zu gewährleisten.

Die räumliche Verteilung der Zellen wurde durch konfokale Laserscanningmikroskopie analysiert und zeigte eine konfluente Zellschicht auf beiden Seiten der Transwell™-Membran. Makrophagen und Mastzellen befinden sich auf der Oberseite der Epithelzellen. Makrophagen und Mastzellen bilden Kolonien unter submersen Bedingungen, die aber verschwinden, sobald die Zellen am Air-Liquid-Interface kultiviert werden (ALI). Das Vitrocell™ Aerosolsystem beeinflusste nicht die Vitabilität der Zellen. Mit Hilfe des Systems wurden die Zellen gegenüber 50 nm SiO_2-Rhodamine Nanopartikeln (NP) in PBS exponiert. Die Fluoreszenz der internalisierten NP konnte lediglich in CD11b-positiven THP-1 Zellen detektiert werden.

Alle Zellen des Tetrakultursystems reagierten auf die Exposition gegenüber xenobiotischen Stoffen, wie Benzo[a]pyrene (B[a]P) oder 2,3,7,8-tetrachlorodibenzo-*p*-dioxin (TCDD), mit der Hochregulation von *CYP1* mRNA. Mit Hilfe des Tetrakultursystems wurde die Reaktion des endothelialen Teils der alveolaren Barriere *in vitro* gegenüber Dieselpartikeln in einem realistischen Expositionszenario für hohe Luftverschmutzung untersucht. Nach der Exposition wurde die Expression verschiedener anti-oxidativer und anti-inflammatorischer Zielgene, wie *NAD(P)H Dehydrogenase Quinone 1* (*NQO1*), *Superoxide Dismutase 1* (*SOD1*) und *Heme Oxygenase 1* (*HMOX1*) analysiert. Außerdem wurde die Translokation des Transkriptionsfaktors Nuclear Translocation Nuclear Factor Erythroid-derived 2 (Nrf2) untersucht.

Die Exposition gegenüber der Dieselpartikel führte nicht zu einer veränderten Expression der Zielgene, aber zu einer signifikanten Translokation von Nrf2. Die Endothelzellen reagierten auf die indirekte Exposition mit einer Hochregulation von *CYP1A1* mRNA und nukleärer Translokation des Aryl-Hydrocarbon-Rezeptors.

Insgesamt sorgte die Exposition gegenüber der geringen aber relevanten Dosen an Dieselpartikeln für eine messbare Antwort im endothelialen Teil der Tetrakultur was die Sensitivität des Systems unterstreicht.

Die Verwendung des Tetrakultursystems zusammen mit der nativen Aerosolexposition kan zu einer realistischeren Einschätzung der Effekte neuer Stoffe und Chemikalien, insbesondere Nanomaterialien, auf die menschliche Lunge, führen. In dieser Arbeit war es zum ersten Mal möglich die zelluläre Antwort von Endothelzellen der Alveolarbarriere *in vitro* in einem realistischen Expositionsszenario zu studieren ohne die Zellen direkt zu exponieren.

1. INTRODUCTION

Since the dawn of mankind, individuals have been exposed to small particulates, either from combustion processes, e.g. fires in caves, forest fires, etc. or other natural processes, such as volcanic eruptions or simply blowing winds or waves on the shore [2, 3].

During the last 250 years, the level of exposure to combustion derived particulates increased dramatically in western countries due to the industrialization but also because of globalization processes, such as increased traffic and shipping activities. During recent years much effort was put into lowering the amount of particulate air pollution in Europe, resulting in better air quality and overall lower particle burdens [4, 5]. However, exposure to small ambient particles like particulate matter (PM; aerodynamic diameter <10 µm), is still of high concern in many industrialized countries. A large number of studies indicate that continuous exposure to air pollution and to PM significantly increase morbidity and mortality related to respiratory but also cardiovascular diseases [6], linking the level of exposure directly to human health. The relationship between daily exposure to polluted air and augmented mortality became dramatically obvious during the London fog episode in 1952, that was followed by a significant increase in mortality [7]. It was estimated that more than 12000 people lost their lives [8]. One possible explanation for the toxicity of atmospheric particles is the fact that these particles can absorb pneumotoxic heavy metals, as well as polycyclic aromatic hydrocarbons (PAHs) attached on their surfaces [9]. Particle bound transport is considered to be a fundamental pathway for the distribution of these, in part toxic, compounds in the environment [10].

Besides the larger particles with an aerodynamic diameter between 10 (PM_{10}) and 2.5 µm ($PM_{2.5}$) smaller particles have detrimental effects on human health. During recent years intensified use of nanotechnology led to the production of many new nanomaterials that can be found in consumer products. The use of these materials may further increase exposure to ultrafine particles (aerodynamic diameter <100 nm) potentially enforcing the risk for respiratory diseases for workers in the nanomaterial production sites but also consumers.

Nanomaterials and nanoparticles (NPs) (the first defined as a material with at least one dimension <100 nm and the latter with all dimensions <100 nm) have become of primary interest for different kinds of industries. These particles possess unique properties compared to their parent compounds making them attractive for application in a wide spectrum of industrial fields. However, these unique properties are not accounted for in the environmental risk assessment methods that the *registration, evaluation, authorization, and restriction of chemicals (REACH)* proposes in their program on environmental exposure estimation [11]. Despite a clear lack of knowledge on the toxicity of NPs and missing regulation, more than 1000 customer products already contain NPs (www.nanotechproject.org). Exposure to NPs has been linked to the induction of adverse effects on human health and to aggravation of pre-existing diseases like asthma [2]. Ambient air also contains considerable amounts of environmental particles, such as PM_{10} and some reports suggest that the toxicity of environmental PM is mainly exhibited by the nano-fraction (reviewed in [12]).

The alveolar epithelium is a very thin gas permeable barrier, composed of alveolar type I and II (AT-I, AT-II) cells with a high number of capillaries underneath. Due to their small size, some ultrafine particles can cross the alveolar barrier and affect the underlying cells or even enter the bloodstream thus causing damage in other compartments of the human body. Animal studies, but also studies with human volunteers, have demonstrated the potential of different kinds of NPs to cross the alveolar barrier [13-16]. In rodents, different NPs were found in lymph nodes [17], the brain [18] and other parts of the central nervous system [19] several hours after exposure.

1.1.1. ABOUT THE ORGANIZATION OF THE LUNG – A SHORT OVERVIEW

The respiratory system is highly specialized and it allows gas exchange between the blood stream and the inhaled air at a high yield. The respiratory system can be subdivided into the

upper respiratory tract and the lung, which represents the lower respiratory tract. The upper respiratory tract comprises the nasal cavity, the pharynx and the larynx. The lung (lower respiratory tract) is composed of the trachea, which is fused to the larynx, the primary bronchi, which lead to the bronchioles and finally the alveolar region (Figure 1).

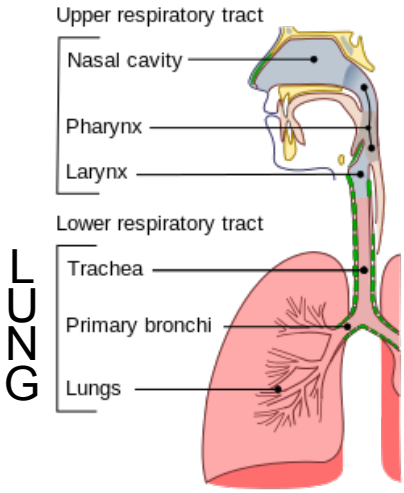

Figure 1: Simplified scheme of the organization of the human respiratory tract. The human respiratory tract can be subdivided into two main parts: the upper respiratory tract and the lower respiratory tract. The latter one is normally referred to as the lung. Adapted and modified from [20].

The bronchial tree in the lower respiratory tract can be roughly described as an accumulation of branching tubes, stemming from the main trachea [21]. The diameter of these tubes (the bronchi) decreases progressively until the terminal bronchioles with the alveolar sacs at the end, which is also referred to as the distal respiratory tract [22]. The main function of the bronchi and bronchioli is to conduct inhaled air to the lower respiratory tract where the actual gas exchange takes place in more than 300 million alveoli in order to provide maximized gas exchange via a vast surface. The conducting zone itself does not allow gas exchange [23]. The total surface area for gas exchange in an adult lung is between 55 m^2 and 80 m^2 [24] and at the end of a normal breath, the lung consists of about 80% air, 10% blood, and only 10% tissue by volume [25].

The surface of the respiratory tree is formed by a continuous layer of epithelial cells, which play an important role in maintaining the functionality of the lung, such as forming a barrier to

pathogens and other harmful compounds, facilitating mucociliary clearance, secreting protective substances, etc. [26]. This epithelium shows a complex and different composition regarding e.g. the bronchioli and the alveoli (Figure 2). In total, more than 40 cell types were described within the epithelia of the respiratory system [27]. Many of these are intermediates or differentiating cells, leaving more or less a dozen morphologically and functionally unique epithelial cell types that can be identified [28]. The epithelium in the lower respiratory tract (trachea and bronchi) is pseudostratified and columnar, composed of secretory goblet cells, which produce mucus and basal cells and ciliated cells, which are necessary for mucociliary clearance (Figure 2). In the bronchioles, the epithelium consists of more cuboidal shaped cells with shorter cilia and secretory clara cells. The distal respiratory tract with the alveoli mainly consists of AT-I and AT-II cells, which cover the alveolar epithelium (Figure 2) [21]. The alveolar epithelium is highly vascularized by capillaries underneath the basal membrane to improve the gas exchange between air and blood. AT-II cells serve many different functions, including surfactant production or as a progenitor of AT-I cells. A resident population of alveolar macrophages resides in the interstitial spaces to perform alveolar clearance of inhaled particles and pathogens [23].

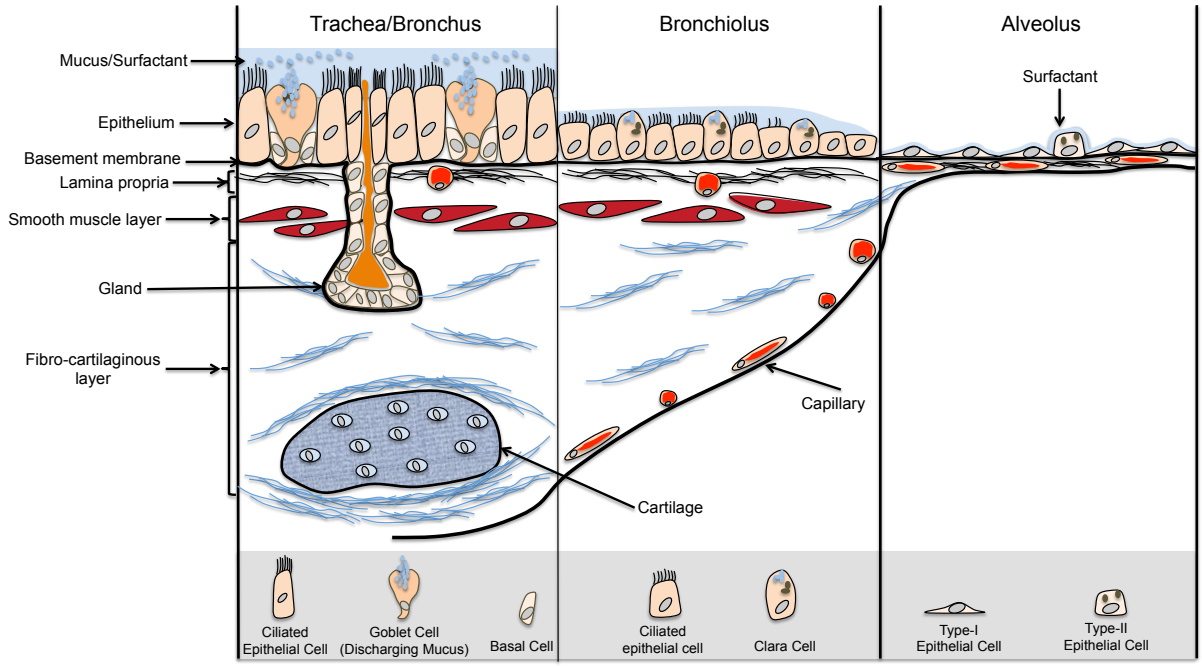

Figure 2: Simplified scheme of the structure of the airway wall at the three principal levels. The epithelial layer gradually becomes reduced from pseudostratified to cuboidal and then to squamous. The organization of the airway wall is mainly a mosaic of epithelial and secretory cells. In the alveoli, the smooth muscle layer is not present. The fibrous layer contains cartilage only in bronchi and gradually becomes thinner as the alveolus approached. Adapted and modified from [29].

1.1.2. Particle deposition and retention in the respiratory tract: Targets for particle interaction

The PAHs that are a component of urban PM and DEPM have been described to possess genotoxic potential [30-32]. They constitute a major class of environmental pollutants and many can be metabolized by macrophages following the induction of CYP1A1 [33-36], to diol-epoxides resulting in strong mutagenic and carcinogenic metabolites [37, 38].

The induction of the phase I enzyme CYP1A1 is important for the detoxification of lipophilic chemicals including PAHs in order to avoid accumulation of toxic concentrations inside the cell. PAHs but also halogenated aromatic hydrocarbons such as 2,3,7,8-tetrachlorodibenzo-p-dioxin (TCDD) can pass the cellular membrane and form a complex with the arylhydrocarbon receptor (AhR) in the cytoplasm [39]. The PAH-AhR-complex acts together

with the arylhydrocarbon receptor nuclear translocator (Arnt) as an activator of the xenobiotic response element (XRE), which can be found in the enhancer region genes coding for several phase I enzymes, such as CYP1A1 [39, 40]. CYP1A1 converts PAHs and other xenobiotics to oxidatively labile metabolites. These metabolites can interact and damage cellular components such as lipids, proteins and especially DNA by forming DNA adducts [30, 41, 42]. Additionally, the quinone metabolites formed by CYP1A1 contribute to enhanced ROS in cells [43-45].

The respiratory system is the main portal for the entrance of small particles into the human body [46]. Ultra fine particles (UFPs) with an aerodynamic diameter of less than 100 nm, are mainly deposited in the alveolar region (Figure 3) [47], which is the most prone region for injuries due to the lack of mucociliary clearance [48, 49].

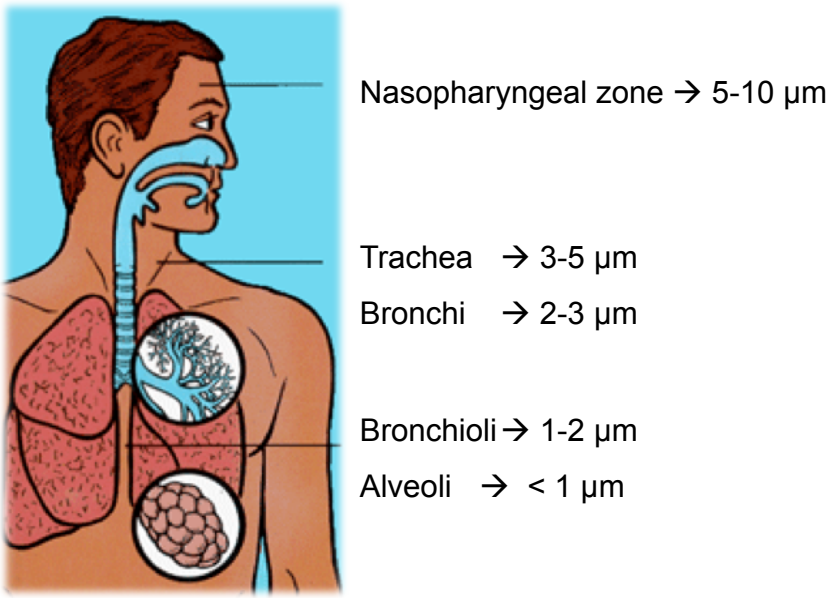

Figure 3: Deposition of particles in the respiratory system in respect to their aerodynamic diameter. Deposition of particles in the lung strongly depends on the aerodynamic diameter of a particle. The smaller a particle the deeper it penetrates into the lung until reaching the alveoli [47].

The behavior and the fate of aerosolized particles are mainly influenced by their aerodynamic properties, the flow dynamics during breathing and the anatomy of the respiratory tract leading to different deposition efficiencies. Upon entering the human

respiratory tract, the environmental conditions change dramatically, regarding temperature and the humidity saturation of the atmosphere [50]. In addition, the structure and composition of the particles itself are not static, but rather undergo various physical and chemical interactions and transformations, resulting in a process called atmospheric aging. This also includes changes in size distribution and aggregation state.

In the environment, particle number and mass concentrations vary typically between 10^2 to $10^5/cm^3$ and 1 to 100 mg/m^3, respectively [50, 51]. After combustion DEPM was found to form aggregates with a diameter between 0.1–0.5 µm. As a result about 90% of these particles can be inhaled due to their small size. From this inhalable fraction up to 33% are likely deposited on the respiratory tract and about one-third of these is expected to reach the area of gas exchange [52]. Particles that are deposited in the mucus layers on top of a ciliated surface of the respiratory tract can be cleared through mucociliary clearance within 24 hours [50, 53, 54]. For particles deposited in the alveolar region, clearance mechanisms must function independently from mucus layers and ciliated surfaces, thus resulting in much longer retention times. Clearance is mainly executed by a resident population of macrophages (alveolar macrophages, AMs) [50]. For rats an alveolar clearance half-life of 62 days was reported for DEPM [55]. This slow clearance of UFPs is partly due to the low efficiency of AMs to ingest high amounts of such small particles *in vivo* [56]. Consequently a portion of these particles can reach the blood stream by crossing the alveolar epithelium [50].

The alveolar epithelium consists of two subtypes: squamous AT-I cells that form the actual lining and the cuboidal AT-II cells that have secretory functions. AT-I cells cover a large area per cell, they are flat and squamous in shape. Their main function is to serve as a thin and gas-permeable epithelial barrier [21]. Although AT-II cells are more numerous than AT-I cells, about 95% of the alveolar surface area is covered by AT-I cells [25, 57, 58]. Furthermore, tight junctions between the cells avoid the entrance of foreign material and pathogens into the interstitium [59]. Since AT-I cells are considered to be terminally differentiated and unable to perform further divisions their replacement depends on the

mitosis and differentiation of AT-II cells [60]. AT-II cells have therefore two main functions: they produce and secrete the protective surfactant layer and they are the progenitors for both types of alveolar cells. Regarding its composition, the surfactant is a mixture of mainly saturated phospholipids together with proteins. Important components of the surfactant are the apoproteins surfactant protein A (SP-A), surfactant protein (SP-B), surfactant protein (SP-C), and surfactant protein (SP-D). The surfactant system serves three major functions in the alveolar system. First, it lowers surface tension at the surface, thus keeping alveoli open and preventing them from collapsing. Second, the surfactant prevents fluid fluxes into the alveolar lumen by lowering alveolar surface tension, thus keeping alveoli relatively dry. Third, it contributes to the lung's innate immune defense, thus keeping alveoli clean. This important function of the surfactant film is due to the nature of SP-A and SP-D. These two surfactant proteins act as collectins that are able to bind to the surface of various pathogens and to act as opsonins in order to facilitate their elimination by alveolar macrophages [61-63]. In addition to SP-A and SP-D, AT-II cells are able to secrete the bacteriolytic lysozyme, which can be found in the surfactant, too [64, 65]. These biophysical and immune-modulatory functions are dependent on a complex system of biochemical and morphological factors (reviewed in [25]).

Because of their importance for the alveolar system and the defence of the alveoli against pathogens, they have been referred to as *"defender of the alveolus"* [66, 67]. In addition to the secretion of the surfactant, these cells are also capable of secreting a spectrum of inflammatory mediators after insult, such as granulocyte macrophage colony-stimulating factor (GM-CSF), monocyte chemotactic protein 1 (MCP-1), the interleukins (IL) 1_{β}, 4, 6, 8 and the chemokine "regulated on activation, normal T cell expressed and secreted" (RANTES) [67]. Among these mediators, IL-1_{β}, and IL-6 are produced by AT-II cells in response to particles [68].

The chemokines RANTES and MCP-1 chemotactically attract macrophages [69], as well as GM-CSF [70, 71], can also stimulate macrophage growth [72]. SP-A, that is produced by AT-II cells, was found to modulate macrophage functions such as, oxygen radical release

[73], and nitric oxide production [74]. In addition, AT-II cells have the potential to interact with leukocytes due to the production of the cytokines IL-6 or IL-8 [67]. By the secretion of these cytokines, AT-II cells potentially induce the differentiation of specific leucocyte subtypes, such as, basophil, eosinophil and neutrophil granulocytes [67].

The uptake and removal of particles and pathogens in the alveoli is predominantly done by macrophage phagocytosis because of the lack of a mucociliary escalator [50]. The AMs are the principal phagocytic and scavenger cells on alveolar surfaces and form up to 90% of cells found in the alveolar spaces [75]. AMs are the first line of protection against inhaled antigens and pathogens [76] and show a strong phagocytic activity that is even enhanced by the contact with opsonized particulates and following inflammatory signals such as IFN-γ [77, 78]. Insoluble particles that reach the alveolar surface are efficiently removed by AMs, as long as they do not affect the phagocytic activity and although, to a lesser extent, are transported into the interstitium via transcytosis [46]. However, particles which are not soluble in mucus or in surfactant, are generally not easily engulfed by macrophages and particles with a size below 0.26 µm can elude the macrophage defense system [79]. Inhalation studies indicate that particle size plays a crucial role in the clearance process. A subchronic inhalation study found after exposure of rats to ultrafine (around 20 nm) and fine (around 200 nm) titanium dioxide (TiO_2) a significantly slower clearance for the smaller particles. This was due to extended translocation of the ultrafine material to interstitial spaces and consequently to the draining regional lymph nodes in comparison to the fine TiO_2 particles [80]. These particles can get easily into contact with the epithelial cells and be translocated through the epithelium and reach interstitial spaces or the blood stream [81].

1.2. PARTICULATE MATTER IN THE ENVIRONMENT AND THEIR ROLE AS AIR POLLUTANT

In many parts of the world, the near surface atmosphere contains considerable amounts of coarse (aerodynamic diameter <10 µm), fine (aerodynamic diameter <2.5 µm) and ultrafine

particles (aerodynamic diameter <0.1 µm). PM in general can be considered to be of complex composition, originating from both natural sources and from anthropogenic activities such as vehicle emissions, industrial combustion processes, thermal power plants and many others [82, 83]. PM comprises a vast range of different particulates and contains many different compounds [84].

Diesel engines emit up to 100 times more particles compared to gasoline engines equipped with modern exhaust treatment systems [85-88]. Regarding the high cost of fuel in many countries, the use of diesel engines has increased due to its superior energy efficiency and increased engine lifetime. In Europe, diesel engines power 37% of all new cars, with reaching the highest rate in France with 62% [89]. In Japan, even 75% of trucks, 98% of buses, and 12% of passenger cars in 1998 were powered by diesel engines [90]. Emissions from diesel vehicles cause up to 70% of the air pollution in metropolitan areas in countries like China, India, Mexico, Chile or Russia [91]. In these countries, the concentration of 50 µg PM_{10} per m^3 air, which is recommended by the world health organization (WHO) [92], is often more than four times exceeded at peak loads. In Chennai (India), PM_{10} concentrations even reach up to 1.47 mg per m^3 air under high traffic conditions [91]. The main reasons for the general omnipresence of DEPM as environmental pollutant is most probably the lack of a general implementation for particle filters for diesel-fuel-powered engines [93].

Human epidemiological studies revealed that high exposure levels of PM_{10}, containing a considerable fraction of DEPM, are associated with increased hospital admissions for respiratory diseases such as asthma or bronchitis [94-96]. Overall the number of individuals suffering from asthma increased dramatically over the last decades in industrialized countries [97] with an augmentation for the prevalence of asthma of approximately 6% per year worldwide [98-102]. An estimated number of 300 million people worldwide suffer from asthma, with 250000 individuals dying each year as a direct consequence of the disease [103].

1.2.1. DIESEL EXHAUST PARTICLES AS MAJOR ENVIRONMENTAL PARTICULATE

In Europe and Japan, DEPM is the main air pollutant [104]. These particles seem to possess a high potential for adverse effects on human health. Evaluation of the hazard of DEPM can be considered to be a special task, since they posses several special characteristics. DEPM was found to act as a carrier for considerable amounts of metals and organic compounds [9]. The surface structure of these particles is complex and heterogeneous. On the outer shell, that is surrounding the carbon core, heavy metals such as lead, chromium, copper and zinc can be found. Those metals were shown to have inhibitory effects on the nitric oxide (NO) production by the inducible form of the nitric oxide synthase (iNOS), which can compromise the regulation of the vascular tone in the blood vessels [105]. Even short exposure times, as little as 1 h, were found to impair already the regulation of the vascular tone due to a reduced production of NO by endothelial cells [106]. An impaired endothelium-dependent regulation of the vascular tone is associated with an increased risk of acute cardiovascular events, such as cardiac death [107].

In addition, other molecules present, such as some PAHs or heavy metals, can be a source of oxidative stress, which seems to be an important mechanism for the adverse effects of DEPM [105, 108-114]. It was shown that the distribution of PAHs and heavy metals in the outer shell is not homogenous and differs from particle to particle, making it even more complex to study and to forecast the effects of these particles [9]. The heterogeneous distribution of heavy metals and PAHs shows highly concentrated hotspots [9]. Even in cases when the total concentration of PAHs and heavy metals in the particles on a total weight basis is low, these hotspots might be able to elicit a reaction when coming into contact with cellular components.

Up to now many *in vitro* studies evaluating the hazard of DEPM were using extracts of particles, since experiments with native aerosol exposure equipment are complex and cost intensive. In respect to the complex structure and composition of DEPM, extracts may not properly reflect the effects for example due to the absence of the carbon core [115].

Furthermore, the composition of DEPM might change in respect to the type of diesel fuel, that is used, or the state of the engine (e.g. load or idle conditions). Potential contamination with bacterial endotoxins such as lipopolysaccharides (LPS) may lead to an overestimation of the pro-inflammatory potential of DEPM under *in vitro* conditions. However, under laboratory conditions, DEPM can be generated and sampled under highly controlled and reproducible conditions for toxicology studies. In respect to the fact that diesel particles are the dominant component of PM in urban regions and industrialized countries they are frequently used as model particles in human and animal *in vivo* and *in vitro* studies (reviewed in [116]) and it is assumed that the ultrafine fraction of DEP is mainly responsible for the observed adverse effects [48].

1.2.2. EFFECTS OF DIESEL PARTICULATE MATTER ON HUMAN HEALTH

In general, the predominant chemical components of ambient PM are sulfate, nitrate, ammonium, sea salt, mineral dust, organic compounds, and black or elemental carbon. Although some of the chemicals that can be found in ambient PM, e.g. benzo[a]pyrene (B[a]P), are definitely toxic, under standard conditions none of them reaches a concentration to be of acute toxicological concern [49]. However, as emerged from a multitude of studies, DEPM possesses a clear adverse potential for human health in acute and chronic exposure scenarios resulting in short-term and long-term effects [52, 106, 112, 115, 117-134]. In real life, observed adverse health effects are unlikely a consequence of just a single PM component, but rather based on complex and synergistic interactions of multiple components in varying physical structures with the respiratory tract and other target organs [49]. Understanding the mechanisms involved in the adverse effects is crucial for the development of protective strategies, but may help to cure PM related diseases, too.

The number of hospital admissions for pulmonary diseases and cardiovascular injury correlates well with PM levels in ambient air, especially during periods with high levels of

particles [7, 94], which is also associated with increased mortality [135, 136]. During recent years, the link between air pollution and the progression of atherosclerosis was elucidated [137]. It is hypothesized that tissue damage due to massively increased oxidative stress is one of the principal mechanisms of PM-induced sub-chronic pulmonary inflammation. Similarly this mechanism is speculated to be responsible for the observed pro-atherogenic effects of urban PM in the long run [138].

1.2.3. THE HIERARCHICAL OXIDATIVE STRESS CONCEPT

The ability of some particles such DEPM, carbon black, or urban PM to induce the production of reactive oxygen species (ROS) [131, 139-141] strengthens the association between elevated exposure to particulates and exacerbations of lung disease [142]. E.g., in the case of allergic asthma the role of ROS is in general often overlooked [143] and intracellular signaling and transcriptional alterations induced by oxidative stress have not been much studied regarding the endothelial homeostasis [118, 144]. In order to better explain the link between air pollution and lung inflammation, the concept of the hierarchical oxidative stress response was developed (Figure 4) [143]. The ultrafine fraction of PM is rich in organic chemicals, such as PAHs and quinones [145]. These chemicals contribute to the generation of ROS by their redox cycling as well as possibly through an impairment of the mitochondrial function [146]. Many studies indicate, that PM can be a direct source for oxidative stress [108-110, 112, 114, 147]. DEPM particles can reduce cytochrome P450 reductase activity, leading to increased superoxide production [148]. The redox cycling organic hydrocarbons and transition metals found in DEPM are capable of generating airway inflammation through their ability to generate reactive oxygen species (ROS) [145, 149]. The intrinsic potential of DEPM to produce ROS was demonstrated using a cell free *in vitro* system with DEPM suspended in phosphate buffer [150].

Local and systemic oxidative stress are likely to be the common link between pulmonary

exposure and systemic effects [151]. Regarding the hierarchical oxidative stress concept different doses of air pollutant particles induce a tiered cellular response [143].

The hierarchical oxidative stress model can be divided into three *tiers* regarding the level of oxidative stress. Once the generated ROS amount overwhelms the antioxidant protection, this results in oxidative stress [152]. In *tier 1* the level of oxidative stress is low and induction of the antioxidant defense mechanisms via nuclear factor erythroid-derived 2 (Nrf2) translocation and new formation of antioxidant enzymes, such as heme oxigenase 1 (HO-1) and superoxide dismutase 1 (SOD1). These enzymes cope with the stress and consequently restore cellular redox homeostasis (Figure 4). For instance SOD1 is able to prevent the more damaging pro-inflammatory and apoptotic effects by converting superoxide anions into hydrogen peroxide [153]. HO-1 is an antioxidant enzyme, whose expression is upregulated via the transcription factor Nrf2 that binds to the antioxidant response element (ARE) in *tier 1* of the oxidative stress response. HO-1 expression can be upregulated by its substrate heme and by various non-heme substances that can be found as components in PM, such as heavy metals, bromobenzene, endotoxins and oxidizing agents [154, 155]. As an example, PM was found to trigger the upregulation of *heme oxygenase 1* (*HMOX1*) mRNA coding for HO-1 in endothelial cells [122, 124]. Besides its role in heme catabolism [155, 156] HO-1 has emerged as an important phase II and anti-inflammatory enzyme, which is highly upregulated by oxidative stress [157]. This enzyme generates biliverdin through the catabolism of heme leading to the generation of a potent antioxidant that is able to scavenge efficiently radicals. In endothelial cells basal levels of HO-1 were found to be important for the protection against inflammation [158]. HO-1 was described to be an important oxidative stress sensor in endothelial cells [124] and to play a critical role in *tier 1* of the hierarchical oxidative stress response in the vasculature for the progression of atherosclerosis [159]. It is assumed that HO-1 is among the most critical cytoprotective mechanisms activated to counteract oxidative stress [157]. In *tier 2* at an intermediate level of oxidative stress a pro-inflammatory response is induced by the activation of mitogen-activated protein kinases (MAPK) and nuclear factor kappa B (NF_k-B) related pathways

(Figure 4). Finally in *tier 3* the highest level of oxidative stress induces a perturbation of the mitochondrial permeability and disrupts the electron transfer chain. Together with an inflammatory response this results in necrotic and apoptotic cell death leading to tissue damage (Figure 4) [143, 160]. The concept of the tiered oxidative stress response after DEPM exposure is well supported by the high correlation between the PAHs content of fine and UFPs and their ability to induce oxidative stress in macrophages [161, 162]. Overall the production of reactive oxygen species is probably the most important mechanism to explain the adverse effects of particles on the lung [143, 149, 162, 163] and the cardiovascular system (reviewed in [160]).

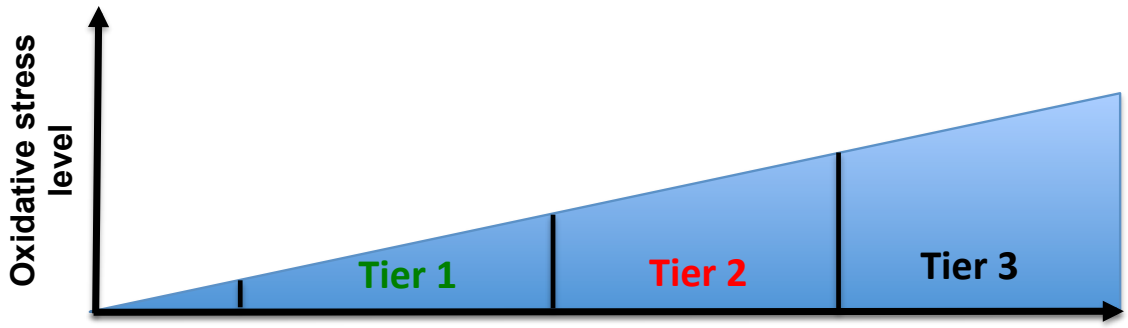

	Tier 1 Antioxidant defense	Tier 2 Inflammation	Tier 3 Cytotoxicity
Pathway	ARE	AP-1 & NF-kB	Caspase activation/ ATP depletion
Transcription factor/ target	Nrf2	Fos, Jun, Rel	Mitochondrial PT pore Mitochondrial respiratory chain
Cell response	HO-1 Phase II enzymes, e.g. GST, NQO1, etc.	Cytokine, Chemokines Adhesion molecules	Apoptosis Necrosis

Figure 4: The concept of the hierarchical oxidative stress response. In order to explain the effects in cells observed after exposure to DEPM, the concept of the hierarchical oxidative stress response was developed [143]. In this concept, the cellular response is divided in three different tiers, depending on the level of oxidative stress. In *tier 1* the level of oxidative stress is moderate and cellular defense mechanisms are able to cope with the radicals. In *tier 2* the level of oxidative stress causes already an inflammatory response and activation of cells. Finally, in *tier 3* the oxidative stress leads to cytotoxicity and cellular damage.

1.2.4. IMPACT OF DEPM ON CARDIOVASCULAR HOMEOSTASIS

Endothelial dysfunction plays a central role in the pathogenesis of several cardiovascular diseases [164] and this dysfunction precedes in general cardiovascular disease [165]. The mechanisms involved in cardiovascular injury, due to exposure to PM, are poorly understood but there is accumulating evidence that exposure to air pollution affects vascular homeostasis and contributes to the progression of vascular systemic diseases [137]. In the lung, the capillary endothelium is in close contact with the alveolar epithelium [166]. Therefore inhaled DEPM and their components may easily interact with the vascular endothelium and may also release radicals and soluble materials into the circulation [127]. PM-associated B[a]P was shown to be systemically available in the circulation [167] as well as some soluble metal components from PM [168] and small amounts of PM were translocated [169], although the mechanism, by which DEPM enters the circulation is not clear.

Animal studies [138, 170] but also human epidemiological studies [170] demonstrated that exposure to ambient PM is able to promote atherosclerosis. Atherosclerotic malady can be defined as an inflammatory process, which takes place in the vascular wall. Atherosclerosis is characterized by the accumulation of lipids in elastic and muscular arteries [171] with the result of reduced vascular elasticity and reduced blood circulation. Studies conducted on vascular endothelial cells and monocytes provided evidence for the central role of the endothelium in orchestrating inflammation. Furthermore, accumulation of oxidatively modified low-density lipoprotein in the intima seems to contribute significantly to monocyte recruitment and foam-cell formation [171, 172].

A key event in early atherosclerosis is the recruitment of monocytes and lymphocytes but not neutrophils to the artery wall triggered by the accumulation of minimally oxidized LDL. This accumulation stimulates the endothelium to produce adhesion molecules, such as vascular cell adhesion molecule 1 (VCAM1), Intercellular adhesion molecule 1 ICAM-1 and E-Selectin and second messengers such as GM-CSF or IL-6. Possibly the hierarchical

oxidative stress response also functions in a similar way in endothelial cells [145] since the endothelium is prone to oxidative stress induced by DEPM [124, 173-176].

One of the fundamental functions of the endothelium is maintaining the vascular tone by modulating vasodilation or vasoconstriction. DEPM and PM were found to interfere with this important process [177, 178]. Likely the impairment of vasodilation is due to an altered release or scavenging of NO from the endothelium by DEPM [127]. Experiments in cell culture models showed that DEPM can also exhibit anti-estrogenic and anti-androgenic effects [179-183]. Estrogen receptors play a role for the activation of the endothelial nitric oxide synthase (eNOS) and a perturbation in the regulation of eNOS will also lead to altered vasodilation [184]. Macrophages that were exposed to DEPM were shown to alter endothelial cell expression of the expression of eNOS but also the expression of the iNOS [185].

Additionally, DEPM was reported to induce unfolded protein response (UPR) [145]. Generally, UPR pathway is activated in cells under stress conditions that compromise the processing and folding of the proteins in the endoplasmatic reticulum [186]. An important stimulus for the induction of the UPR pathway is the presence of oxidative stress, which leads to modification of proteins and causes misfolding. Interestingly, it was already demonstrated that exposure to DEPM stimulates the UPR pathway in lung cells [187]. Furthermore, UPR has emerged as a key mechanism in the pathogenesis of a number of factors that promote atherosclerosis in the vasculature [188]. The barrier function of the endothelium can also be affected by DEPM since they were found to cause redistribution of endothelial VE-cadherin [169]. Moreover, PM induces apoptosis in endothelial cells *in vitro* [176] suggesting a potential to cause tissue damage *in vivo*.

In summary, the observed systemic effects could either be due to release of inflammatory mediators from the lung or from the possible translocation of particles and/or chemicals to the circulation. However, in both scenarios the interplay of PM components and the endothelium seems to be relevant for the generation of the above-mentioned effects [145].

1.2.5. DEPM AS ADJUVANTS IN ALLERGIC REACTIONS

Besides the already described cardiovascular effects of DEPM there is growing evidence that these particles can act as an adjuvant to common environmental allergens, contributing to respiratory diseases, such as asthma [139, 189-197]. DEPM seems to be able to exacerbate existing diseases, but also to enhance the sensitization to allergens via the production of immunoglobulin E antibodies [193, 198]. During the past 20 years the reported cases of asthma increased dramatically in industrialized countries [97] and childhood asthma was reported to be more predominant in urbanized areas [199].

In addition, there is a large body of evidence that oxidative stress plays a role not only in the pro-inflammatory but also for the adjuvant effects of these particles [57-68]. Radical generation has been demonstrated at sites of allergen challenge in human lungs [200]. The results could be confirmed using large animals (e.g. sheep) [201, 202] where it was demonstrated that oxygen radicals could contribute to airway hyperreactivity induced by the encountered antigen [203]. Experiments with mice showed the development of asthma-like symptoms after DEPM instillation [204]. Interestingly, patients suffering from asthma showed different levels of enzymes responsible for antioxidant defense compared to healthy individuals [155, 205-207] underlining the importance of the oxidative stress concept in asthmatic malady. Another potential mechanism to explain the adjuvant effects of DEPM in allergic inflammation is the potential enhancement of the role of macrophages as antigen presenting cells [139]. Respiratory sensitization as a consequence of chronic exposure to particulates or chemicals is a problem of high concern [208, 209] and understanding in detail the involved mechanisms is an important task for the future.

1.3. CHALLENGES IN STUDYING THE UNDERLYING MECHANISMS IN PM-INDUCED ADVERSE EFFECTS *IN VITRO*

Studying the hazard of DEPM and urban PM is a challenging task since DEPM and also urban PM are complex mixtures comprising a myriad of different chemicals and metals that are adsorbed to these particles [90, 210-212]. Most of the data that are available on the hazard of DEPM are based on *in vivo* studies and from *in vitro* studies under submerged conditions [213].

The most common way to expose laboratory animals to environmental particles is to prepare a suspension of the particles in phosphate buffer and to instill this suspension into the respiratory system [204, 214-217]. However, this approach is not properly reflecting the particle's properties, since it influences the size of the particles and may wash out heavy metals and other components from the parent particles leading to altered availability. The same is true for most of the *in vitro* experiments that were done with DEPM and urban PMs. The particles are generally suspended using either an organic solvent such as dimethylsulfoxid (DMSO) or some standard cell culture medium [213]. In either case the physico-chemical properties of the particles are modified reflecting not accurately the parent material [118]. In addition, it is very challenging to prepare homogeneous solutions with heavily charged particles such as DEPM. These particles have the tendency to stick to every kind of material resulting in a loss of material that is neither traceable nor repeatable.

Other studies used extracts of DEPM that were prepared using organic solvents for extraction. However, these DEPM extracts cannot properly reflect the effects triggered by the parent particle since they are not considering the role of the carbon core [115]. To study properly the hazard of environmental particles and nanomaterials studies performed under realistic exposure conditions are needed [113]. These studies need to be designed carefully and several key-points need to be considered as the route of exposure may have tremendous impact on the overall results [218]. Dependent on sample preparation, the

physico-chemical properties of a particle may become altered compromising the relevance of the results.

Another very complex task for every study is the choice of a proper dosimetry approach. The dose is generally defined as µg/mL of cell culture medium. Common values for concentrations of DEPM used *in vitro* range from 0.2 µg/mL up to 1 mg/mL (reviewed in [213]). Most of the doses that are applied *in vitro* are far beyond any physiological relevance, and would never be accumulated in the respiratory tract during anyone's life. The concentrations to be used for *in vitro* studies should rather be defined in respect to well established epidemiological studies and deposition models in order to define *in vitro* relevant doses [219].

Another important issue is the way how cells are exposed to particles to allow exposure of cell cultures at the so called air-liquid-interface (ALI) avoiding altering particle's properties due to contact with medium components or organic solvents. Such exposure units start to become more important to study the hazard of particles. However, translating doses from classical submerged *in vitro* approaches to an ALI exposure scenario is very difficult, as the dose at the ALI is usually defined by the deposition rate per cm^2 of cell culture area.

1.3.1. SUBMERGED CULTIVATION VS. CULTIVATION AT THE AIR-LIQUID-INTERFACE (ALI)

The submerged cultivation is the classical method to grow cells and to study effects of different agents. Depending on the assay this model is relatively simple to use, shows high reproducibility and is rather cost-efficient. Submerged cultures are particularly relevant to study the toxicity of chemicals that are water soluble, i.e. pneumotoxic heavy metals. These can be dissolved in cell culture medium and then be used to expose the cells. In a submerged culture the cells are studied growing on the bottom of culture wells covered by the medium, reflecting a rather unphysiological situation (Figure 5 A). The surface of the cells has no contact with the ambient air and therefore PM or NPs have to cross the medium

before they can reach the cell surface. Modification of particles due to the proteins and supplements of the medium may take place, which can enhance or totally quench potential toxic effects. The outer layer of proteins around a particle is recognized by the cells especially of the immune system and induce responses [220]. The interaction between proteins and particles can also be limited in a submerged system by using serum-free exposure conditions to study the toxicity [221, 222].

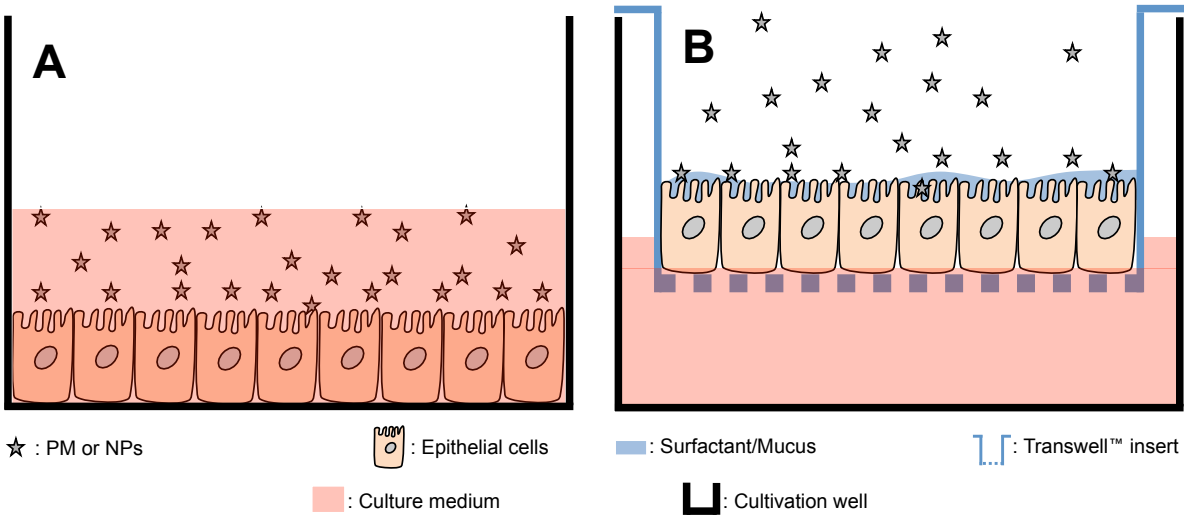

Figure 5: Submerged cultivation vs. cultivation at the ALI. A: Scheme of the submerged cultivation of a monoculture system. **B:** Scheme of the ALI cultivation of a mono-culture system for aerosol exposure.

The administered mass of a particle in a submerged *in vitro* system will never reflect properly the deposited mass on the cell surface *in vivo* because of effects like the Brownian motion or non-physiological agglomeration processes [223, 224]. Due to these conditions dose determination in submerged cultures and thus evaluation of toxicity can lead to huge errors for particles. To circumvent all these issues, cells can be cultivated at the ALI [225] and be exposed in a special chamber [226], which provides the possibility of creating an aerosol and using a microbalance for dose determination [227].

Cells cultivated in this way are seeded in a Transwell™ insert and are fed from the medium

below (Figure 5 B). During the ALI cultivation the cells in the apical part will have no contact with the medium on the apical cell side but will be in direct contact with the airphase. A549 lung epithelial cells cultivated at the ALI start to secrete surfactant under optimal conditions, which is forming a protection layer against drying and agents [228, 229]. The surfactant is also important for particle retention and displacement under *in vivo* conditions [230, 231] and its presence in the *in vitro* system increases the similarity of a model with the *in vivo* situation.

Primary tracheal epithelial cells have been shown to contain considerably more ciliated surface cells when cultivated at the ALI compared with submerged cultures. Extensive ciliogenesis is dependent on growth at the ALI and also on the presence of retinoic acid in the culture medium [232]. These morphological differences were also attributed to the higher exposure to oxygen under ALI conditions [23].

A lot of efforts were put into standardization of aerosol exposure chambers for reproducible exposure of cells cultivated at the ALI [226, 233-235]. A crucial benefit of the ALI cultivation is the fact that the particle properties should not be changed, as there is no contact with cell culture medium components. However, particle agglomeration state or corona formation may change due to the interaction with surfactant or mucus, although this is likely to happen under *in vivo* conditions, too. Dependent on the system for ALI used the administered dose may be continuously determined via microbalance-measurements thereby allowing exact dosimetry [227]. Altogether the ALI exposure system is a promising approach to study and simulate the toxicity of aerosols, which possesses clear advantages compared to submerged cultivation (Table 1).

Table 1: Submerged cultivation vs. ALI cultivation, advantages and disadvantages in summary

Submerged cultivation	Air-liquid-interface cultivation
✚ technically simple and cost efficient ✚ high reproducibility	✚ No alteration of particles properties ✚ Microbalance-based dose determination ✚ Better simulation of inhalation exposure ✚ high reproducibility
− Dose determination is difficult − Medium can alter particles properties	− Complex and cost extensive system

1.4. AN *IN VITRO* APPROACH TO STUDY THE INFLAMMATORY POTENTIAL OF PARTICULATE MATTER AND NANOMATERIALS

Due to the increasing number of PM and UFPs such as NPs in the environment it becomes more and more relevant to have fast, easy and reliable methodologies to forecast their toxic potential [81]. In this respect, complex *in vitro* coculture systems may be valuable tools to study pulmonary processes and further evaluate the effects of particles on the lung and human health [236].

The pulmonary system with almost 40 different cell types is highly heterogeneous [27]. While any state-of-the-art coculture system is still far from completely mimicking an *in vivo* tissue the coculture systems allow cell-to-cell communications and interactions [237]. The possibility of spatial interaction between the cell types may change the observed effects and thereby result in a more realistic judgment regarding the hazardous potential of compounds, making coculture systems more relevant than monoculture models. Such models have a high potential to unravel some of the mechanisms involved, and are likely to serve as a partial replacement for *in vivo* studies in the future.

1.4.1. COCULTURE MODELS OF CELLS RELEVANT FOR THE PULMONARY SYSTEM

The respiratory system with its vast surface area serves as a major portal for ambient materials such as PM and NPs. There is an ongoing effort to develop and improve *in vitro* models, which should be suitable for studying inflammatory and toxic effects of chemicals and particles on the respiratory tract [238, 239]. A challenging aspect for the development of coculture *in vitro* model systems is the question regarding the cell types to be used and if it is better to choose primary cells or cell lines. The isolation of human primary cells is often experimentally challenging and labor-intensive, due to the problems to find adequate donors to assure the constant and homogenous supply with cell material. Freshly isolated human primary cells are highly differentiated, but will start dedifferentiation soon after isolation when cultured *in vitro* [240]. In addition, isolates of primary cells represent a highly heterogeneous population in respect to state of differentiation and cell types present. The latter aspect is mainly a question of good isolation procedures and could be partially overcome. Cell lines are more homogenous, but show only few characteristics of differentiated cells, wherefore they often only poorly represent the *in vivo* situation [240]. In addition they may be less uniform than previously thought depending on their passage and culture conditions used [241]. Nevertheless, for establishing a new assay it is often better to use cell lines instead of primary cells to avoid possible donor variations, otherwise experiments could be hard to standardize [238, 240]. Regarding the complex cellular structure of the human lung, a single *in vitro* model system using just a few different cell types will not be able to represent such a complex system. Therefore it is more reasonable to develop specialized models for certain anatomical parts of interest, e.g. the alveoli or bronchioli.

Phagocytic cells are playing a dual role in the respiratory tract: first as a phagocyte to engulf particulates, to process foreign antigens and to kill ingested microorganisms and second as an effector cell in the course of an immune response in order to initiate immune and inflammatory responses [242, 243]. Phagocytosis of deposited particles in the alveoli by macrophages can result in the activation of AMs and the secretion of chemokines, cytokines,

ROS, etc. By the secretion of pro-inflammatory chemotactic factors, like the chemokine family of cytokines, alveolar macrophages can induce the migration of polymorphonuclear cells (PMNs) and other cells to the lung and an inflammation emerges [76, 244-246]. Airway epithelial cells can also generate pro-inflammatory cytokines to assist with PMNs attraction [67, 247]. Therefore, the different cells of the pulmonary defense system are not functionally distinct players, but they communicate with each other by a great amount of cytokines and receptors [248-252] (Figure 6).

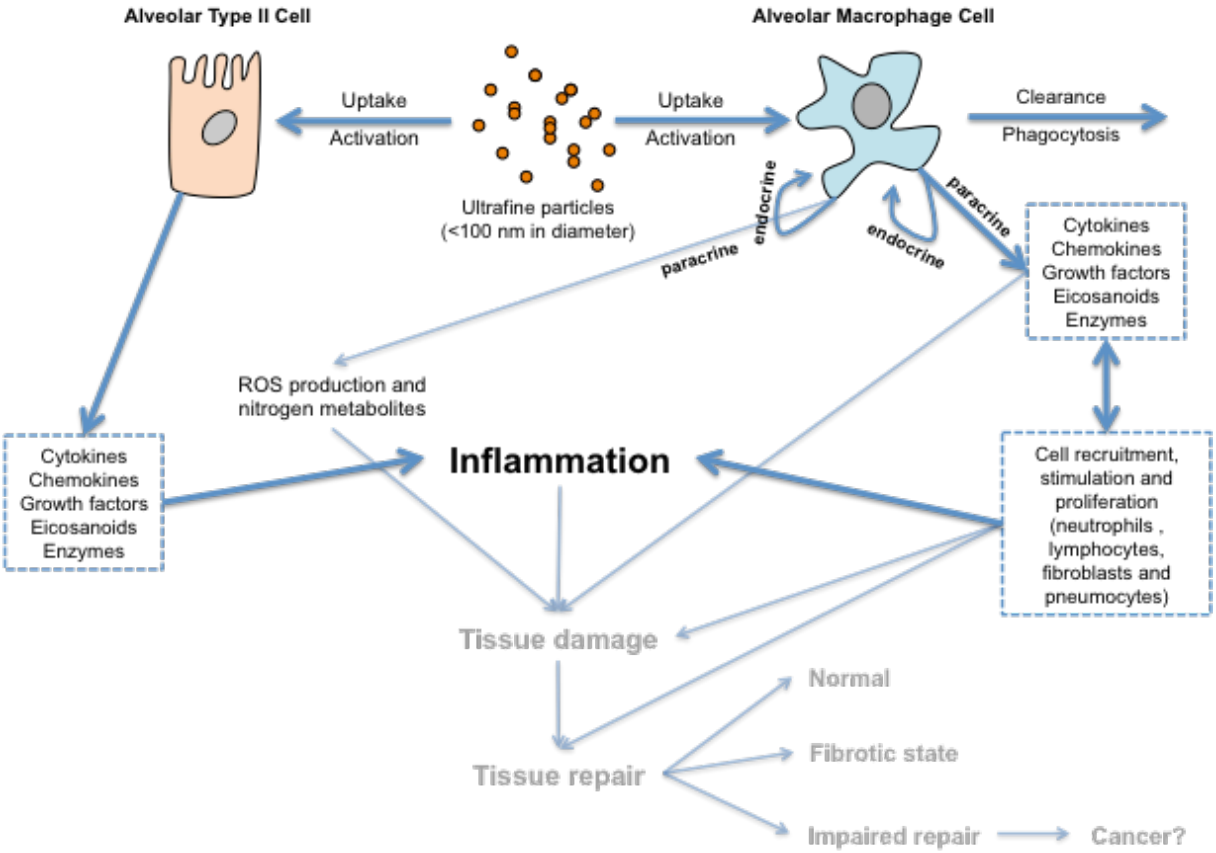

Figure 6: Suggested role of the alveolar type II cells and macrophages in particle-induced inflammation. Alveolar type II cells and macrophages play an important role in defending the alveolar region and in modulating immune responses. Adapted and modified from [253].

Since macrophage activation is one of the most important events among the pulmonary responses to inhaled substances [253], it seems reasonable to develop alveolar *in vitro*

model systems consisting of the predominant epithelial cell type supplemented with macrophage cells to evaluate the hazard of small particles. Although the surface of the alveoli is mainly composed of AT-I cells, many proposed *in vitro* systems [1, 254-258] are using the AT-II-like cell line A549, which is derived from a human adenocarcinoma [259]. The morphology and functionality of A459 cells, e.g. surfactant synthesis, oxidative metabolism and transport properties, are consistent with that of AT-II pulmonary epithelial cells *in vivo* [260, 261]. This cell type provides certain benefits such as the protective surfactant film and the potential of secretion of pro-inflammatory mediators. In addition, these cells are able to perform phase I xenobiotic biotransformation, although the capacity does not fully reflect that of the human lung. However, phase II activity levels found in A549 cells are in the same range found in lung tissue. A549 cells are appropriate to investigate the mechanism of active toxins, but compounds that have to be biotransformed in order to elicit toxicity are less accurately detected [262].

1.4.2. A COCULTURE *IN VITRO* MODEL TO STUDY RESPIRATORY INFLAMMATION

An interesting *in vitro* approach combining A549 AT-II cells [259], THP-1 cells differentiated to macrophage-like cells [263, 264], a human mast cell line (HMC-1 [265]) and EA.hy 926 endothelial cells [266] in coculture has been developed to assess the hazard of PM_{10} on the alveolar epithelium [1]. In this system endothelial cells were seeded in a Transwell™ insert and a tripleculture consisting of A549 cells, differentiated THP-1 cells and HMC-1 cells was seeded inside the well of a multiwell plate. Generally, primary AMs can be isolated by performing bronchoalveolar lavage, where alveoli are washed out repeatedly with a sterile solution that finally contains the cells present on top of the alveolar epithelium [267, 268]. Due to the fact that the procedure of isolating and purifying human AMs is not trivial and volunteers are not always readily available, the monocytic cell line THP-1 [263], differentiated to macrophages, was used. Mast cells are also present within the alveolar

wall and particularly on the alveolar surface [269], but their role in aggravating alveolar inflammation has not been studied intensively in relation to urban PM or NPs. Histamine plays an important role in the systemic effects after exposure to PM *in vivo* [14, 133, 270]. Histamine is mainly secreted by mast cells and therefore mast cells may be crucial for the understanding of systemic effects of PM and NPs [1]. Since urban PM is capable of inducing an endothelial dysfunction phenotype [178, 271, 272] and has pro-thrombotic effects [14, 273], a fourth cell line (EA.hy 926, endothelial cells [266]) was added to the system. With the addition of the endothelial cells in a Transwell™ on top of the system (Figure 7 A), it is possible to study second messenger-induced effects after PM_{10} exposure. The communication between endothelial cells and the cells that have primary contact with particles may play an important role in the systemic effects of PM secondary after an inflammatory reaction. The system should also offer possibilities to evaluate the inflammatory effects of NPs via aerosol exposure at the air-liquid-interface (ALI).

However, for the ALI exposure the epithelial cells as well as the immune cells should be seeded in the Transwell™ insert and not on the bottom of the well (Figure 7 B). After a certain time in culture, the medium will be removed from the Transwell™ insert, while the endothelial cells will grow to confluency in the well (Figure 7 B). Cultivating both, endothelial cells and the tripleculture in the same insert will give the possibility to the cells to communicate with each other via soluble second messengers. This communication between endothelial cells and the cells that have direct contact with particles may play an important role in the systemic effects of DEPM and urban PM secondary after an inflammatory reaction. In addition, this change is necessary to avoid an unintended diffusion of particles or chemicals from the upper to the lower compartment across the microporous membrane.

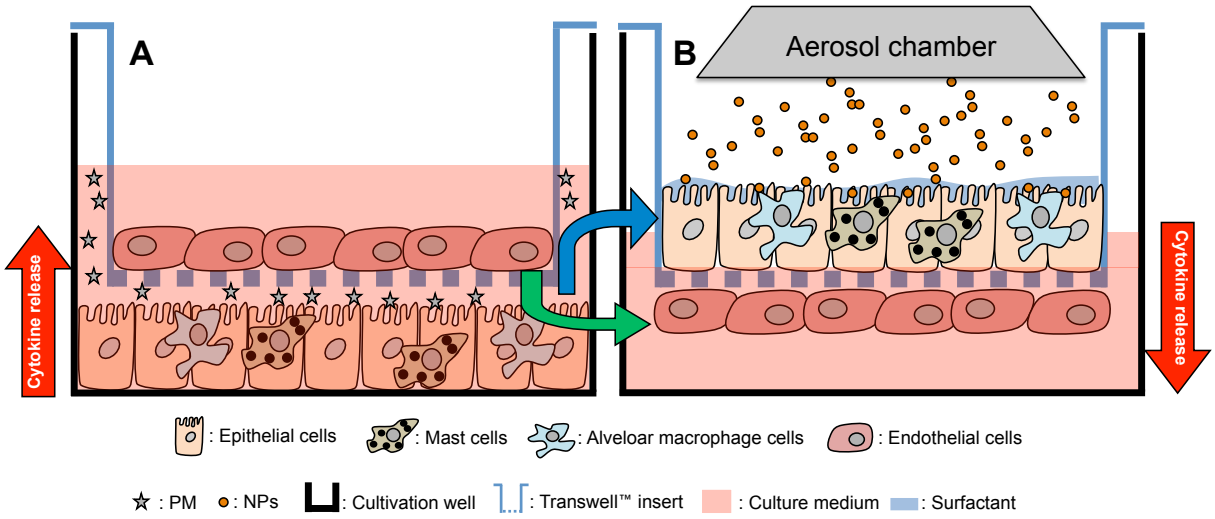

Figure 7: Tetraculture *in vitro* system, relevant for the alveolar barrier. A: Triculture system with endothelial cells to study the inflammatory effects and pulmonary cell communication *in vitro* after exposure to PM_{10} [1]. **B:** variant of the system to study the potential inflammatory effects of NPs at the ALI with native aerosol exposure.

The upper compartment that is comprising the triculture can then be exposed to the NPs or chemicals in the form of an aerosol. Eventually secreted second messengers can cross the microporous membrane and potentially affect the endothelial cells in the lower compartment. Regarding the barrier qualities, the epithelial integrity in a system consisting of A549 cells is controversially discussed due to the lack of sealing tight junctions, [257, 274, 275]. Not all NPs are able to cross microporous membranes with a 0.4 µM pore size in a significant amount even without a cell layer on top [276]. For the skin it has been shown that an impairment of the presence of tight junctions can contribute to allergic reactions, e.g. allergic contact dermatitis due to an increased permeability of the epithelium and thereby causing an enhanced uptake of the allergen, underlining the importance of tight junctions for the integrity of an epithelial barrier *in vivo* [277, 278].

Applying the above-mentioned changes in orientation of the cell layers, it is also possible to study second messenger mediated effects on the endothelial cells after NPs exposure without the risk that NPs could reach the cells at the bottom by crossing the microporous membrane. Nevertheless, several *in vivo* and *in vitro* studies have demonstrated a possible

translocation of UFPs through the epithelium [50]. Therefore it is reasonable to design and develop *in vitro* model systems suitable for the study of direct effects due to the transport of particles through the epithelial barrier. However, the setup of the model system is dependent on the scientific question.

The combination of a complex triculture *in vitro* system, cultivated at the ALI and exposed to an aerosol of a particle or chemical with a state-of-the-art exposure system [235, 279] offers the possibility of studying the interaction of aerosol particles of native atmospheres without altering particle's properties, in a non-physiological way.

1.5. AIMS AND OBJECTIVES

The aim of this PhD work can be divided into two main parts: first to modify and to further improve the coculture system developed by Alfaro-Moreno et al. [1]. Within this part, the tetraculture system was carefully characterized to ensure its performance and repeatability of the results. In the second part, the response of the endothelial part of the alveolar barrier after exposure to relevant doses of DEPM was studied by using the tetraculture *in vitro* system.

1.5.1. DEVELOPMENT OF AN *IN VITRO* COCULTURE SYSTEM SUITABLE TO STUDY ENVIROMENTAL PARTICLES UNDER NATIVE EXPOSURE

In this part, I focused on the establishment and the modification of the tetraculture system, so that it could be used in conjunction with native aerosol exposure equipment. In contrast to the original system, where the actual tetraculture is divided into the part that is seeded in the multiwall plate (tripleculture: A549, THP-1, HMC-1), and the endothelial cells (EA.hy 926) seeded in the Transwell™ insert, in the modified version the Transwell™ insert has an even more important and central role, as it serves as support for the complete tetraculture system.

The coculture was redesigned in order to have a 3D-organisation of the cells, which closely resembles the *in vivo* histology of the alveolar barrier: endothelial cells are seeded on the basolateral side of a microporous membrane; epithelial cells together with the models for the innate immune system (mast cells and macrophage-like cells) are seeded in the apical compartment followed by cultivation at the ALI. The system offers possibilities to evaluate the inflammatory effects of NPs and PM via aerosol exposure at the ALI. Eventually secreted second messengers can cross the microporous membrane and potentially affect the endothelial cells in the lower compartment. In the first part of the thesis, the modified three-dimensional model of the alveolar barrier is presented in detail.

1.5.2. STUDYING THE RESPONSE OF THE ALVEOLAR ENDOTHELIAL BARRIER TO RELEVANT DOSES OF DEPM USING AN INDIRECT EXPOSURE METHOD

Direct exposure of endothelial cells to air pollutants is poorly justified in respect to the *in vivo* anatomy of the respiratory tract and the efficient barrier function of the lung [118]. Therefore the second aim was to evaluate the hazard of ambient DEPM on the endothelium under realistic conditions with relevant doses of DEPM in order to study the processes in the endothelial cells at the early stages of the oxidative stress response. In this part, particular attention was given to the potential of DEPM to induce a Nrf2-mediated response and potential pro-inflammatory effects in the endothelial cells. In addition, we addressed the question on the susceptibility of endothelial cells to DEPM as a potential AhR agonist.

Deciphering early stages of the inflammatory response in endothelial cells of the alveolar barrier after DEPM exposure will contribute to the mechanistic understanding of the adverse effects of DEPM on the cardiovascular system and the exacerbation of other related diseases. The particle loads used in the presented experiments were considerably lower than what is commonly used for submerged exposure to diesel particles in order to have a realistic approach. In addition, it was necessary to develop a dosimetry approach for DEPM

suitable for ALI exposure since DEPM were found to interfere with the microbalances provided by Vitrocell™.

2. MATERIALS AND METHODS

Ethical statement

The experiments in this PhD thesis were conducted neither using primary material from humans or animals nor performing *in vivo* studies on animals. The human cell lines A549 [259], THP-1 [263] and EA.hy 926 [266] were obtained from the American Type Culture Collection (Manassas, VA, USA). HMC-1 [265] cells were kindly provided by J.H. Butterfield, Mayo Clinic (Rochester, MN, USA).

Conflict of interest

Nothing declared.

Reagents

All reagents, unless otherwise specified, were purchased from Sigma Chemical (Deisenhofen, Germany). Cell culture media were purchased from Invitrogen (the Netherlands), fetal bovine serum (FBS Gold) was obtained from PAA (Paschl, Austria). SiO_2-Rhodamine (50 nm) particles were purchased from Corpuscular (Cold Spring, NY, USA).

Cell culture

The different mammalian cell lines were cultured using different media (Table 2). Cells were seeded at specified densities (cells/cm^2) (Table 3) on BD Falcon cell culture inserts (surface area of 4.2 cm^2; 0.4, 1 and 3 µm pore size; high pore density PET membranes for 6-well plates; BD Biosciences, Basel, Switzerland) and grown until confluency. Inserts were placed in BD Falcon tissue culture plates (6 well plates; BD Biosciences) with 2 mL medium in the upper and 2 mL in the lower compartment. Cells were grown in T75 flasks and trypsinized twice a week. Medium (inserts and cell culture flasks) was changed every other day. Cells were maintained in a humidified atmosphere with 5% CO_2 at 37 °C and tested regularly for

contamination by mycoplasma using the PCR mycosplasm testing kit (AppliChem, Darmstadt, Germany).

Table 2: Medium conditions for mono- and cocultures. Unless otherwise mentioned, mono- and cocultures were handled in the absence of antibiotic and antimycotic agents. All media contained Glutamax instead of L-glutamine.

Monocultures			
Cell Line	**Medium**	**Serum**	**Supplements**
A549	Dulbecco's Modified Eagle's Medium (DMEM)	10 % (v/v) Fetal Bovine Serum Gold	
THP-1	Roswell Park Memorial Institute (RPMI) 1640		25 mM HEPES; 50 µM β-mercaptoethanol
HMC-1	Iscove's Modified Dulbecco's Medium (IMDM)		25 mM HEPES; 1,2 mM α-thioglycerol
EA.hy 926	Dulbecco's Modified Eagle's Medium (DMEM)		25 mM HEPES
Tetraculture			
75% HEPES-buffered DMEM; 15% RPMI; 10% IMDM		10 % (v/v) Fetal Bovine Serum Gold	25 mM HEPES

Table 3: Seeding densities for the different mammalian cell lines.

Cell line	**Seeding density per cm^2**
A549	1.2×10^5
EA.hy 926	2.4×10^5
THP-1	2.4×10^5
HMC-1	1.2×10^5

Differentiation of THP-1 cells into macrophage-like cells

Human THP-1 cells (human acute monocytic leukemia cell line) [263] were grown in RPMI 1640 media containing 10% (v/v) FBS Gold (PAA, Paschl, Austria). Differentiation was achieved by resuspension of THP-1 cells at 4 x 10^5 cells/mL in growth medium with addition of phorbol-12-myristate-13-acetate (PMA; 20 ng/mL) and incubation over night at 37 °C and 5% CO_2 [280]. PMA was prepared as a stock solution (10 mg/mL) in ultrapure absolute ethanol. Stocks were kept at -20 °C in the dark. Differentiated THP-1 cells were rinsed with PBS and detached by using accutase in order to harvest them. To remove traces of PMA, detached cells were centrifuged and washed twice with PBS. The upregulation of CD11b as a marker for mature macrophage cells [264] was evaluated by confocal laser scanning microscopy (CLSM) (see cell labeling and fixation for further details).

Tetraculture

EA.hy 926 endothelial cells were seeded on inverted Transwell™ inserts (2.4 x 10^5 cells/cm^2; BD Falcon inserts, 1 µm pore size; Figure 8). Upon attachment on the basolateral side of the Transwell™ insert the plate with the Transwell™ inserts was turned back to its original orientation (Figure 8, Step 4) before the A549 cells were seeded inside the Transwell™. Epithelial and endothelial cells were grown for three days at 37 °C and 5% in a humidified atmosphere. On day 3 THP-1 cells were stimulated to differentiate into macrophage-like cells by addition of PMA. On day 4, THP-1 cells and HMC-1 cells were added into the inserts with A549 and EA.hy 926 cells to complete the tetraculture system. The medium for the complete tetraculture contained only 1% FBS to avoid extensive proliferation of HMC-1 cells. THP-1 cells and mast cells were found to be attached on the epithelial layer after 4 h. The attachment of the cells was verified by light microscopy. Upon attachment the medium was removed from the upper compartment and the tetraculture was cultivated at the ALI for 24 h prior to exposure (Figure 9).

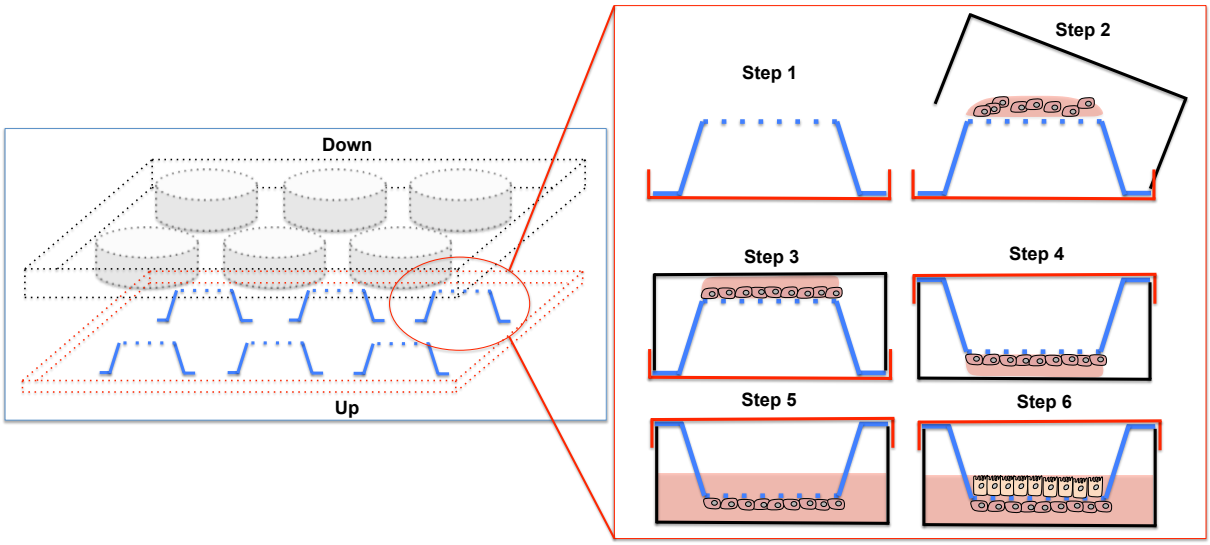

Figure 8: Seeding of endothelial and epithelial cells on inverted inserts. EA.hy 926 endothelial cells were seeded on inverted Transwell™ inserts (Step 1 to Step 6). First, Transwell™ inserts were placed into a corresponding 6 well plate and the plate with the inserts was turned upside-down (Step 1). Endothelial cells were seeded on the inverted inserts and the bottom of the 6-well plate was used as lid (Step 2). Upon attachment to the basolateral side of the Transwell™ insert, the plate with the Transwell™ inserts was turned back to its original orientation (Step 3, 4 and 5) before the A549 cells were seeded inside the Transwell™ (Step 6).

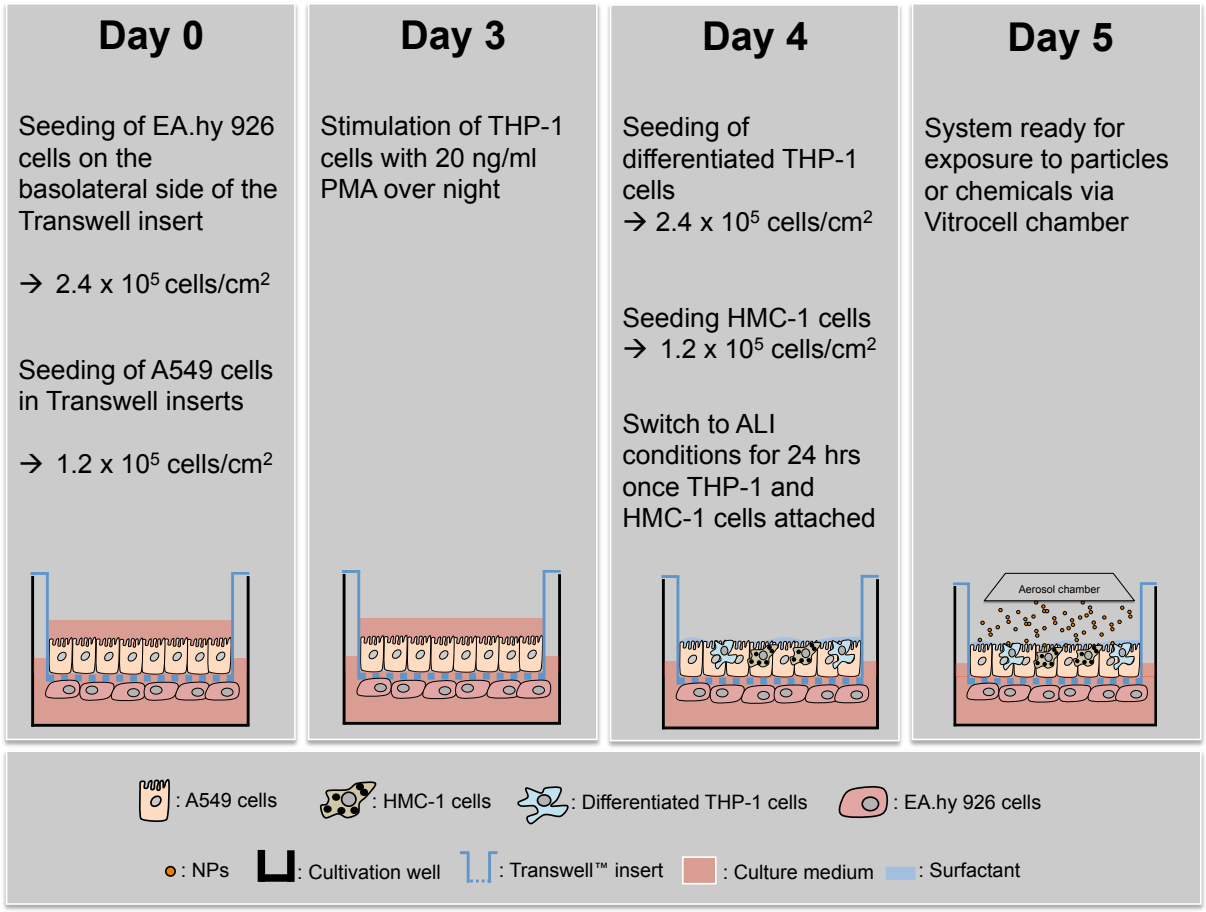

Figure 9: Workflow to setup an aerosol exposure experiment with the tetraculture system.

Transepithelial transport of sodium fluorescein

A solution of sodium fluorescein (1 mg/mL in medium) was added into the apical compartment and a solution of medium without sodium fluorescein was added into the lower compartment. The cultures were incubated for 60 min at room temperature in the dark. Empty inserts without cells served as a control to evaluate the maximum leakage. After 60 min the inserts were carefully discarded and samples were taken from the basolateral compartment. The fluorescence of sodium fluorescein was measured with a multi-mode microplate reader (ex: 495 nm; em: 519 nm; Biotek, Germany).

Adaptation of the DCFH-DA assay for oxidative stress for the use with Transwell™ inserts

2,2'-azobis-2-methyl-propanimidamide-dihydrochloride (AAPH; Merck), a water-soluble azo-compound, which is commonly used in studies of lipid peroxidation, was chosen as positive control for oxidative stress. Working solutions were prepared freshly in cell culture medium before use. The evaluation of oxidative stress was performed by the use of dichlorodihydrofluorescein diacetate (DCFH-DA) dye. DCFH-DA enters the cell and the diacetate is cleaved, which results in the trapping of the dye inside the cell. In the presence of reactive oxygen species (ROS) the dye is oxidized and emits green fluorescence, which is directly proportional to the amount of oxidative stress [281].

DCFH-DA was suspended in cell culture medium (100 µM) and cells were preloaded with the dye for 45 min at 37 °C and 5% in the dark. After the preloading step the cells were rinsed with PBS to remove the non-internalized DCFH-DA and immediately exposed to the compound of interest. Fluorescence reading was done with a multi-mode microplate reader (ex: 485 nm, em: 528 nm; Biotek, Germany). Empty inserts did not emit significant fluorescence at the above-mentioned wavelengths.

Adaption of the resazurin metabolism assay for the 3D tetraculture

Transwell™ inserts were washed twice with PBS. Afterwards, 2 mL of medium containing 400 µM resazurin were added to the upper and the lower compartment. Cells were incubated for one hour at 37 °C and 5% CO_2. After the incubation, aliquots of 500 µL were taken from the upper and the lower compartment and transferred into a 12 well plate to measure separately the fluorescence for both compartments (inside and outside of the Transwell™ insert). Fluorescence reading was done with a multi-mode microplate reader (ex: 530 nm, em: 590 nm; Biotek, Germany).

Transepithelial Electrical Resistance Measurements

Transepithelial electrical resistance (TEER) was measured with the Millicell-ERS system (MERS 000 01; Millipore AG, Volketswil, Switzerland). The mean of three measurements per insert was determined. The electrical resistance of inserts without cells was subtracted from all samples, and the resistance values were multiplied with the surface area of the inserts (4.2 cm^2). Electrical resistance was measured in single A549, EA.hy 926 cell cultures, coculture of A549 and EA.hy 926 and in tetraculture to follow tightness of the cell layer in respect to the cellular composition.

Cytokine measurements

Single cultures, cocultures and tetracultures were exposed to 20 mM of AAPH for two hours. After treatment, aliquots from the undernatant were taken and the amounts of GM-CSF, IL-1_β, IL-6, IL-8 and TNF-α were analyzed. Quantification was performed on a Luminex 100™ (Luminex Oosterhout, the Netherlands) using the inflammatory cytokine human magnetic 5-plex panel produced by Invitrogen (Invitrogen, Leusden, the Netherlands) following manufacturer's instruction.

Cell labeling and fixation

The cells were washed twice in PBS and fixed for 15 min at room temperature in 4% formaldehyde in PBS (v/v). Fixed cells were incubated for 30 min with 10% bovine serum albumin (BSA) in PBS (w/v) to block unspecific bindings. After blocking, cells were incubated with primary and secondary antibodies for 60 min each at room temperature in the dark.

Antibodies were diluted in immunostain enhancer (Thermo Scientific, Belgium) or PBS containing 1% FBS (Table 4). Nuclei were counterstained with 4',6'-diamidino-2-phenylindole (DAPI) and cellular membranes were stained with cell mask deep red (C10046; Invitrogen, Leusden, the Netherlands).

Table 4: List of antibodies used for immunohistochemistry labeling

Target	Species	Dilution	Reference
Primary antibodies			
CD11b	Rabbit	1:200	clone EPR1344; Novus Biologicals, UK
Histamine	Rabbit	1:200	ABIN115761; antibodies-online Inc., USA
Nrf2	Rabbit	1:100	ab31163; Abcam, UK
AhR	Rabbit	1:200	sc-5579; H-211; Santa Cruz, Heidelberg, Germany
SP-A	Rabbit	1:200	ABIN672996; antibodies-online Inc., USA
SP-B	Mouse	1:100 to 1:200	ABIN384606; antibodies-online Inc., USA
SP-C	Rabbit	1:200	ABIN679643; antibodies-online Inc., USA
Secondary antibodies			
Anti-rabbit	Goat	1:2000 to 1:3000	AS09 633; Agrisera, Vännas, Sweden
Anti-mouse	Goat	1:100 to 1:200	405309; Poly4053; Biolegend, Eching, Germany

Confocal Microscopy and Image Restoration

A Zeiss LSM 510 Meta with an inverted Zeiss microscope (Axiovert 200M, Lasers: HeNe 633 nm, HeNe 543 nm, Ar 488 nm and Diode 405 nm; Zeiss, Jena, Germany) was used. Image processing and visualization was done using the Zeiss Software ZEN 2011 and Image*J* (http://rsbweb.nih.gov/ij/).

Aerosol exposure

The Vitrocell™ aerosol exposure device (Vitrocell™, Taufkirchen, Germany) was used for dynamic delivery and exposure of cells to aerosolized PBS and to PBS containing 50 nm SiO_2-Rhodamine nanoparticles. This system was designed for toxicology studies to directly expose target cells at the ALI, which resembles the *in vivo* anatomical situation [238, 279]. The uniformity of the particle population was confirmed by scanning electron microscopy (SEM).

Briefly, the used device (Vitrocell™ 6/3 CF stainless, Vitrocell™ Systems, Germany) contains three exposure chambers (Vitrocell™ module), which holds one separate insert each, allowing simultaneous exposures of 3 Transwell™ inserts. In order to keep the cells viable, the module is equipped with a heated water jacket at a steady temperature of 37 °C. For the exposure, cell culture inserts are placed into the exposure chambers containing the culture medium.

The aerosol is generated by a pneumatic nebulizer (AGF 2.0 PALAS, Karlsruhe, Germany) and is delivered through a trumpet device at a low flow rate (5 ± 0.1 mL/min/module) for a defined time of exposure to the modules.

Before the experiments, all Transwell™ inserts were routinely checked by light microscopy to assure a uniform distribution of DEPM and to verify the integrity of the cell layer. All inserts showed homogenous particle distributions and no abnormalities of the cellular layers could be discovered.

What can be considered to be a relevant dose for *in vitro* experiments?

For *in vitro* and *in vivo* toxicology dosimetry plays always an important role. As already mentioned above particle doses used for *in vitro* experiments under submerged conditions are generally too high and beyond any realistic range. However, following considerations published that are describing carefully relevant parameters [219], calculations in order to determine a relevant dose-range for *in vitro* studies at the ALI can be performed.

The alveolar surface of a normal human individual has a surface area of ≈ 140 m^2. We can assume, that small particles below 2.5 µm or smaller, can penetrate deep into the lungs, reaching the area of gas exchange. While working and performing light physical exercises, humans breath between 40 and 60 L/min. The minute volume while sleeping or relaxing is much lower and is around 8.5 L/min. For our calculations, we assume a physical exercise of 10 hours a day, resulting in an air intake of 24 m^3 (40 L/min x 60 min x 10 h). This together with the 6.1 m^3 (8.5 L/min x 60 x 12 h) that we breathe without physical exercise result in a complete air intake of ≈ 30 m^3 in 24 hours.

In India or China the rapid growth of the number of motorized vehicles (cars and motorcycles) and also the rapid growth of the industry contribute to high particle burden in the ambient air. In large cities particle concentrations of 1.4 mg/m^3 can be present in the ambient air [91]. Taking this as a worst case scenario we can multiply this value by a daily air intake of 30 m^3, which results in about 42 mg of particles that are inhaled per day. This means, that each cm^2 of the alveolar surface may be exposed to approximately 30 ng of particulates on a single day. For Europe this is still an unlikely scenario, which is however quite realistic for several non-western industrialized countries.

Using these considerations as a baseline, the ALI *in vitro* exposure experiments were designed with exposures to 40, 80 and 240 ng/cm^2, the latter being a dose, which may be accumulated over several days during a smog episode.

Surfactant droplet test

The surfactant droplet test was performed as described [229]. Briefly, A549 cells were cultured under submerged conditions in Transwell™ inserts. The medium was then removed from the apical compartment well and the cells were cultivated at the ALI for 24 h. In order to determine the surface tension, DMP/O droplets were placed on the cell surface. Droplet diameters, d0 and d, were measured before and after deposition. A large diameter indicates a high surface tension, e.g. of cells grown under submerged conditions. A small diameter of the drop indicates a lower surface tension, e.g. of cells grown under ALI conditions with secreted surfactant.

qRT-PCR

Cells were washed twice with PBS and centrifuged 2 min at 800 g and supernatants were discarded. Total RNA was isolated from cell pellets with RNeasy Mini Kit (Qiagen, Leusden, Netherlands), following the manufacturer's instructions. RNA integrity control was assessed with the RNA Nano 6000 assay (Agilent Technologies, Diegem, Belgium) using a 2100 Bioanalyzer (Agilent Technologies, Diegem, Belgium). All RNA samples displayed RINs

(RNA integrity number) above 8. Concentration and purity determination of the RNA were performed by using Nanodrop ND1000 spectrophotometer (Thermo Scientific, Villebon-sur-Yvette, France). Reverse transcription was performed with New England BioLabs (Ipswich, MA, US) reagents: M-MuLV Reverse Transcriptase (RNase H), the murine RNase Inhibitor (New England Biolabs, Ipswich, MA, USA) using Random primers (Invitrogen, Carlsbad, NM, USA) following the manufacturer instructions. 20 µL final volume containing 5 µg of total RNA were used to perform the reverse transcriptase. Four reference genes *B2M*, *HPRT*, *SDHA*, *YWHAZ* (Table 5) [282] primers pairs were ordered from Eurogenentec (Liege, Belgium). The reference genes were validated as stable candidates between the conditions using GeNorm in the Biogazelle qBase PLUS software. Gene expression was evaluated using a real-time PCR system (Life technologies) together with mesa green low rox real-time PCR kits (Eurogentec, Liège, Belgium). PCR were performed in 25 µL with final concentrations as follows: 1X MasterMix, 100 nM for each primers except for *CYP1B1* where 300 nM forward and 100 nM reverse primers were used, 0.4 ng/µL cDNA. Each sample was performed in triplicate. Template control and RT- control samples were added to each plate. Thermal cycling conditions were: initial 5 min denaturation at 95 °C, followed by 45 cycles of 15 s at 95 °C and 1 min at 60 °C, and a final dissociation step (melting curve) was used to determine the primer specificity by revealing the presence of a single peak. PCR efficiency was performed using decreasing five-fold dilution from THP-1 and A549 cDNA pool (from 25 ng to 0.04 ng and no template control). Contamination by genomic DNA was verified by using total RNA as sample for PCR. The relative gene expression was calculated taking into account gene-specific PCR efficiency [283, 284] using the Biogazelle qbase PLUS software 2.5 software with the $^{\Delta\Delta}$CT method. Table 5 summarizes the primers that were used in this PhD work.

Table 5: Summary about the primers that were used for qRT-PCR experiments with the endothelial cells of the tetraculture. Unless further mentioned, qRT-PCR primer were designed for the experiments of this PhD work.

Gene	Primer F	Primer R	Reference
HMOX1	TTCTCCGATGGGTCCTTACACT	GGCATAAAGCCCTACAGCAACT	[134]
CASP7	CGGTCCTCGTTTGTACCGTC	GGTGGTCTTGATGGATCGCA	[134]
SOD1	GTGCAGGTCCTCACTTTAAT	CTTTGTCAGCAGTCACATTG	[134]
FAS	AGCTTGGTCTAGAGTGAAAA	GAGGCAGAATCATGAGATAT	[134]
NF_kB	GCTTGTAGGAAAGGACTGCC	GTTGTTGTTGGTCTGGATGC	[285]
CYP1A1	GGAGGCCTTCATCCTGGAGA	CCTCCCAGCGGGCAACGGTC	[286]
CYP1B1	CTTTATGAAGCCATGCGCTTCT	GCCACTTCACTGGGTCATGATT	[287]
IL-6	GGAGACTTGCCTGGTGAAAA	GTTGGGTCAGGGGTGGTTAT	
NEF2	ACATTGAGCAAGTTTGGGAG	TGTGGACTACAGTTACCTAC	
NQO1	GGAGAGTTTGCTTACACTTACGC	TTCTCCAGGCGTTTCTTCCA	
ICAM-1	GCAAGGTGACCGTGAATGT	GCATAAAGCCCTACAGCAAC	
GST1	ACAGTTGTACAAGTTGCAGGATG	TGCCAAAGAGATTGTGCTTG	
HSP70	CCTACTCCGACAACCAACCC	GGTGATCTTGTTGGCCTTGC	
HMOX2	GGGAAAGGAGACATGCGTAA	CAAGAGTCCAGCAGCTAGGG	
E-Selectin	ACCTCCACGGAAGCTATGACT	CAGACCCACACATTGTTGACTT	
VCAM1	CTTAAAATGCCTGGGAAGATGGT	GTCAATGAGACGGAGTCACCAAT	
B2M	TGCTGTCTCCATGTTTGATGTATCT	TCTCTGCTCCCCACCTCTAAGT	[282]
HPRT1	TGACACTGGCAAAACAATGCA	GGTCCTTTTCACCAGCAAGCT	[282]
YWHAZ	ACTTTTGGTACATTGTGGCTTCAA	CCGCCAGGACAAACCAGTAT	[282]
SDHA	TGGGAACAAGAGGGCATCTG	CCACCACTGCATCAAATTCATG	[282]

Catalytic activity of CYP1A1

Ethoxyresorufin-O-deethylase assay was performed as described in [241]. A549 cells were seeded at a density of 1.2 x 10^5 cells/cm^2 in BD Falcon 6 well plates. Cells were washed two times with DMEM without phenol red and treated with 2.5 µM dicumarol [3,39-methylene-bis(4-hydroxycoumarin)] and 7,5 µM ethoxyresorufin. Cells were incubated for 60 min at 37 °C. A kinetic was recorded by measuring every 5 min. The formation of resorufin was measured using a multi-mode microplate reader (ex: 485 nm, em: 528 nm; Biotek, Germany).

Scanning electron microscopy (SEM)

The Vitrocell™ aerosol exposure device (Vitrocell™, Taufkirchen, Germany) was used for dynamic delivery and exposure of cells to aerosolized PBS and to PBS containing 50 nm SiO_2-Rhodamine nanoparticles. Empty Transwell™ inserts were exposed for 30 min as described for Transwell™ inserts containing the tetraculture system. Afterwards samples were metallized with a 20 nm golf film under vacuum. Scanning electron microscopy was done with a FIB-SEM (FEI, Eindhoven, The Netherlands) at 25 kV and 25 mA.

NanoSIMS analysis

Samples were analyzed with a NanoSIMS 50 (Cameca, Courbevoie, France) using a Cs^+ primary source (8 keV), rasterizing the surface of the sample (-8 keV) with a raster between 40 x 40 µm and 20 x 20 µm to generate secondary negative ions. The energy of the impact of the primary beam was 16 keV with an intensity range of 1.0-0.8 pA. In these conditions the probe-working diameter was in the range 80–100 nm. The masses studied simultaneously in multicollection mode were: $^{31}P^-$ (m=30.97376), ^{54}Cr (m = 53.9388804), ^{58}Ni (m = 57.9353429), ^{67}Cu (m = 66.9277303) and ^{64}Zi (m = 63.9291422). Images were recorded in a pixel format of 256 x 256 image points with a counting time of 20 ms per pixel.

Aerosol particle counting

An optical particle counter (GRIMM EDM 164 portable fine dust aerosol spectrometer) was used. A continuous flow of sample air (1.2 L/min ± 5% continuously regulated) is directly led into the measuring cell where the dust particles are measured by the physical principle of orthogonal light scattering. A laser light illuminates the particles. The laser signals, 90° scattered by the particles passing through the laser beam, are collected by a mirror and transferred to a recipient diode. Each signal of the diode is transmitted, after a corresponding reinforcement, to a pulse height analyzer, then classified to size and transmitted in each size channel. The laser spectrometer detects all airborne particles in a

size range from 0.25 µm up to 32 µm in real-time, with a particle size distribution in 31 channels.

12 Nano channels:

0.25 / 0.28 / 0.3 / 0.35 /0.4 / 0.45 / 0.5 / 0.58 / 0.65 / 0.7 / 0.8 / 1.0 and

19 micro channels:

1 / 1.3 / 1.6 / 2 / 2.5 / 3 / 3.5 / 4 / 5 / 6.5 / 7.5 / 8.5 / 10 / 12.5 / 15 / 17.5 / 20 / 25 / 30 / 32

The data are stored on an internal memory card. The GRIMM instruments have the European Equivalence Approval for PM10 and PM2.5 as well as the US-EPA Approval for PM2.5.

Statistics

Data represents the mean of at least four independent Transwell™ inserts ± standard error of mean (SEM). Statistical analysis was done using SPSS, version 19 (IBM, Mainz, Germany). Statistical comparison of the means was performed by ANOVA, followed by the Tukey posthoc test. In graphs, groups that are sharing the same letters are not significantly different (P>0.05).

3. RESULTS

3.1. CHARACTERIZATION AND ESTABLISHMENT OF THE TETRACULTURE *IN VITRO* SYSTEM

In this part of the results section, the findings about the abilities and the limitations of the tetraculture *in vitro* system of the human alveolar barrier that was carefully adapted and modified for the use with native aerosol exposure equipment will be described.

3.1.1. CHARACTERIZATION OF THE CELL LINES OF THE TETRACULTURE *IN VITRO* SYSTEM

In order to fully understand the potential and limits of the proposed *in vitro* model system, the most important characteristics of each cell line as well as the inducibility of *CYP1A1* and *CYP1B1* genes were evaluated.

3.1.1.1. PRODUCTION AND SECRETION OF SURFACTANT IN A549 TYPE II EPITHELIAL CELLS

The production of the most abundant surfactant proteins A, B and C (SP-A, SP-B and SP-C) was evaluated using immunohistochemistry together with confocal microscopy in alveolar type II epithelial cells (A549). A549 were cultivated in LabTek-II chambered coverslides and then fixed and stained for cellular membranes, nuclei and surfactant proteins. The cells were found to produce large amounts of SP-A and SP-C (Figure 10). However, the amount of produced SP-B was at the limit of detection and was only slightly different from the background noise (data not shown).

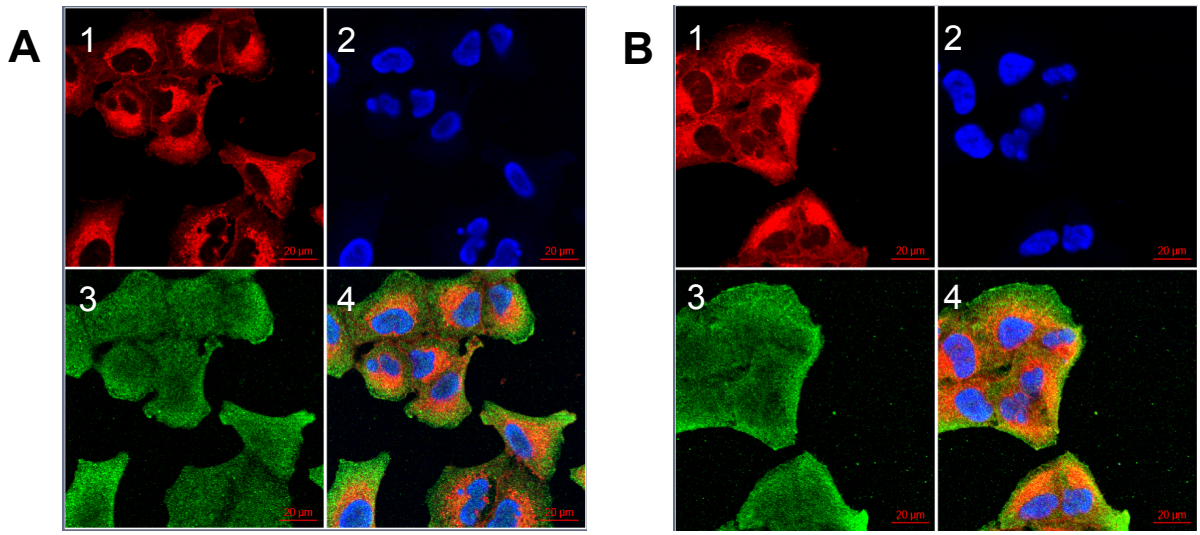

Figure 10: Immunohistochemistry staining of surfactant protein A and C in A549 cells. A549 cells were grown in Labtek-II chambers for 48 h. Afterwards, cells were fixed, permeabilized and stained for cellular membranes, nuclei and surfactant protein (**A:** surfactant protein A; **B:** surfactant protein C)**.**

1: membranes stained with cell mask deep red. **2:** Nuclei stained with DAPI. **3:** Surfactant protein stained with anti-surfactant-protein antibody (1:200). **4:** Overlay.

To demonstrate the ability of A549 cells not only to produce surfactant related proteins but also to secrete a functional surfactant layer the Transwell™ inserts with confluent A549 cells were kept at the ALI and under submerged conditions for 24 h. Surfactant production was compared using the surfactant droplet test to confluent endothelial cells (EA.hy 926) cultivated also for 24 h under submerged conditions as a negative control.

The surfactant droplet test allows a direct evaluation of the surface tension of a cellular layer. The smaller the size of the droplet, the lower the surface tension of the epithelium. Among the conditions tested, A549 cells cultivated for 24 h at the ALI show the smallest droplet compared to the submerged A549 cells and the endothelial EA.hy 926 cells, where the droplet spreads completely (Figure 11).

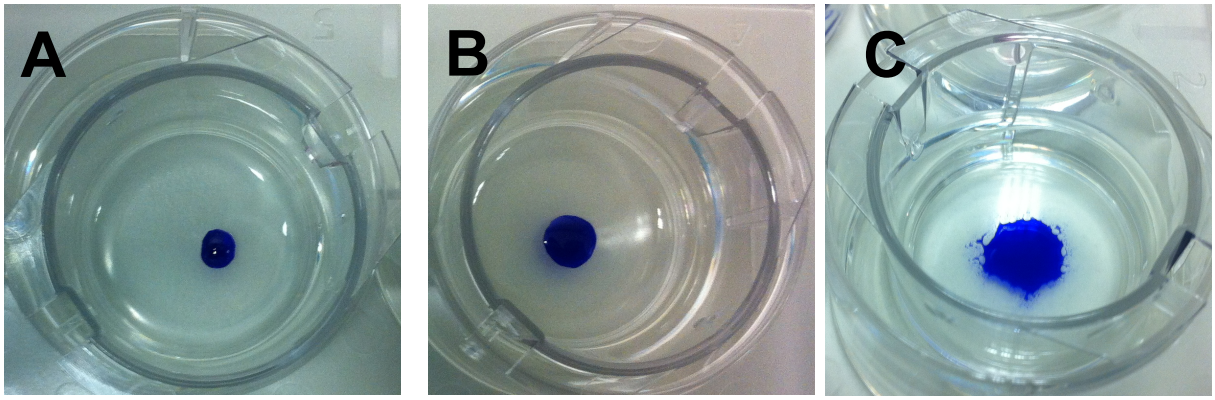

Figure 11: Surfactant droplet test to evaluate the production of a functional surfactant film on top of A549 cells. A: A549 cell exposed for 24h at the ALI; **B:** A549 kept under submerged conditions; **C:** EA.hy 926 cells kept under submerged conditions.

3.1.1.2. XENOBIOTIC METABOLISM IN A549 CELLS

The lung can be considered as an important target organ for the toxicity of inhaled particles and xenobiotics. Cytochrome P450 enzymes play an important role in the metabolization of xenobiotics. In order to evaluate whether or not the different cell lines of the tetraculture system were able to respond to xenobiotics, they were exposed to 5 µM B[a]P and 600 pM TCDD (positive control) for 24 and 48 h. Afterwards the levels of *CYP1A1* and *CYP1B1* mRNA were evaluated using qRT-PCR.

A549 cells responded the strongest to the B[a]P treatment with an increase in *CYP1A1* mRNA expression of 324.4 ± 170 (24 h) respectively 422.3 ± 88.6 (48 h) fold relatively compared to control cells treated with DMSO ($P<0.05$) (Figure 12 A). The effect of 600 pM TCDD on the mRNA expression of *CYP1A1* in A549 cells was found to be lower than after B[a]P treatment, with a fold increase of 285.8 ± 226.6 (24 h) and 234.2 ± 97.9 (48 h), but still significantly increased compared to the control cells ($P<0.05$). The basal level of CYP1A1 mRNA expression in A549 cells was close to the limit of detection in our experimental setup. In analogy to the experiments for *CYP1A1* (Figure 12 A), the expression level of *CYP1B1* was evaluated under identical conditions.

Compared to the findings for *CYP1A1* mRNA in A549 cells, *CYP1B1* mRNA was found to be less inducible. After 24 h of treatment with 5 µM B[a]P A549 cells showed a 14.8 ± 2.1 fold increase for *CYP1B1* mRNA, which is similar to the response after 48 h (16.9 ± 2.6) (both time-points were significantly different from the control $P<0.05$) (Figure 12 B). The effect of the positive control (600 pM TCDD) on the mRNA expression of *CYP1B1* in A549 cells, was found to be slightly lower than after B[a]P treatment with a significant increase of 12.1 ± 2.9 (24 h) and 12.2 ± 1.9 (48 h) fold compared to the control cells ($P<0.05$). In contrast to *CYP1A1* the basal level of *CYP1B1* mRNA was in a good detectable range in the experimental setup (Figure 12 B).

For both experiments, the differences between B[a]P and TCDD treatments as well as between both time-points, were not significant ($P>0.05$).

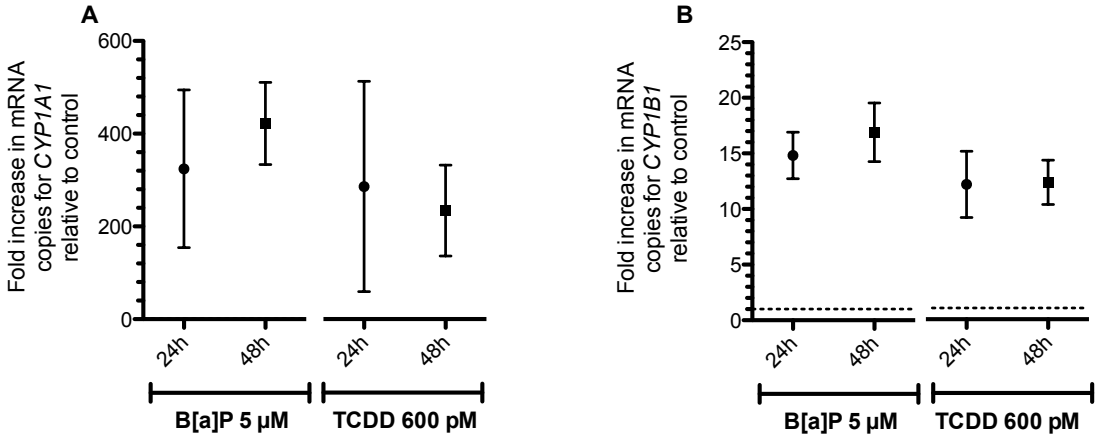

Figure 12: Fold increase of *CYP1A1* (A) and *CYP1B1* (B) mRNA copies in A549 alveolar type II epithelial cells. Cells were exposed to 5 µM of B[a]P or 600 pM TCDD for 24 h and 48 h. Cells treated with DMSO for the same time were used as control to which the results were normalized. Data represents the mean of three independent samples ± SEM. B[a]P and TCDD treatment lead to significant upregulation of *CYP1A1* (A) and *CYP1B1* (B) relatively compared to the control cells ($P<0.05$). The dotted line represents the level of expression in the control cells.

3.1.1.3. EROD ACTIVITY IN A549 CELLS

To determine CYP1A1 catalytic activity in A549 cells after treatment with B[a]P and TCDD, cells were incubated together with resorufinethylether and dicumarol [241]. The catalytic activity was recorded as a function of time for 60 min. However, no signal was detected for A549 cells in our experimental setup (data not shown).

3.1.1.4. PRODUCTION OF HISTAMINE IN HMC-1 MAST CELLS

The HMC-1 cell line is the only available human mast cell line and these cells were intensively studied in the past to describe their exact phenotype [265, 288-290]. However, as the production and intracellular storage of histamine is one of the major characteristics of mast cells the histamine production was evaluated using immunohistochemistry together with confocal microscopy.

HMC-1 cells were grown over night in LabTek-II chambers coated with poly-l-lysine to enhance the attachment. Afterwards cells were fixed permeabilized and stained for cellular membranes, nuclei and histamine. HMC-1 cells were found to produce large amounts of intracellularly stored histamine (Figure 13).

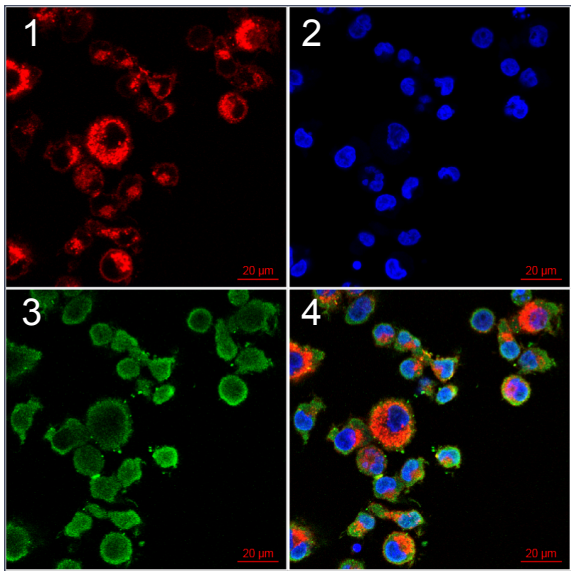

Figure 13: Immunohistochemistry staining of histamine in HMC-1 cells. HMC-1 cells were grown over night in LabTek-II chambers coated with poly-l-lysine. Afterwards cells were fixed, permeabilized and stained for cellular membranes, nuclei and histamine. **1:** membranes stained with cell mask deep red. **2:** Nuclei stained with DAPI. **3:** Histamine with anti-histamine antibody (1:200). **4:** Overlay.

3.1.1.5. Inducibility of *CYP1A1* and *CYP1B1* mRNA in HMC-1 mast cells

To evaluate the ability of HMC-1 mast cells to upregulate *CYP1A1* and *CYP1B1* mRNA, cells were exposed to 5 µM BaP and 600 pM TCDD (positive control) for 24 and 48 h. Afterwards the levels of *CYP1A1* and *CYP1B1* mRNA were evaluated using qRT-PCR.

The response of HMC-1 cells after 24 h of treatment with B[a]P and TCDD was almost identical (2.9 ± 0.3, respectively 2.2 ± 0.7 fold increase) but significantly increased compared to the DMSO-treated control cells ($P<0.05$). After 48 h of treatment HMC-1 cells showed the highest increase in *CYP1A1* mRNA expression for both, B[a]P and TCDD, with 7.0 ± 1.4, respectively 6.2 ± 0.7 fold relatively compared to the control (Figure 14 A). The longer exposure time significantly increased the amount of mRNA copies for *CYP1A1* for both treatments compared to the response after 24 h ($P<0.05$). The B[a]P and TCDD treatment produced almost identical responses in the HMC-1 cells.

In analogy to the experiments for *CYP1A1* (Figure 14 A) the expression levels of *CYP1B1* were evaluated under identical conditions. Compared to the findings for *CYP1A1* mRNA in HMC-1 cells *CYP1B1* mRNA was found to be poorly inducible. After 24 h of treatment to 5 µM B[a]P the, HMC-1 cells showed no difference relatively compared to the control cells (1.2 ± 0.3 fold) and after 48 h, there was a decrease in the expression of *CYP1B1* mRNA compared to the control cells (0.7 ± 0.1) (Figure 14 B) (not significant). The positive control (600 pM TCDD) had also only limited potential to induce the mRNA expression of *CYP1B1* in HMC-1 cells (24 h: 1 ± 0.2; 48 h: 1.2 ± 0.2) relatively compared to the control (Figure 14 B) (not significant).

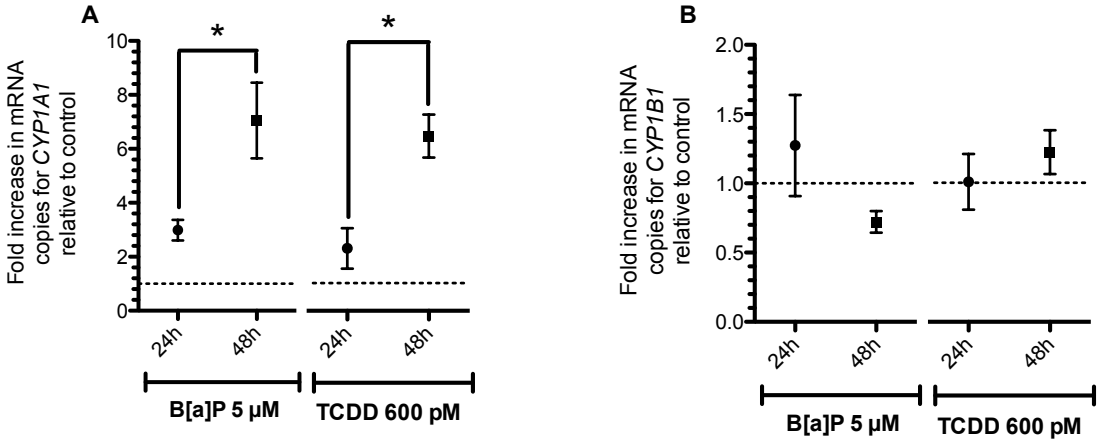

Figure 14: Fold increase of *CYP1A1* (A) and *CYP1B1* (B) mRNA copies in HMC-1 human mast cells. Cells were exposed to 5 µM of B[a]P or 600 pM TCDD for 24 h and 48 h. Cells treated with DMSO for the same time were used as control to which the results were normalized. Data represents the mean of three independent samples ± SEM.

B[a]P and TCDD treatment lead to significant upregulation of *CYP1A1* (A) relatively compared to the control cells ($P<0.05$). Asterisks indicate significant differences between different time-points ($P<0.05$). The level of *CYP1B1* mRNA (B) did not change significantly during the treatment ($P>0.05$). The dotted line represents the level of expression in the control cells.

3.1.1.6. DIFFERENTIATION OF THP-1 CELLS INTO MACROPHAGE-LIKE CELLS

In vivo, AMs contribute to defense and clearance of the alveoli from foreign material, such as bacteria, viruses and particulates. THP-1 cells are a well-known and well-characterized surrogate for dendritic-like cells *in vitro,* but they can also be differentiated into macrophage-like cells using agents such as vitamin D3 or PMA [264, 280]. The upregulation of the surface receptor CD11b was described as a marker for differentiated macrophages [264]. The expression of CD11b on the surface of THP-1 cells was verified by immunohistochemistry and confocal microscopy. THP-1 cells were differentiated over night with 20 ng/mL PMA in Labtek-II chambers or cultivated in the absence of PMA for the same time. Cells were fixed and stained for cellular membranes, nuclei and CD11b. THP-1 cells that were in contact with PMA attached stably to the cultureware (data not shown) and expressed CD11b on their surface (Figure 15 A). Undifferentiated THP-1 showed also a weak expression of CD11b. However, the signal for CD11b in the cells without PMA was found intracellularly and not co-localized within the cell membrane (Figure 15 A and B).

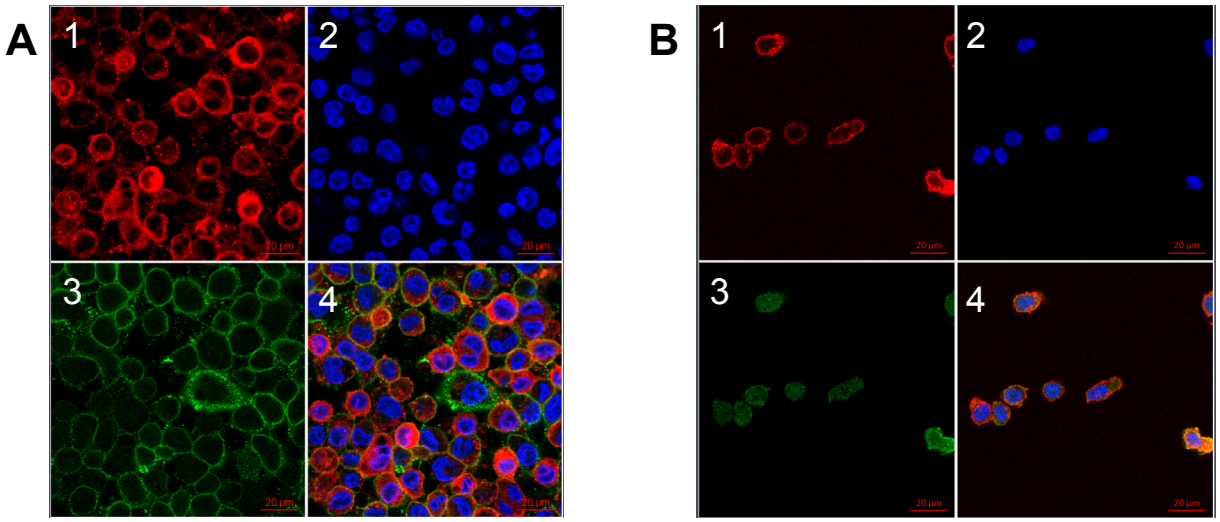

Figure 15: Immunohistochemistry staining of CD11b receptor of differentiated and undifferentiated THP-1 cells. THP-1 cells were differentiated over night with 20 ng/mL PMA in Labtek-II chambers (**A**) or cultivated in the absence of PMA for the same time (**B**). Afterwards, cells were fixed and stained for cellular membranes, nuclei and CD11b. **1:** membranes stained with cell mask deep red. **2:** Nuclei stained with DAPI. **3:** CD11b receptor with anit-CD11b antibody (1:200). **4:** Overlay.

3.1.1.7. Differences in the inducibility of *CYP1A1* and *CYP1B1* mRNA in THP-1 cells before and after PMA differentiation

To evaluate potential differences in the ability of THP-1 cells and their PMA-differentiated counterparts to upregulate *CYP1A1* and *CYP1B1* mRNA cells were exposed to 5 µM B[a]P and 600 pM TCDD (positive control) for 24 and 48 h. Afterwards the levels of *CYP1A1* and *CYP1B1* mRNA were evaluated using qRT-PCR.

Undifferentiated THP-1 cells showed very limited potential to upregulate *CYP1A1* mRNA after exposure to B[a]P or TCDD after 24 and 48 h and the results were almost identical with the results of the control cells that were treated with DMSO. There was no significant difference between B[a]P and TCDD treatments as well as between the evaluated time- (P>0.05) (Figure 16 A).

In analogy to the experiments for *CYP1A1* (Figure 16 A) the expression level of *CYP1B1* was evaluated under identical conditions. Compared to the findings for *CYP1A1* mRNA in THP-1 cells, *CYP1B1* mRNA was found to be also very little inducible for both, B[a]P and TCDD treatments compared to the control. There was no significant difference in the expression level after 24 and 48 h or between the treatments (Figure 16 B).

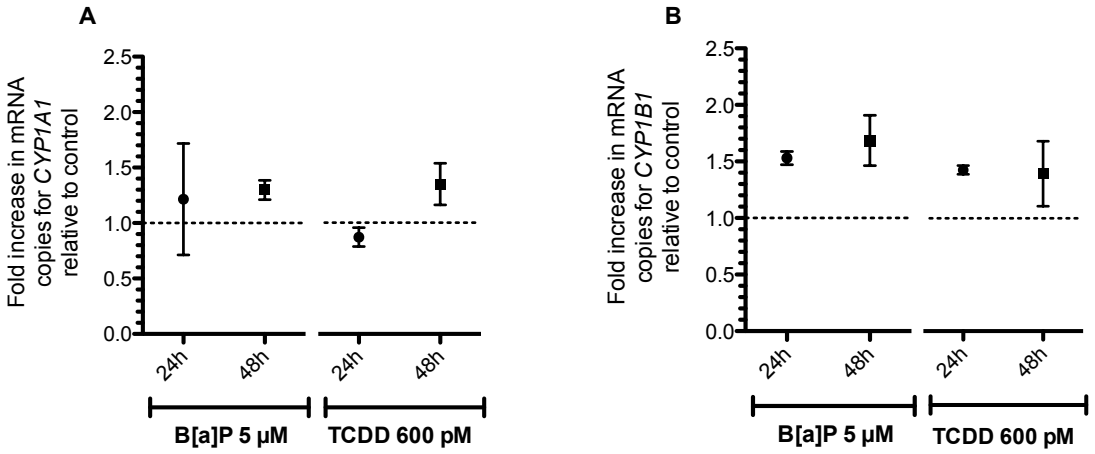

Figure 16: Fold increase of *CYP1A1* (A) and *CYP1B1* (B) mRNA copies in THP-1 cells. Cells were exposed to 5 µM of B[a]P or 600 pM TCDD for 24 h and 48 h. Cells treated with DMSO for the same time were used as control to which the results were normalized. Data represents the mean of three independent samples ± SEM. The levels of *CYP1A1* (A) and *CYP1B1* (B) did not change significantly during the experiments ($P>0.05$). The dotted line represents the level of expression in the control cells.

To evaluate the effect of the PMA differentiation on the potential of THP-1 cells to respond to the B[a]P and TCDD treatment with an upregulation of *CYP1A1* and *CYP1B1* mRNA, the experiment described above was repeated. Instead of normal THP-1 cells, THP-1 cells differentiated with 20 ng/mL PMA over night were used for the exposure and qRT-PCR experiments.

PMA-differentiated THP-1 cells showed an increased potential to respond to the treatment, compared to normal THP-1 cells (Figure 16 A and 17 A). In differentiated cells, the exposure

to 5 µM B[a]P lead to a significant increase of 3.3 ± 0.8 fold for *CYP1A1* mRNA after 24 h compared to the DMSO-treated control ($P<0.05$). The level of expression after 48 h was constant (3.7 ± 0.93 fold). Differentiated THP-1 cells exposed to 600 pM TCDD showed a decreasing response. After 24 h the increase for *CYP1A1* mRNA is similar compared to the B[a]P treatment (3.4 ± 1.4 fold). After 48 h, *CYP1A1* mRNA level was slightly lower (2.4 ± 0.5) (Figure 17 A). The differences between B[a]P and TCDD treatments were not significant.

The impact of the differentiation on the ability of THP-1 cells to respond to the treatment with *CYP1B1* mRNA induction was stronger compared to *CYP1A1*. After 24 h, B[a]P- and TCDD-treated cells showed a similar significant increase (3.5 ± 0.3, respectively 3.3 ± 0.5 fold) compared to control cells with DMSO ($P<0.05$). After 48 h of treatment, B[a]P and TCDD lead also to similar significant responses (7.2 ± 1.4, respectively 5.8 ± 1.2 fold) compared to the control ($P<0.05$). The differences between B[a]P and TCDD treatments were not significant.

Overall, differentiated THP-1 cells were found to be more responsive to both, the B[a]P and TCDD treatments.

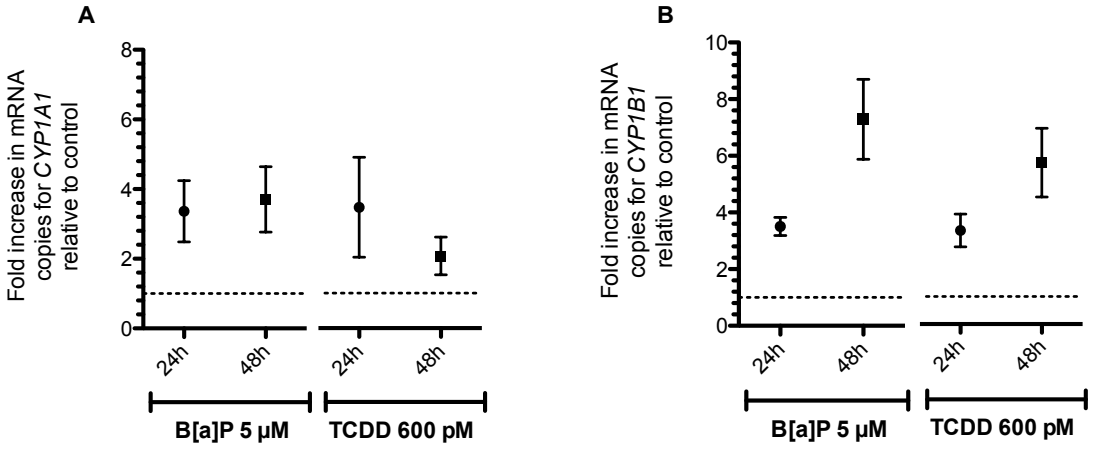

Figure 17: Fold increase of *CYP1A1* (A) and *CYP1B1* (B) mRNA copies in differentiated THP-1 cells. Differentiated cells were exposed to 5 µM of B[a]P or 600 pM TCDD for 24 h and 48 h. Cells treated with DMSO for the same time were used as control to which the results were normalized. Data represents the mean of three independent samples ± SEM. B[a]P treatment lead to significant upregulation of *CYP1A1* (A) relatively compared to the control cells (P<0.05). For *CYP1B1* mRNA both, B[a]P and TCDD treatment, lead to significant upregulation of *CYP1B1* (B) mRNA relatively compared to the control cells (P<0.05). The dotted line represents the level of expression in the control cells.

3.1.1.8. Inducibility of *CYP1A1* and *CYP1B1* mRNA in EA.hy 926 endothelial cells

To evaluate the ability of EA.hy 926 endothelial cells to upregulate *CYP1A1* and *CYP1B1* mRNA, cells were exposed to 5 µM BaP and 600 pM TCDD (positive control) for 24 and 48 h. Afterwards the levels of *CYP1A1* and *CYP1B1* mRNA were evaluated using qRT-PCR. The fold increase of *CYP1A1* mRNA in EA.hy 926 cells after 24 h treatment to B[a]P and TCDD was similar (4.4 ± 0.3, respectively 4.6 ± 0.2 fold) and significantly increased relatively compared to the DMSO-treated control (P<0.05). After 48 h the response remained constant for both treatments and showed no further increase compared to DMSO-treated cells (Figure 18). The differences between B[a]P and TCDD treatments were not significant (P>0.05).

The expression level of *CYP1B1* mRNA was not detectable in the experimental setup (data not shown).

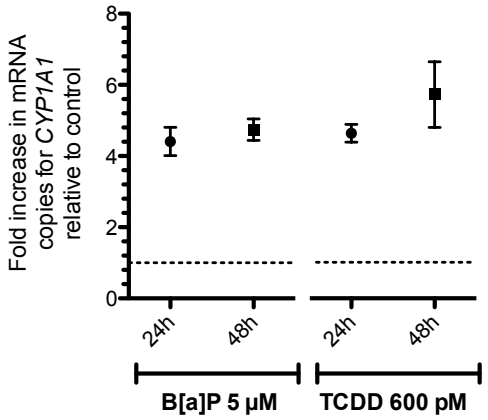

Figure 18: Fold increase of *CYP1A1* mRNA copies in EA.hy 926 endothelial cells. EA.hy 926 cells were exposed to 5 µM of B[a]P or 600 pM TCDD for 24 h and 48 h. Cells treated with DMSO for the same time were used as control to which the results were normalized. Data represents the mean of three independent samples ± SEM. B[a]P and TCDD treatment, lead to significant upregulation of *CYP1A1* mRNA relatively compared to the control cells ($P<0.05$). The dotted line represents the level of expression in the control cells.

3.1.2. STRUCTURE OF EPITHELIAL AND ENDOTHELIAL CELL LAYERS ON THE MICROPOROUS MEMBRANE

Transwell™ (1 µm pore size) inserts seeded with cells (A549 and EA.hy 926 in coculture) were stained with DAPI (blue) and cell mask deep red dye (red) and analyzed by CLSM. EA.hy 926 cells seeded on the basolateral side and A549 cells on the apical side of the Transwell™ did not show any evidence of multilayer formation and the cells were distributed in a confluent monolayer. EA.hy 926 endothelial cells on the basolateral side of the membrane seemed to cover a larger surface area compared to A549 cells and to have a flatter shape, while the A549 cell on the apical side appeared to be more cuboidal-shaped (Figure 19).

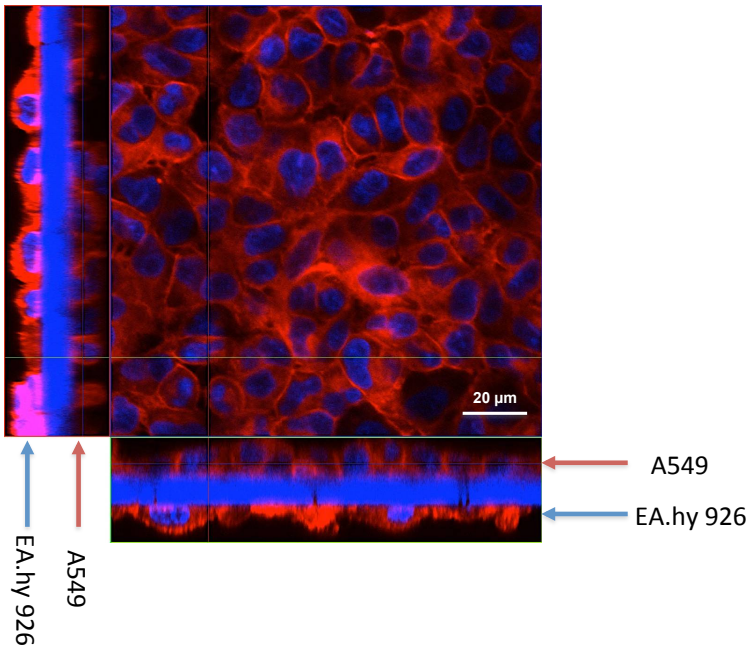

Figure 19: Z-stack image series to evaluate the distribution of A549 and EA.hy 926 cells on opposite sides of a Transwell™ insert. The cells form a closed monolayer on both sides of the 1 µm Transwell™ membrane. Cellular membranes are stained in red (cell mask deep red dye), nuclei in blue (DAPI). X–y projection with the respective side views (magnification: 630x).

3.1.3. Distribution of differentiated THP-1 cells and HMC-1 cells in the *in vitro* system

Differentiated macrophage-like THP-1 cells were seeded on top of A549 cells in Transwell™ inserts. Cells were allowed to attach for 24 hours and then stained and the membranes were mounted. Nuclei were stained with DAPI (blue), a fluorescent dye (red) specific for the plasma membrane and an antibody against CD11b (green) were used to highlight differentiated macrophages. The macrophage cells were triple positive showing a signal for DAPI, the plasma membrane and for CD11b. A549 cells did not express CD11b and a monolayer of cells can be observed (Figure 20 A). In submerged conditions, once in contact with the epithelial cells, the differentiated THP-1 cells tend to form small colonies on top of the epithelial cell layer (Figure 20 A and B). This effect was not observed in monocultures of THP-1 cells after differentiation.

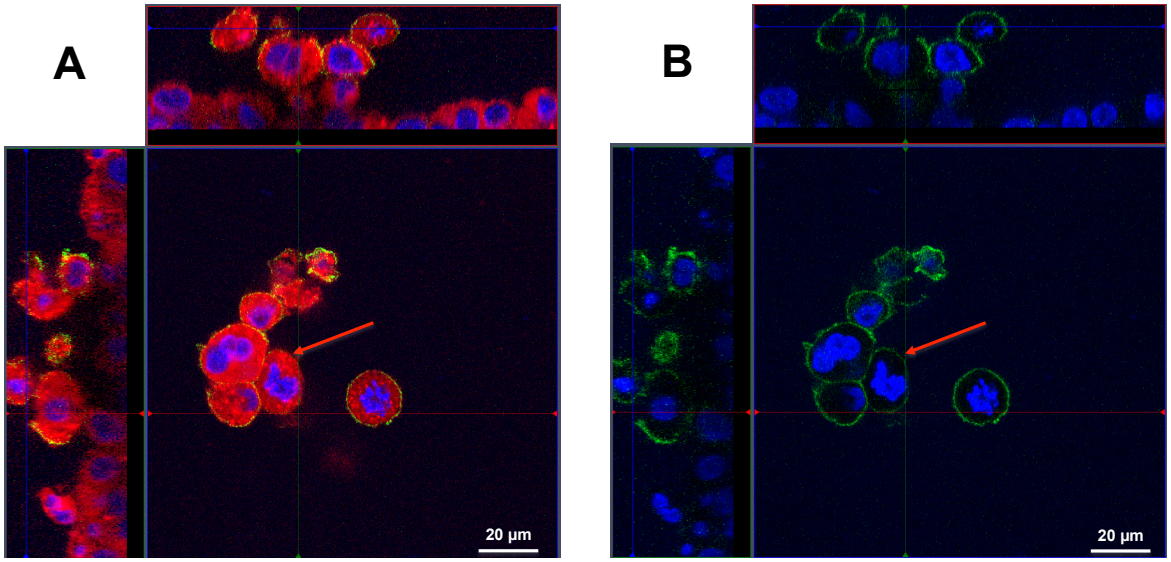

Figure 20: Colonies of differentiated THP-1 cells on top of epithelial A549 cells. A: Analysis of the distribution of THP-1 cells in the coculture system by a z-stack image series. THP-1 cells form colonies of several cells on top of A549 cells. THP-1 cells are stained with anti CD11b (green); nuclei are counterstained with DAPI (blue). X–y projection with the respective side views (magnification: 630x). **B:** Same image as shown in A but only with the channels for DAPI and CD11b. Red arrows indicate representative colonies (magnification: 200x).

A similar observation was made in the tetraculture system, composed of A549, differentiated THP-1, HMC-1, and EA.hy 926 cells. After seeding the HMC-1 cells into the tetraculture system, the originally floating HMC-1 cells disappeared from the culture medium and attached to the epithelial cell layer. The macrophage-like cells and mast cells can be found on top of the epithelial cells (Figure 21 A and B). THP-1 cells are in direct contact with HMC-1 cells and they form heterogeneous colonies (Figure 21 B).

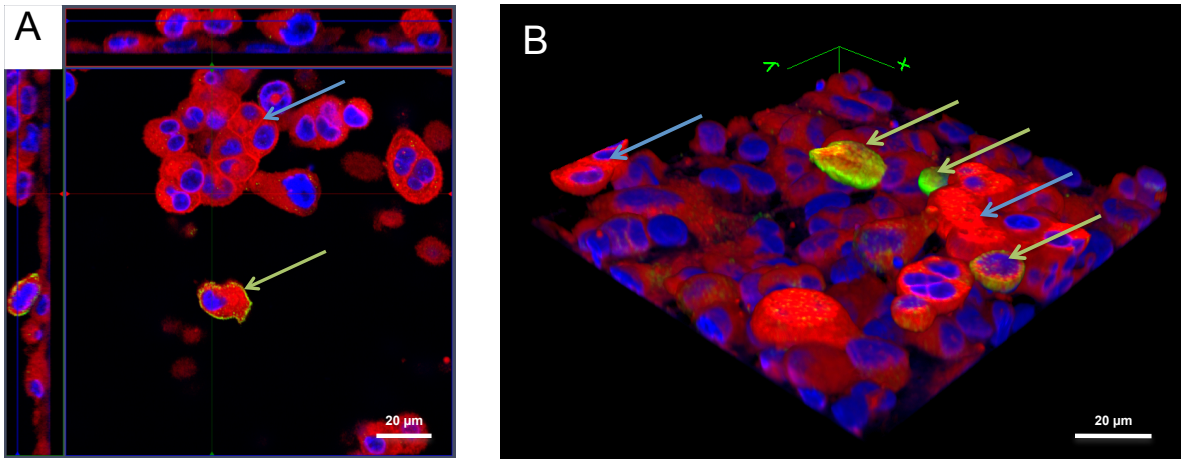

Figure 21: Z-stack image series to analyze the distribution of THP-1 macrophages and HMC-1 in the tetraculture system present in the apical compartment of the insert. The distribution of A549, differentiated THP-1, HMC-1 and EA.hy 926 cells in the tetraculture was analyzed via CLSM. Cellular membranes are stained with cell mask deep red dye (red) and nuclei are stained with DAPI (blue); Macrophage-like cells are counterstained with an anti-CD11b-antibody. **A:** X–y projection with the respective side views. **B:** 3D reconstruction of the tetraculture based on the results of the z-stack from A. THP-1 (green arrows) and HMC-1 (blue arrows) cells are found on top of the epithelial cells. EA.hy 926 cells were not considered in the 3D reconstruction.

However, once the system was shifted to ALI conditions, the colonies that were observed under submerged conditions disappeared and the cells spread more equally on top of the epithelial cells (Figure 22 A and B).

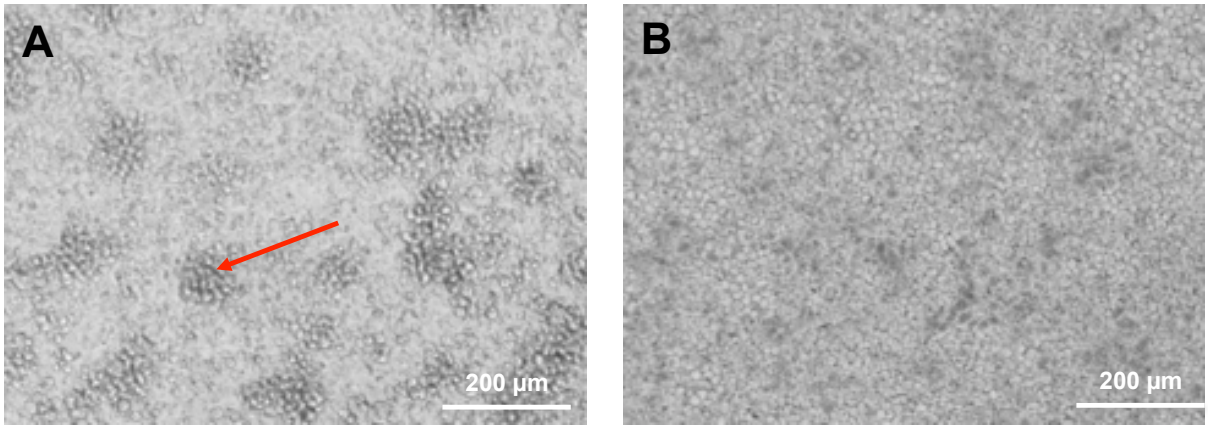

Figure 22: Colonies of differentiated THP-1 cells and HMC-1 cells on top of epithelial A549 cells. A: Brightfield image of THP-1 cells and HMC-1 that form colonies on top of A549 epithelial cells. The red arrow indicates a representative colony. **B:** same Transwell™ insert cultivated at the ALI without showing colonies. (Magnification: 200x).

3.1.4. BARRIER QUALITIES OF THE *IN VITRO* SYSTEM

A549 in monoculture, EA.hy 926 in monoculture, A549 plus EA.hy 926 in coculture and the tetraculture were exposed for 60 minutes to a sodium fluorescein tracer solution in the apical compartment and the fluorescence leakage was measured in the basolateral compartment as absolute fluorescence of sodium fluorescein. Inserts of different pore sizes (0.4, 1 and 3 µm) were compared as well (Figure 23 A, B and C). The 0.4 µm inserts showed a great ability to block the fluorescent tracer solution, regardless of the presence or absence of cells (Figure 23 A). In inserts with 1 and 3 µm pore size, the presence and the composition of the cell layers influences the amount of leaked fluorescence. The overall leakage in an empty 0.4 µm Transwell™ insert (w/o cells) was four times less compared to inserts with 1 and 3 µm pores (compare empty inserts in Figure 23 A, B, and C). For cell cultures prepared in 0.4 µm inserts, no statistical significant differences were observed (Figure 23 A). When 1 µm inserts were used, the monoculture of EA.hy 926 shows with 9103 ± 545 significantly the highest leakage (P<0.05). When A549 and EA.hy 926 cells were in coculture, the leakage (4944 ± 93) was slightly lower than in the A549 monoculture (5241 ± 161). In the tetraculture

system with A549, EA.hy 926, differentiated THP-1 and HMC-1 cells, the leakage was with 6339 ± 249 again higher than for the A549 monoculture and the coculture of A549 and EA.hy 926 but still significantly lower than for the monoculture of EA.hy 926 (P<0.05) (Figure 23 B). In Transwell™ inserts with 3 µm pores, the amount of leaked fluorescence for A549 monoculture was 4928 ± 57 and for EA.hy in monoculture 6134 ± 572. The coculture of A549 and EA.hy 926 cells showed a fluorescence leakage of 5250 ± 84. The differences between A549 and EA.hy 926 cells in monoculture and the corresponding coculture were not significant. In these inserts the tetraculture showed the highest amount of leaked fluorescence with 11584 ± 865 (Figure 23 C).

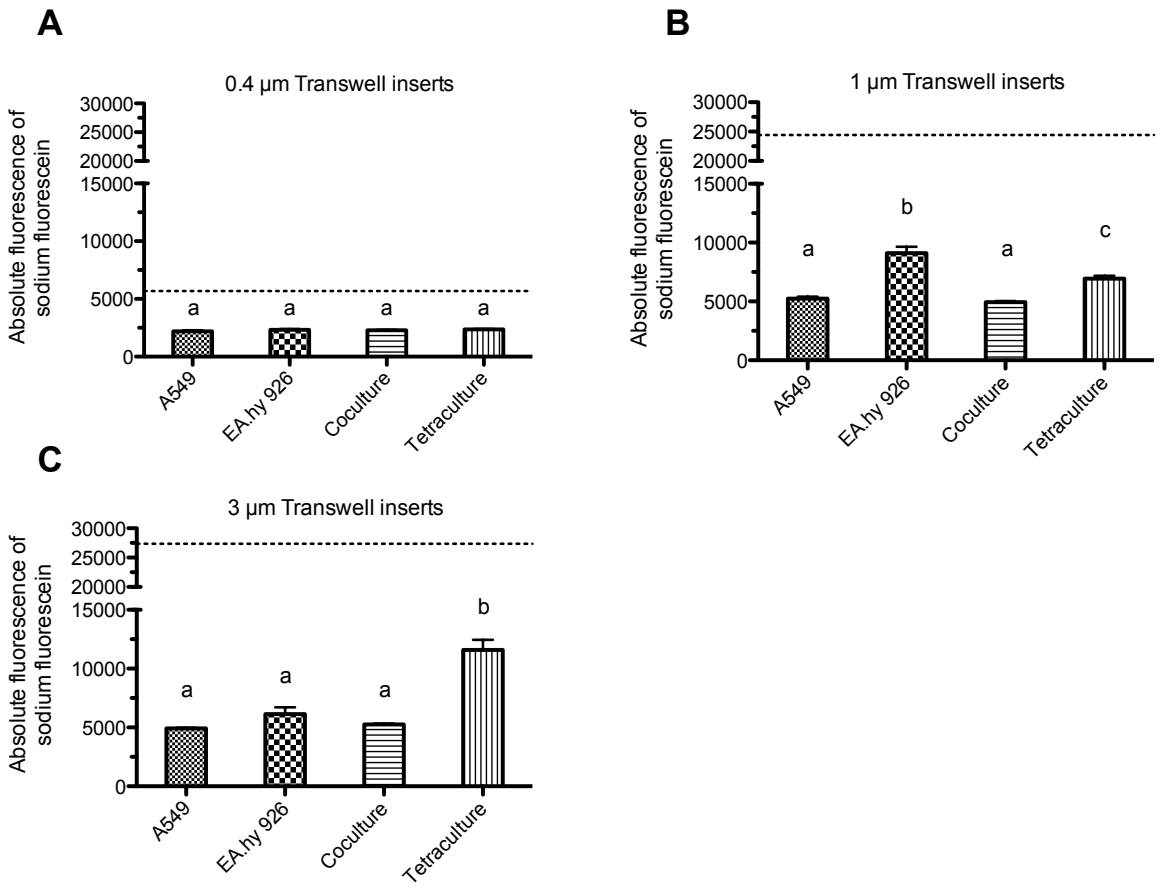

Figure 23: Sodium fluorescein leakage for mono-, co-, and tetraculture in Transwell™ inserts with 0.4, 1 and 3 µm pore size. Medium containing 1 mg/mL of sodium fluorescein was administered to the apical compartment. Medium w/o sodium fluorescein was administered to the basolateral compartment and the leaked fluorescence was measured after 60 minutes incubation at room temperature in the dark. Results obtained for inserts with a pore size of 0.4 µm, 1 µm and 3 µm are given in A, B and C respectively. Data represents the mean of four independent Transwell™ inserts ± SEM. Groups that are sharing the same letters are not significantly different (P>0.05).

The same phenomenon was observed when the accessibility of resazurin for cells grown in Transwell™ inserts of different pore sizes was evaluated. For cells cultivated in Transwell™ inserts with a pore size of 0.4 µm, resazurin on the opposite side of the membrane was not accessible for conversion. However, when Transwell™ inserts of 1 and 3 µm pore size were tested, the resazurin became accessible to the cells (Figure 24).

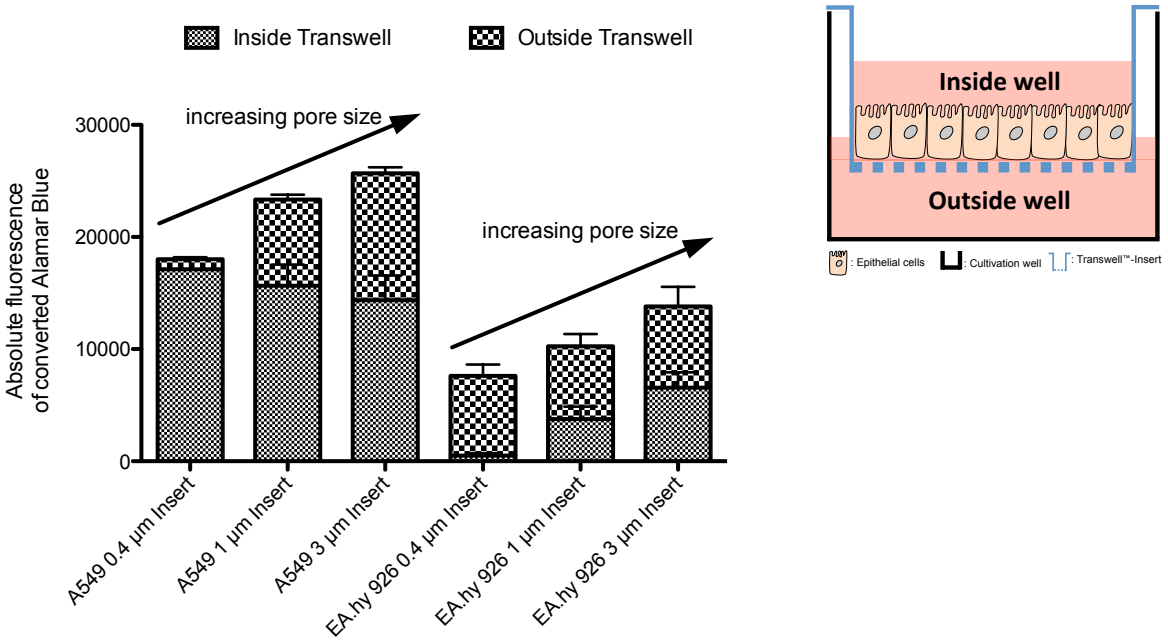

Figure 24: Accessibility of resazurin depends on the pore size of the membrane. Different cultures were exposed to cell culture medium containing 400 µM of resazurin. Both compartments, the apical and the basolateral, were filled with this solution. The conversion of resazurin on the opposite site of the cell layer was dependent on the pore size of the used Transwell™ inserts. Data represents the mean of two independent Transwell™ inserts ± SEM.

In parallel to the evaluation of the leaked fluorescence, the tightness of the epithelium was evaluated by measuring the transepithelial electrical resistance of A549 cells in monoculture (Figure 25), EA.hy 926 cells in monoculture (Figure 26), A549 cells and EA.hy 926 cells in coculture (Figure 27) and the tetraculture (Figure 28) in different Transwell™ inserts with 0.4, 1 and 3 µm pore size. None of the evaluated culture setups was able to produce a stable TEER value over the evaluated 10 days.

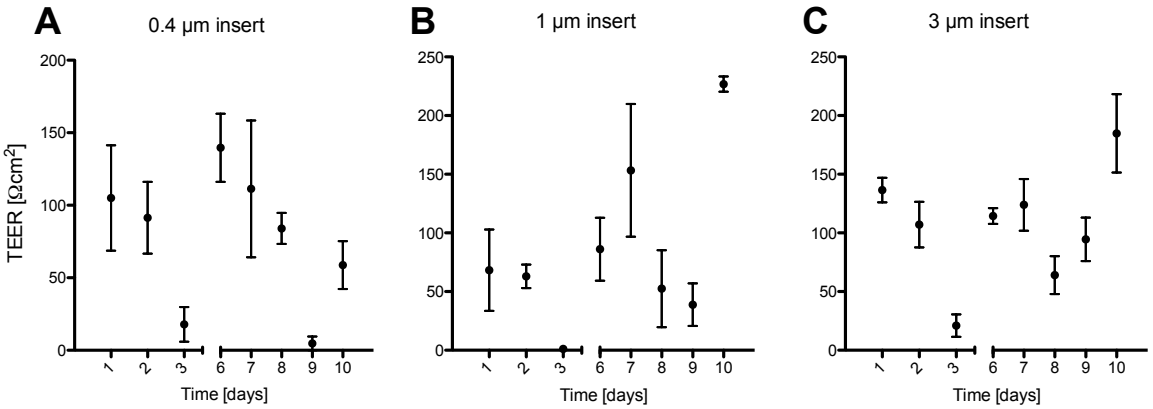

Figure 25: Transepithelial electrical resistance (TEER) of A549 cells grown in inserts of different pore sizes. Electrical resistance was measured to follow tightness of the cell layer. **A:** TEER measured in inserts with 0.4 µm pore size; **B:** TEER measured in inserts with 1 µm pore size; **C:** TEER measured in inserts with 3 µm pore size. Data represents the mean of two independent Transwell™ inserts ± SEM.

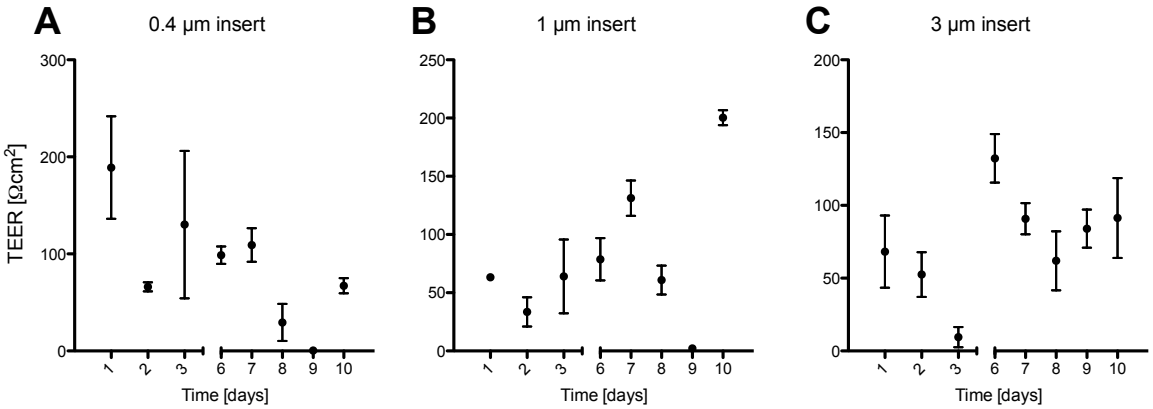

Figure 26: Transepithelial electrical resistance (TEER) of EA.hy 926 cells grown in inserts of different pore sizes. Electrical resistance was measured to follow tightness of the cell layer. **A:** TEER measured in inserts with 0.4 µm pore size; **B:** TEER measured in inserts with 1 µm pore size; **C:** TEER measured in inserts with 3 µm pore size. Data represents the mean of two independent Transwell™ inserts ± SEM.

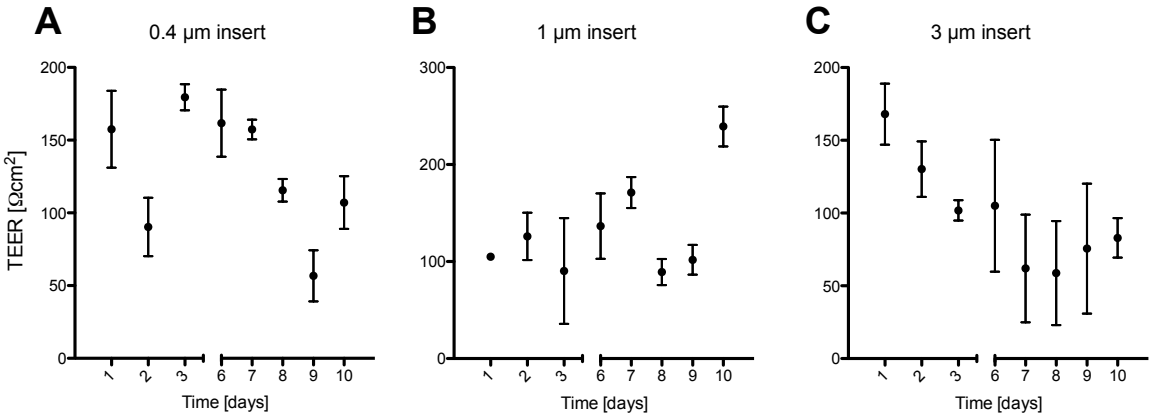

Figure 27: Transepithelial electrical resistance (TEER) of cocultures of A549 and EA.hy 926 cells grown in inserts of different pore sizes. Electrical resistance was measured to follow tightness of the cell layers. **A:** TEER measured in inserts with 0.4 µm pore size; **B:** TEER measured in inserts with 1 µm pore size; **C:** TEER measured in inserts with 3 µm pore size. Data represents the mean of two independent Transwell™ inserts ± SEM.

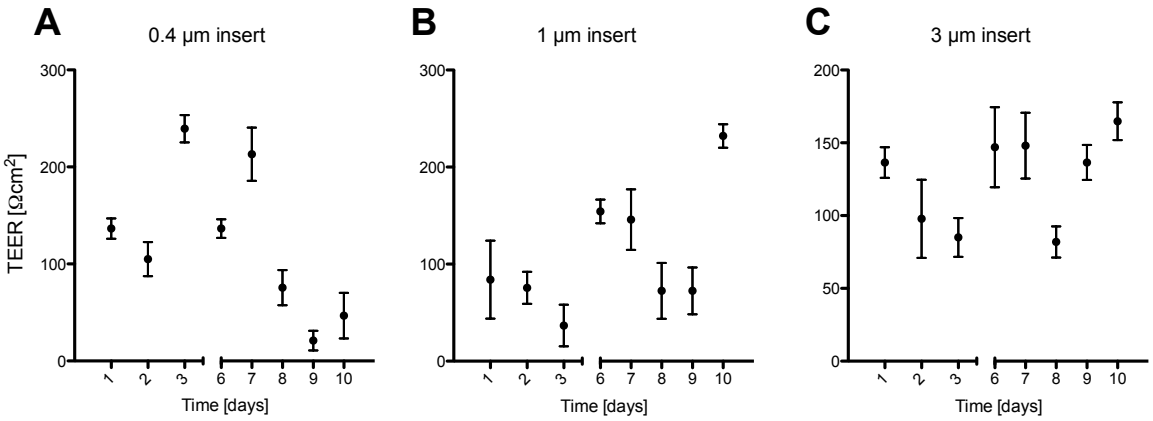

Figure 28: Transepithelial electrical resistance (TEER) of tetracultures of A549, EA.hy 926, THP-1 and HMC-1 cells grown in inserts of different pore sizes. Electrical resistance was measured to follow tightness of the cell layers. **A:** TEER measured in inserts with 0.4 µm pore size; **B:** TEER measured in inserts with 1 µm pore size; **C:** TEER measured in inserts with 3 µm pore size. Data represents the mean of two independent Transwell™ inserts ± SEM.

3.1.5. BEHAVIOR OF THE TETRACULTURE IN RESPONSE TO AN OXIDATIVE STRESS INDUCER

The production of ROS as a response to the exposure to small particulates is an important effect of particles and ROS production by particles has also been linked to their adverse effects on the cardiovascular system [160]. In order to investigate differences of the cultures in response to an oxidative stimulus, monocultures, cocultures, and tetracultures were exposed to 20 mM 2,2'-azobis-2-methyl-propanimidamide-dihydrochloride (AAPH) for 2 h after which the oxidation of the dye DCFH-DA as indicator of ROS production was measured. The differentiated THP-1 cells showed the highest fold increase in ROS production (30.9 ± 2.5; $P<0.05$) for all the cultures tested. Among the monocultures, the response of HMC-1 and EA.hy 926 cells was comparable with a fold increase of 18.6 ± 1.3, respectively 21.9 ± 2.9. A549 cells were cultivated at the ALI and under submerged conditions and then exposed to AAPH. The cells cultivated at the ALI showed the lowest fold increase of all tested monocultures (12.6 ± 1; $P<0.05$ when compared to EA.hy 926 and THP-1). The fold increase of ROS production for the coculture of A549 and EA.hy 926 cells at the ALI as well as the fold increase for the tetraculture at the ALI was comparable to the results obtained with A549 cells alone (Figure 29).

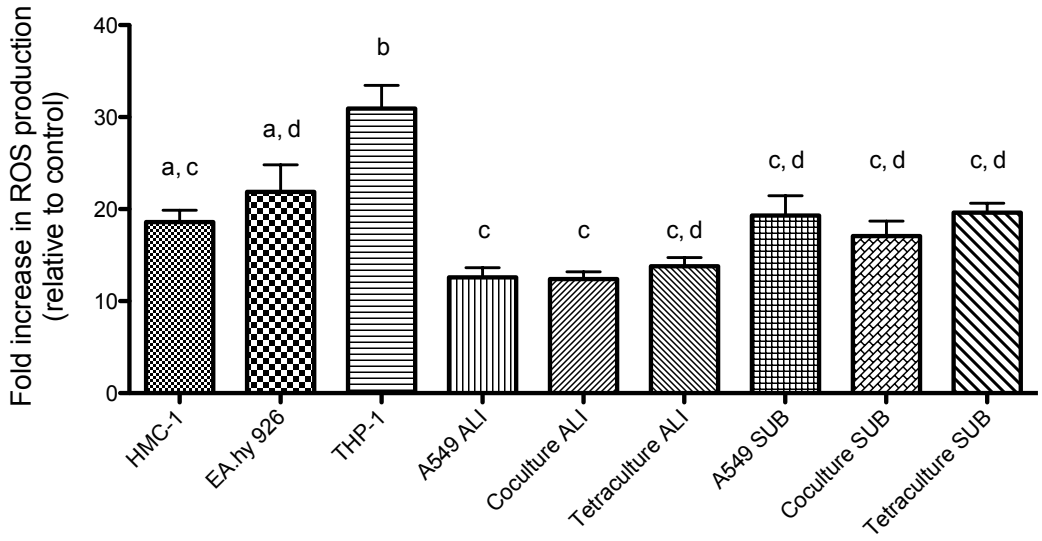

Figure 29: DCFH-DA assay to analyze the behavior of the different cultures in response to oxidative stress. Cultures were preloaded with DCFH-DA dye for 45 min and subsequently exposed to 20 mM AAPH in medium for 2 h. The oxidation of DCFH-DA was measured as an augmentation of green fluorescence. The increase of oxidative stress was compared to cells that were treated with medium without AAPH. Data represents the mean of at least four independent Transwell™ inserts ± SEM. Groups that are sharing the same letters are not significantly different (P>0.05).

3.1.6. SECRETION OF PRO-INFLAMMATORY CYTOKINES AFTER TREATMENT WITH AAPH

In vivo cells have the possibility to communicate and to influence each other. This crosstalk between cells also influences the production of mediators. Here the secretion of the pro-inflammatory cytokines IL-1$_\beta$, IL-6, GM-CSF, IL-8 and TNF-α was measured to evaluate possible differences in the cytokine production pattern between cultures in the acute phase after being treated with AAPH for 2 h. The levels of the cytokines were compared between A549 in monoculture, the coculture of A549 and EA.hy 926 cells and the tetraculture. In addition submerged and ALI culture were also compared.

Following exposure to 20 mM AAPH for 2 h A549 cells in monoculture secreted 124.7 ± 7.4 pg/mL when submerged and 168 ± 5.8 pg/mL IL-8 when cultivated at the ALI (n≥4). The results obtained for A549 cells alone were the lowest compared with the coculture and the

tetraculture (*P*<0.05). The coculture, cultivated under submerged conditions showed a significantly elevated IL-8 secretion of 588 ± 57 pg/mL, respectively 736 ± 88 pg/mL compared to the submerged counterpart (*P*<0.05). The response of the tetraculture at the ALI with 660 ± 57 pg/mL IL-8 was comparable to the response of the coculture. The tetraculture cultivated under submerged conditions showed the highest IL-8 levels with 1118 ± 66 pg/mL compared to all other cultures (*P*<0.05) (Figure 30).

The comparison between submerged culture and ALI culture showed that the IL-8 secretion was significantly increased for the tetraculture with almost a two-fold difference when compared to the submerged counterpart (*P*<0.05) (Figure 30). Levels for IL-1$_\beta$, IL-6 and GM-CSF were below the limit of detection (data not shown).

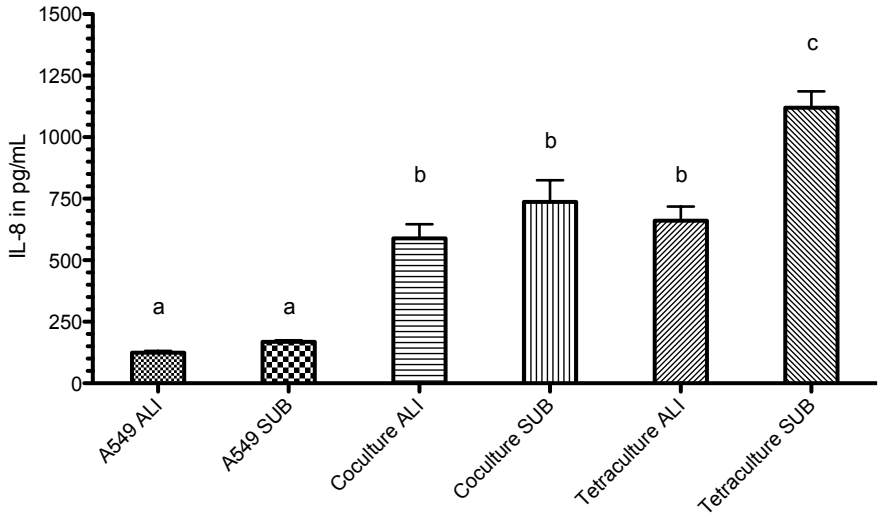

Figure 30: Evaluation of the secretion of IL-8 after treatment with AAPH. Cultures were exposed to 20 mM AAPH in medium for 2 h. Afterwards samples of the undernatant were collected and analyzed to evaluate the amount of secreted IL-8. Data represents the mean of at least four independent Transwell™ inserts ± SEM. Groups that are sharing the same letters are not significantly different (*P*>0.05).

3.1.7. CELL VIABILITY AFTER AEROSOL TREATMENT WITH THE VITROCELL™ EXPOSURE SYSTEM

The effect of exposure conditions present in the Vitrocell™ aerosol exposure system on cellular viability was evaluated by exposing different cell cultures to an aerosol of PBS and ambient sterile filtered air for 30 min. The cultures (A549 in monoculture, in coculture with EA.hy 926 cells and in tetraculture with EA.hy 926, THP-1 and HMC-1) were kept under ALI conditions in the incubator for 24 h and were then exposed. Immediately after exposure the integrity of the cell layers was verified by light microscopy and no visible alterations were observed (data not shown). Subsequently the cultures were placed back into the incubator and the cellular viability was measured 24 h later. Cell viability was compared to cultures under submerged conditions and cultures kept in the incubator at the ALI for 48 h (Figure 31). Compared to cells under submerged conditions, the viability was not significantly reduced for ALI cultures. No significant differences between cells exposed in the aerosol chamber and cells incubated at ALI conditions in the incubator were observed.

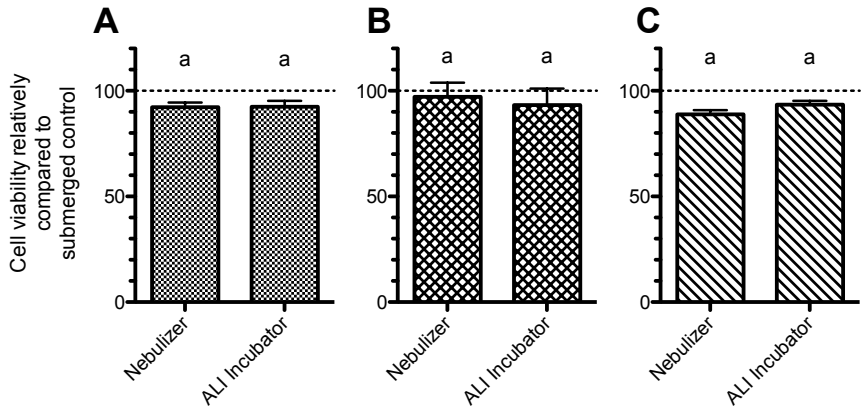

Figure 31: Viability of cultures exposed to an aerosol of PBS by using the Vitrocell™ aerosol exposure system. Cultures were exposed to an aerosol of PBS for 30 min using the Vitrocell™ aerosol exposure system. **A:** A549 monoculture; **B:** Coculture of A549 and EA.hy 926 cells; **C:** Tetraculture. The line represents the viability of cells kept under submerged conditions to which the ALI samples were compared. Data represent the mean of four independent Transwell™ inserts ± SEM. Groups that are sharing the same letters are not significantly different (P>0.05).

3.1.8. Behavior of macrophage-like cells in submerged exposure and at the air-liquid-interface

In vivo alveolar macrophages are efficiently intercepting particles and foreign materials in the alveolar region, contributing to clearance and defense of the alveolar region. The ability of the macrophage-like cells to intercept particles in the tetraculture was evaluated. The tetraculture was incubated for 24 h with 50 nm SiO_2-rhodamine particles suspended in tetraculture cell medium (10 mg/L) with 1% serum. Afterwards cells were fixed and stained with DAPI, cell mask deep red dye and CD11b and analyzed via CLSM. Signals for internalized SiO_2-Rhodamine NPs were detected inside of CD11b-positive macrophage-like THP-1 cells. In the A549 cell layer as well as in the HMC-1 cells no internalized SiO_2-Rhodamine NPs could be detected (Figure 32).

In analogous conditions to the submerged exposure tetracultures were exposed to an aerosol of PBS containing 50 nm SiO_2-rhodamine particles. The aerosol was generated by a pneumatic nebulizer (AGF 2.0 PALAS, Karlsruhe, Germany) and was delivered to the modules through a trumpet device at a flow rate of 5 ± 0.1 mL/min/module for a defined time of exposure (30 minutes). The concentration of the particle suspension in the reservoir of the AGF 2.0 nebulizer was 1 g/L.

After exposure, the cells were allowed to recover for 48 h before fixation and staining. Inserts were stained with DAPI, cell mask deep red dye and CD11b and analyzed via CLSM. Signals for internalized SiO_2-Rhodamine NPs were detected inside of CD11b-positive macrophage-like THP-1 cells only. In the A549 cell layer as well as in the HMC-1 cells and the endothelial layer (not shown), no internalized SiO_2-Rhodamine NPs could be detected (Figure 33 A, B and C).

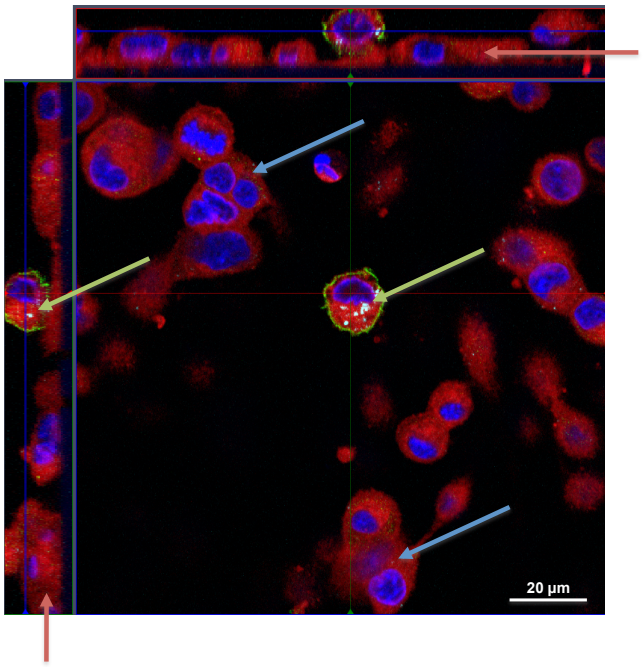

Figure 32: Z-stack image series to analyze the phagocytic activity of THP-1 macrophages in the triculture present in the apical compartment of the system. Tetracultures of A549, differentiated THP-1, HMC-1 and EA.hy 926 were exposed to cell culture medium containing 10 mg/L of 50 nm SiO_2-Rhodamine particles for 24 h. SiO_2-Rhodamine particles distribution was analyzed via CLSM. Cellular membranes are stained with cell mask deep red dye (red) and nuclei are stained with DAPI (blue). Macrophage cells are counterstained with an anti-CD11b-antibody (green). Fluorescence from ingested SiO_2-Rhodamine particles was detected in differentiated THP-1 cells situated on top of the A549 cells (green arrows) but not in A549 (red arrows) or HMC-1 (blue arrows). The image shows an x–y projection with the respective side views.

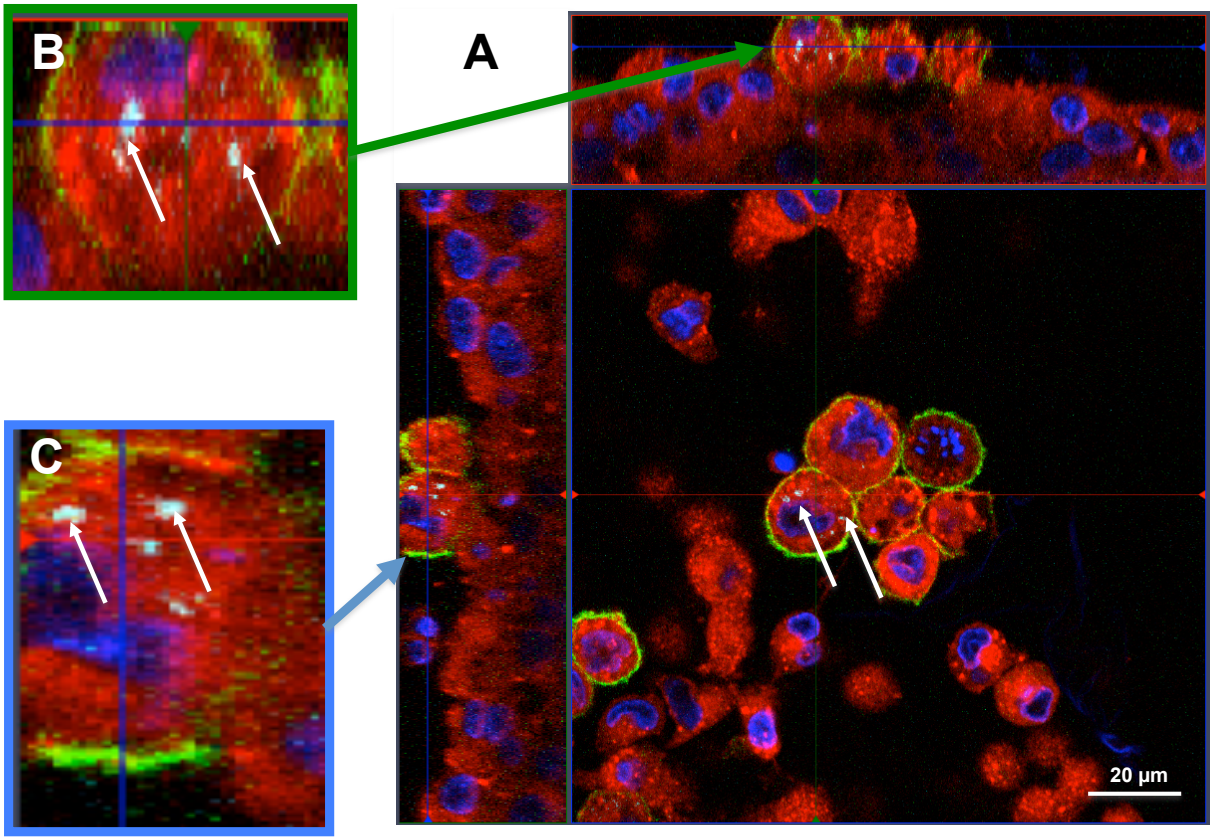

Figure 33: Z-stack image series to analyze the phagocytic activity of THP-1 macrophages in the triculture present in the apical compartment of the system after exposure to 50 nm SiO_2-Rhodamine nanoparticles with the Vitrocell™ system. Tetracultures of A549, differentiated THP-1, HMC-1 and EA.hy 926 exposed to an aerosol of 50 nm SiO_2-Rhodamine particles for 30 minutes using the Vitrocell™ aerosol exposure system. Afterwards cells were fixed, labeled and the distribution of SiO_2-Rhodamine particles was analyzed via CLSM. Cellular membranes stained with cell mask deep red dye (red) and nuclei with DAPI (blue) are shown. Macrophage cells are counterstained with an anti-CD11b-antibody. Signals of ingested SiO_2-Rhodamine particles were detected in differentiated THP-1 cells (white arrows), sitting on top of the A549 cells (blue arrows) but not in A549 or HMC-1 cells. **A:** The image shows an x–y projection with the respective side views. **B** and **C** show a macrophage cell from **A** in a higher magnification.

3.2. RESPONSE OF THE ENDOTHELIAL PART OF A 3D TETRACULTURE *IN VITRO* MODEL IN A DOSE-CONTROLLED EXPOSURE SCENARIO TO DIESEL EXHAUST PARTICULATE MATTER AT THE AIR-LIQUID-INTERFACE (ALI)

In this part of the PhD work, the results obtained after challenging the tetraculture *in vitro* system with native DEPM aerosol, using realistic doses, to study the response of the endothelium are presented. As a first step, it was necessary to validate and characterize the aerosol production with the PALAS steel-brush-generator provided from Vitrocell™.

3.2.1. DEPM AEROSOL CHARACTERISATION AND DOSIMETRY

In order to be able to study cellular responses in the tetraculture system under relevant conditions, a set of important values, such as particle counting and size distribution as well as particle deposition rates need to be evaluated.

3.2.1.1. PARTICLE COUNTING

Aerosols can be described by two main characteristics: particle size distribution and particle counting. In general, particle size distribution of ideal aerosols, e.g. an aerosol of nanoparticles can be described by a Gaussian distribution. Ideal aerosols consist of particles that differ only little in size, resulting in a very uniform size distribution. On the other hand, environmental aerosols, such as aerosols of DEPM, have in general particles, that are very different in size, ranging from a few nm to several µm in the aerodynamic diameter.

Here we analyzed the DEPM aerosol that was produced by the PALAS steel-brush-generator using a standard reference material from the national institute for standards and technology (NIST) (SRM2975). The particle generator was operated under the same conditions as for the exposure experiments with the cells: 1200 rpm brush speed and 30 mm/h piston speed. For the measurements, the exhaust tube of the particle generator was connected to a GRIMM laser spectrometer and particle sizes and counts were recorded for 1 minute.

The majority of the particles were below 500 nm in size and the smallest particle size, detectable by the laser spectrometer, was 250 nm. The upper size limit of the aerosol particles was around 2 µm, which is in line with the cutoff level defined for the cyclone (particle fractionizer) in the PALAS steel-brush-generator. Compared to a homogenous nanoparticle aerosol, the size distribution of the DEPM is quite heterogeneous with a big fraction of particles below 500 nm (Figure 34).

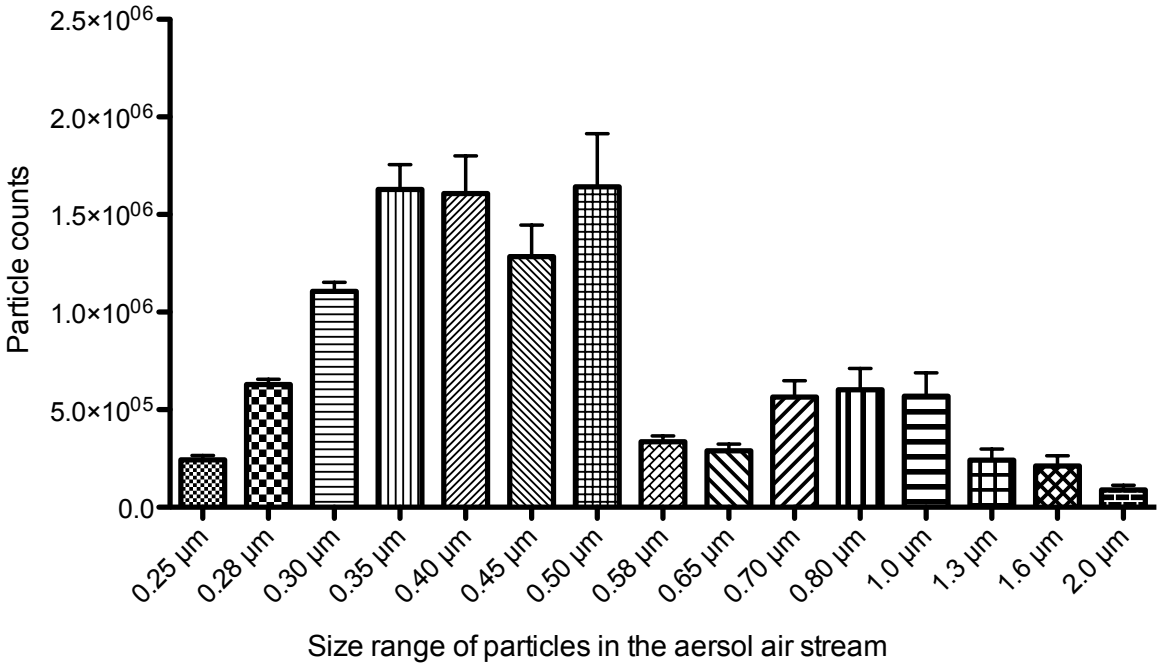

Figure 34: Size characterization of the DEPM aerosol that was produced with the PALAS aerosol generator and analyzed using a GRIMM laser spectrometer. Particle counts were registered for one minute with the rotating steel brush at 1200 rpm and the piston to deliver the diesel particles at 30 mm/h. Data represents the mean of three independent Transwell™ inserts ± SEM.

3.2.1.2. DOSIMETRY APPROACH FOR DEPM

In order to define a working range for the particle doses that should be used for the experiments, it was necessary to establish a method that allowed us to measure the deposited dose of DEPM per cm^2.

First experiments to establish a dosimetry approach that provides deposition rates in real-time were conducted with TiO_2 and should later on be transferred to DEPM.

For the evaluation of the deposition of particles per cm^2 in real-time, we used a quartz-microbalance system from Vitrocell™. The system uses an oscillating quartz crystal. The deposition of material on the surface of this crystal results in a change of the oscillation frequency, which can then be calculated by software into the mass that is deposited on top. The Vitrocell™ exposure system can be equipped with three of these balances allowing three independent real-time measurements at once. First experiments with TiO_2 nano powder gave repeatable results and uniform deposition curves for all three balances (Figure 35).

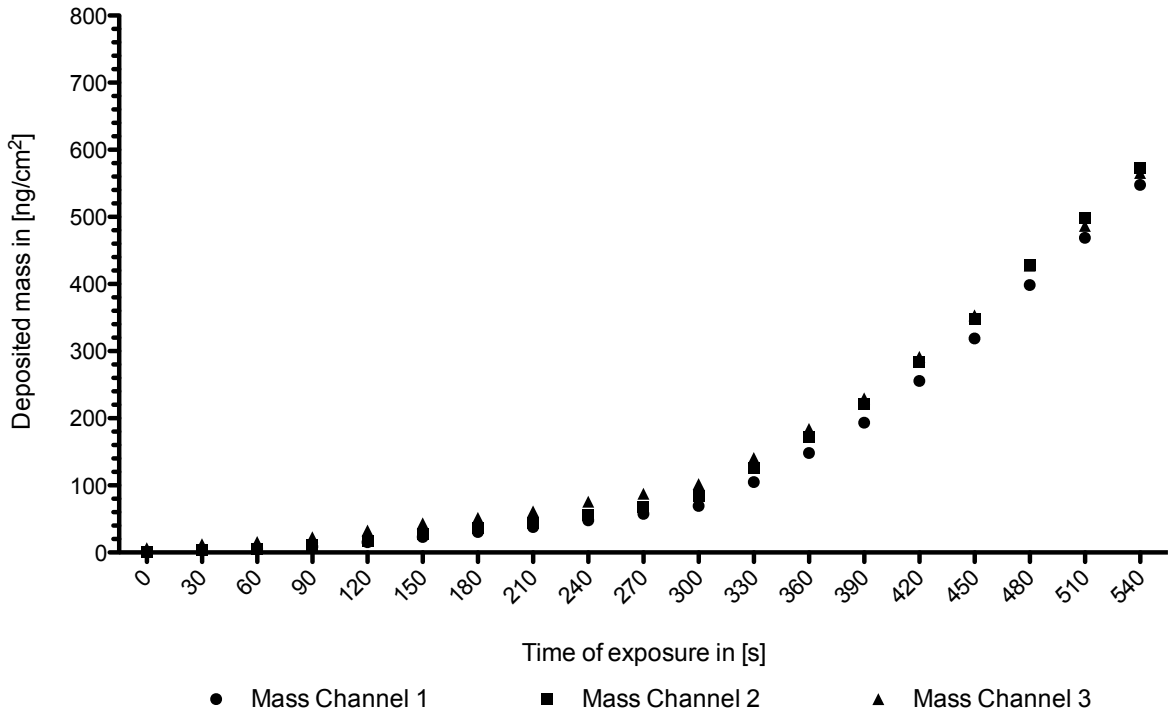

Figure 35: Performance of the quartz crystal microbalances from Vitrocell™ to detect particles deposited after aerosolition. Bulky titanium dioxide powder from sigma was used to create an aerosol with the PALAS aerosol generator to test the Vitrocell™ microbalances. Particle deposition was measured every 30 seconds for three independent channels corresponding to an independent Transwell™ each.

As a next step, dosimetry experiments were repeated by replacing the TiO_2 nano powder by the DEPM from NIST, with no other parameters changed. As a result, the balances from Vitrocell™ were not able to detect the DEPM deposited on top, even when changing the piston speed to the maximum. The crystal surface of the balances was found to be not compatible with the lightweight and electrostatically charged DEPM.

In order to be able to evaluate the particle dose per cm^2, we established an alternative method, based on the approach published by Rudd and Strom [291]. The method uses the absorption of DEPM at 750 nm.

To evaluate the amount of particles per cm^2, pre-wetted Transwell™ inserts were exposed for different times and subsequently washed with 200 µL of 0.1 N NaOH to collect all particles from the membrane. The absorption of these particles suspensions was then measured with a spectrophotometer and compared to a DEPM standard curve to calculate the amount of deposited particles.

Particle deposition for DEPM was found to be uniform for up to 20 min of exposure, resulting in a deposition maximum of 600 ng/cm^2 (Figure 36). The results were used to extrapolate the exposure times needed to expose tetracultures to 40, 80 and 240 ng/cm^2 of DEPM. These particle doses can be considered to be of relevance for a realistic exposure scenario.

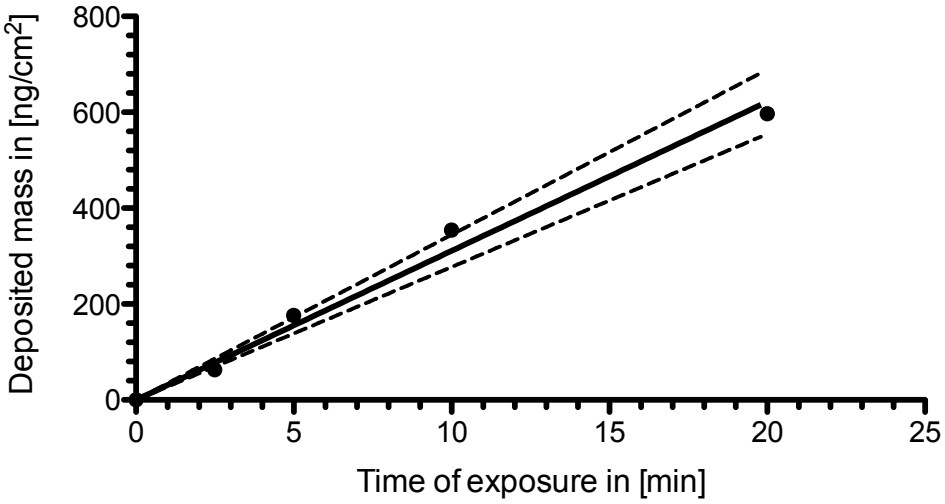

Figure 36: An alternative way to evaluate the deposited amount of DEPM per cm² in a Transwell™ insert based on the method published by Rudd and Strom [291]. Diesel particles were found to be of high electrostatical charge and to be too light for being registered by the microbalances from Vitrocell™. In order to correctly determine the deposited mass per cm², empty Transwell™ inserts were pre-wetted using 0.1 N NaOH and then exposed for different times using the aerosol system. Afterwards inserts were washed with 200 µL of 0.1 N NaOH and the absorbance of the suspended particles was measured at 750 nm. A standard curve was used to calculate the amount of particles deposited in the Transwell™ inserts.

In order to make a statement about the homogeneity of the distribution of the deposited material, Transwell™ inserts were exposed under the same conditions as described above and analyzed by scanning electron microscopy (SEM).

Regarding the results obtained with the GRIMM laser spectrometer (Figure 35), the SEM data also showed a heterogeneous size distribution with some bigger agglomerates (Figure 37, red arrows) and a big population of small particles. There was a clear tendency for the DEPM to form agglomerates when increasing the time of exposure (Figure 37). Overall, the distribution of DEPM was uniform for all three exposure times: 1 min 8 s for 40 ng/cm², 2 min 17 s for 80 ng/cm² and 6 min 52 s for 240 ng/cm².

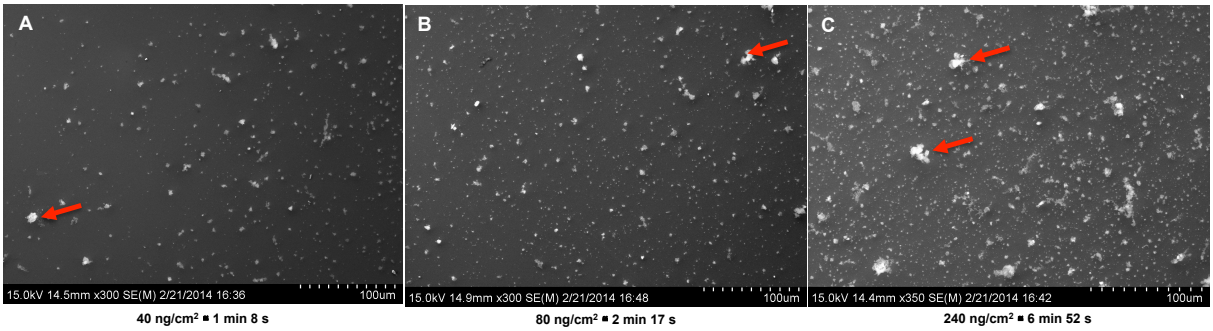

Figure 37: Scanning electron microscopy micrographs of Transwell™ inserts after exposure to DEPM aerosol using the PALAS steel-brush generator. Empty Transwell™ inserts were pre-wetted using 0.1 N NaOH and then exposed for different times using the aerosol system. Afterwards inserts were analyzed via SEM.

A: Transwell™ insert exposed to 40 ng/cm^2: At the lowest dose, DEPM form only few agglomerates (red arrow). **B: Transwell™ insert exposed to 80 ng/cm^2:** At the medium dose, DEPM have the tendency to form agglomerates (red arrow), but the surface of the membrane is still covered by a uniform layer of small particles. **C: Transwell™ insert exposed to 240 ng/cm^2:** At the highest dose DEPM were also found to form bigger agglomerates. This image is a good example to illustrate the heterogeneity of the DEPM aerosol, which is results in the deposition of particles that are very different in size, ranging from a few nanometers to several micrometers.

3.2.1.3. PRESENCE OF HEAVY METALS ON TOP OF DEPM ANALYZED BY NANOSIMS

With the SRM2975, NIST provides a well-characterized reference material. Even though in their datasheet they addressed a lot of parameters, such as size distribution, PAHs content, etc. data about the content of heavy metals are missing. Heavy metals are known to be an important source for oxidative stress in cellular systems and environmental PM was found to carry heavy metals on their outer shell.

In this experiment, DEPM samples were analyzed by using the NanoSIMS approach. This secondary ion mass spectrometer offers the possibility to visualize the heavy metal content of the DEPM samples, showing also potential hotspots on the outer shell of the particles.

DEPM samples were analyzed for the presence of the heavy metals nickel (Ni), copper (Cu), chromium (Cr) and zinc (Zn). Phosphorus was used as reference element to draft the shape of the particles (Figure 38). The results of the experiment can be visualized as color-coded images with a logarithmic scale, ranging from black for the lowest intensity to red for the highest signal (on the right hand of the Figure 38). DEPM from NIST was found to carry only low amounts of chromium. All other heavy metals were below the limit of detection.

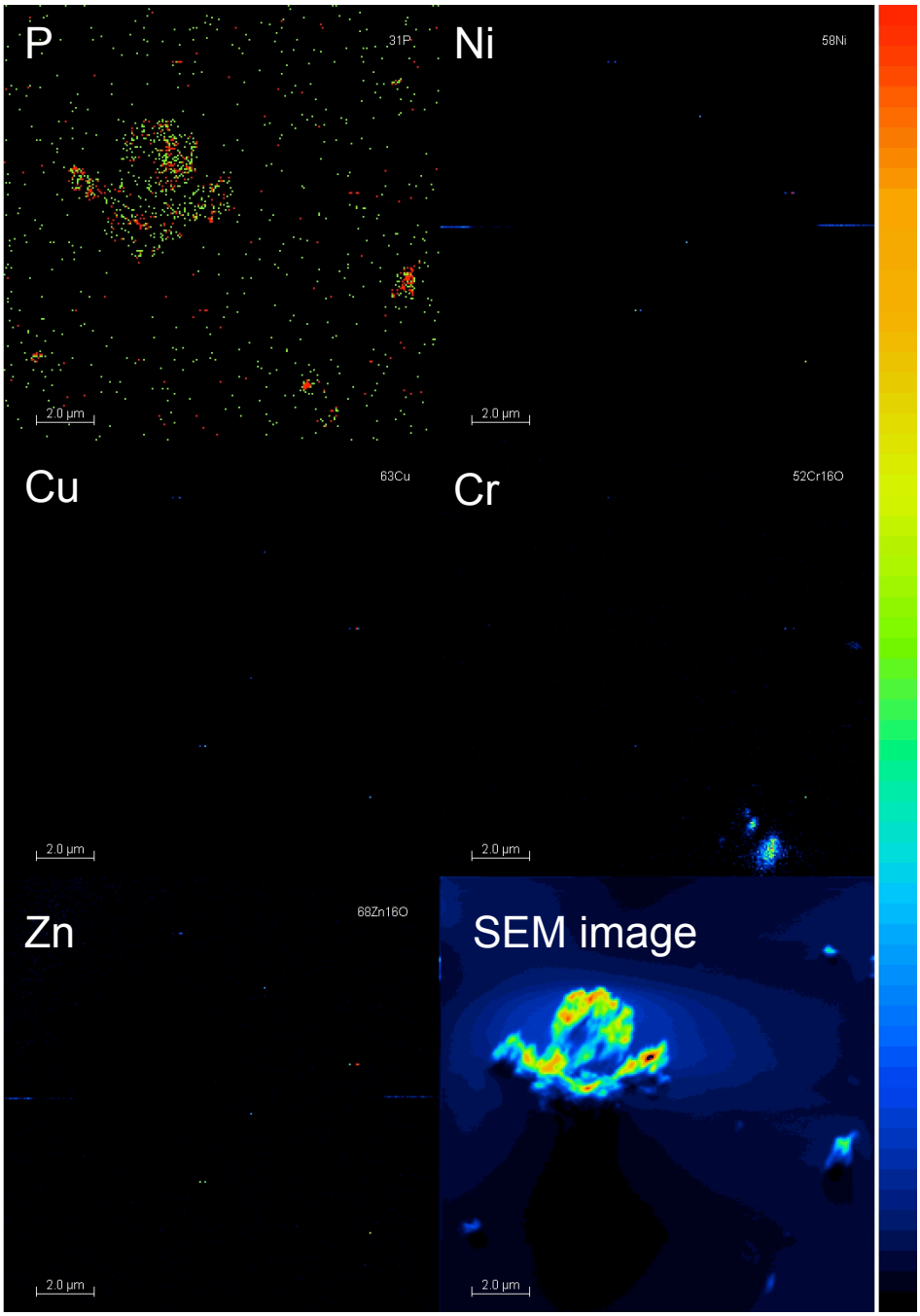

Figure 38: Distribution of heavy metals on the outer shell of DEPM analyzed by NanoSIMS. DEPM samples were analyzed for the presence of the heavy metals nickel (Ni), copper (Cu), chromium (Cr) and zinc (Zn). Phosphorus (P) was used as reference to draft an image of the outer shell of the particle. The relative amounts of the elements are presented as intensities with a logarithmic scale from black (lowest) to red (highest) (on the right hand of the figure).

DEPM from NIST was found to carry only low amounts of chromium. All other heavy metals were below the limit of detection.

3.2.2. INFLUENCE OF RELEVANT DOSES OF DEPM ON THE CELLULAR VIABILITY

Cellular viability is an important parameter for the evaluation of the hazard potential of environmental particles. Dependent on their chemical composition, DEPM affects cellular viability, which is supported by a growing body of evidence from literature. However, the majority of these studies were conducted by using highly concentrated extracts from DEPM (up to 1 mg/mL), which is far beyond the *in vivo* relevant range.

In this experiment, tetracultures were exposed to different doses of DEPM by using the Vitrocell™ aerosol exposure system. The doses were chosen following the considerations given in the materials and methods part about *in vitro* relevant doses for the exposure of cells to aerosolized particles. In respect to this, it was decided to choose 40 and 80 ng/cm^2 as particle doses that could be aspirated during a single day in polluted areas and 240 ng/cm^2 as a subchronic extreme exposure scenario.

The viability of the tetracultures that were exposed to the different doses of DEPM was evaluated at 6, 24 and 48 h after exposure. Tetracultures that were kept in the aerosol chamber for the same exposure time but with the particle generator in standby mode served as control. DEPM were not significantly affecting the viability of the tetracultures compared to the control cells at any of the evaluated time-points (Figure 39).

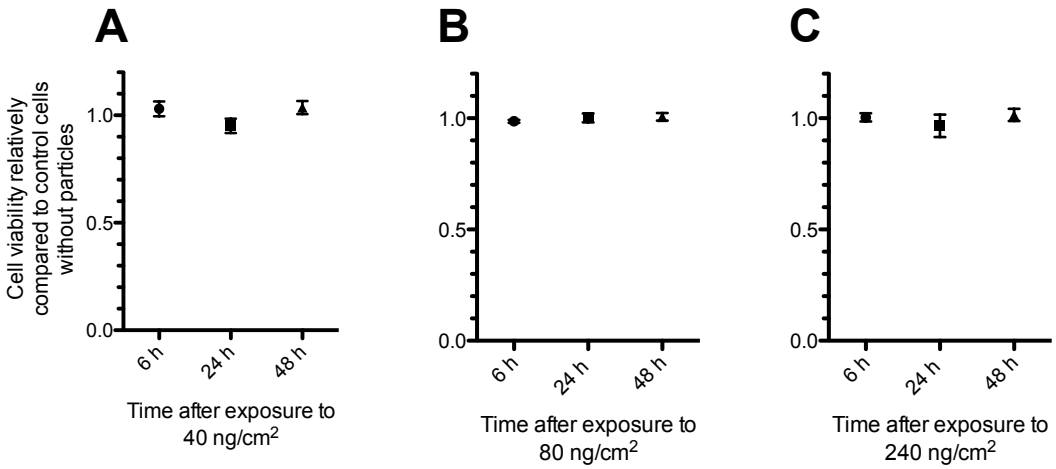

Figure 39: Impact of the exposure to different amounts of DEPM on the cellular viability of the tetraculture at different time-points after exposure. Tetracultures were exposed to 40 ng/cm^2 (**A**), 80 ng/cm^2 (**B**) or 240 ng/cm^2 (**C**) of DEPM. The viability of the tetracultures was evaluated at 6, 24 and 48 h after exposure. Tetracultures that were kept in the aerosol chamber for the same exposure time but with the particle generator in stand-by mode served as control. DEPM were not significantly affecting the viability of the tetracultures compared to the control cells at any of the evaluated time-points. Data represents the mean of three independent Transwell™ inserts ± standard error of mean.

3.2.3. PRO-INFLAMMATORY EFFECTS OF LOW DOSES OF DEPM ON THE ENDOTHELIAL PART OF THE TETRACULTURE

In the framework of the *hierarchical oxidative stress response* the elicitation of an inflammatory reaction is an important indicator for *tier 2.* In this experiment the potential of *in vivo* relevant DEPM doses to trigger an inflammatory response, shifting cellular response potentially towards *tier 2* of the *hierarchical oxidative stress response* was evaluated. In literature, several marker genes were described that can serve as indicators of early endothelial inflammation. In general, these genes are upregulated and become detectable before the secretion of second messengers. Among these genes, it was decided to use the three surface adhesion molecules *ICAM-1*, *VCAM1* and *E-Selectin*, which are important for the recruitment of immune cells from the blood into the inflamed tissue [175, 292, 293]. In

addition, the upregulation of the second messenger *IL-6*, which is also a marker for an emerging endothelial inflammation and the transcription factor NF_kB, which is involved in the regulation of inflammation, was analyzed.

Tetracultures were exposed to 80 ng/cm^2 or 240 ng/cm^2 of diesel exhaust particles. Total mRNA of the endothelial cells of the tetracultures was sampled at 6, 24 and 48 h after exposure, reversely transcribed and analyzed via qRT-PCR. Tetracultures that were kept in the aerosol chamber for the same exposure time but with the particle generator in stand-by mode served as control.

For the target genes *ICAM-1* and *IL-6* there was no difference compared to the control cells. *VCAM1* and *E-Selectin* were below the limit of detection under assay conditions in the exposed and the control samples (Table 6).

Table 6: Impact of the exposure to different amounts of DEPM on the expression level of relevant marker genes for endothelial inflammation in the endothelial part of the tetraculture system at different time-points after exposure to DEPM.

Tetracultures were exposed to 80 ng/cm^2 or 240 ng/cm^2 of DEPM. Total mRNA of the endothelial cells of the tetracultures was sampled at 6, 24 and 48 h after exposure, reversely transcribed and analyzed via qRT-PCR. Tetracultures that were kept in the aerosol chamber for the same exposure time but with the particle generator in stand-by mode served as control. The expression levels of *VCAM1* and *E-Selectin* were not detectable under assay conditions, using 1 µg of isolated mRNA for reverse transcription.

Data represent the mean of at least four independent samples ± SEM. Results were normalized to the level of expression of the control cells.

	80 ng/cm^2			240 ng/cm^2		
Gene	**6h**	**24h**	**48h**	**6h**	**24h**	**48h**
ICAM-1	0,93 ± 0,07	0,86 ± 0,03	0,93 ± 0,04	0,83 ± 0,06	0,83 ± 0,06	1,14 ± 0,17
VCAM1	**Not detecable under assay conditions**			**Not detecable under assay conditions**		
E-SELECTIN	**Not detecable under assay conditions**			**Not detecable under assay conditions**		
IL-6	0,93 ± 0,13	0,94 ± 0,15	0,93 ± 0,24	0,76 ± 0,06	0,96 ± 0,11	0,79 ± 0,07

For the transcription factor *NF$_k$B,* no increase could be detected for the cells exposed to 80 ng/cm^2 of DEPM (Figure 40 A). 48 h after the exposure to 240 ng/cm^2, the expression of *NF$_k$B* was slightly (1.2 ± 0.07), but significantly increased compared to the other time-points (P<0.05) (Figure 40 B).

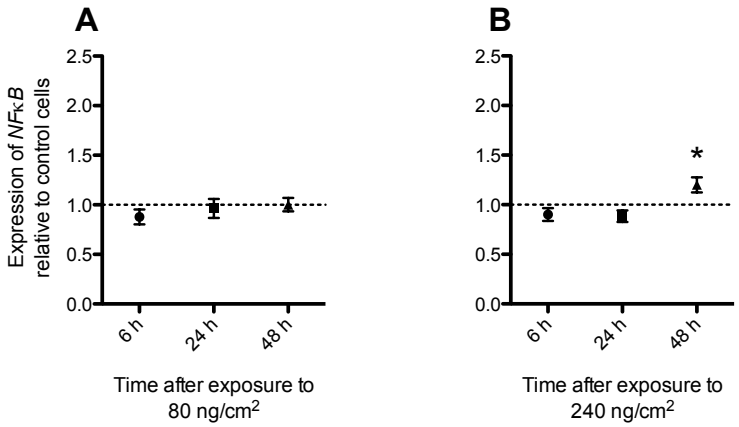

Figure 40: Impact of the exposure to different amounts of DEPM on the expression level of *NF$_k$B* in the endothelial part of the tetraculture system at different time-points after exposure to DEPM. Tetracultures were exposed to 80 ng/cm^2 (**A**) or 240 ng/cm^2 (**B**) of DEPM. Total mRNA of the endothelial cells of the tetracultures was sampled at 6, 24 and 48 h after exposure, reversely transcribed and analyzed via qRT-PCR. Tetracultures that were kept in the aerosol chamber for the same exposure time but with the particle generator in stand-by mode served as control.
Data represents the mean of at least four independent samples ± SEM. Asterisks indicate significant differences between the evaluated time-points (P<0.05). The dotted line indicates the level of expression of the control cells to which the results were normalized.

To confirm the results obtained for the qRT-PCR experiment, we evaluated the potential secretion of second messengers in the undernatant of the tetracultures. The tetracultures were exposed 80 ng/cm^2 or 240 ng/cm^2 of diesel exhaust particles. Aliquots of the undernatant were taken at 6, 24 and 48 h after exposure and stored upon analysis at -80 °C. The levels of secreted second messengers were evaluated using a multiplexed assay from MSD for pro-inflammatory cytokines, cytokines and chemokines. Tetracultures that were kept in the aerosol chamber for the same exposure time but with the particle generator in standby mode served as control. No significant increase in the production of pro-inflammatory cytokines, cytokines or chemokines could be observed (Table 7).

Table 7: Secretion of second messengers after exposure to different doses of DEPM at different time-points after exposure. Tetracultures were exposed 80 ng/cm^2 or 240 ng/cm^2 of diesel exhaust particles. Aliquots of the undernatant were taken at 6, 24 and 48 h after exposure and stored upon analysis at -80 °C. The level of secreted second messengers was evaluated using a multiplexed assay from MSD for pro-inflammatory cytokines **(A)**, cytokines **(B)** and chemokines **(C)**. Tetracultures that were kept in the aerosol chamber for the same exposure time but with the particle generator in stand-by mode served as control. Data represents the mean of at least four independent Transwell™ inserts ± SEM.

A **pro-inflammatory cytokines panel**

Cytokine		80 ng/cm^2 6h	80 ng/cm^2 24h	80 ng/cm^2 48h	240 ng/cm^2 6h	240 ng/cm^2 24h	240 ng/cm^2 48h
IFN-γ	*control*	7,5 ± 2,6	8,2 ± 2,4	8,8 ± 3,4	4,2 ± 0,9	8,1 ± 2,5	9,0 ± 3,9
	exposed	4,9 ± 2,7	8,5 ± 3,4	14,0 ± 3,7	2,9 ± 1,1	5,6 ± 1,7	10,1 ± 3,7
IL-10	*control*	3,9 ± 1,4	10,0 ± 5,7	6,3 ± 2,9	2,7 ± 1,0	7,0 ± 2,3	7,7 ± 4,0
	exposed	4,5 ± 1,3	5,3 ± 2,0	8,4 ± 2,8	3,2 ± 0,5	3,9 ± 1,4	6,6 ± 2,6
IL-12p70	*control*	3,2 ± 0,8	3,5 ± 0,9	5,0 ± 1,1	1,2 ± 0,1	3,3 ± 1,0	3,9 ± 1,4
	exposed	1,8 ± 1,0	3,4 ± 1,3	3,3 ± 1,4	1,1 ± 0,4	2,7 ± 0,9	3,7 ± 1,2
IL-13	*control*	48,4 ± 17,4	75,6 ± 17,3	38,6 ± 14,0	44,4 ± 9,5	65,3 ± 18,1	50,9 ± 20,8
	exposed	45,2 ± 9,4	43,6 ± 17,4	72,7 ± 23,4	43,6 ± 10,7	35,8 ± 11,1	51,3 ± 17,4
IL-1β	*control*	16,2 ± 2,9	31,2 ± 7,9	25,3 ± 4,9	28,1 ± 17,3	23,8 ± 5,7	16,1 ± 9,0
	exposed	9,8 ± 3,3	18,3 ± 7,1	16,1 ± 9,2	10,4 ± 2,4	13,7 ± 2,9	21,2 ± 4,6
IL-2	*control*	4,6 ± 3,3	6,6 ± 7,9	5,5 ± 4,9	2,8 ± 2,4	10,8 ± 5,7	25,5 ± 9,0
	exposed	14,2 ± 10,3	18,2 ± 13,7	31,2 ± 24,4	2,3 ± 0,6	12,0 ± 7,7	6,6 ± 2,2
IL-4	*control*	0,7 ± 0,2	1,2 ± 0,3	1,5 ± 0,3	0,3 ± 0,1	1,0 ± 0,4	1,0 ± 0,5
	exposed	0,5 ± 0,5	1,0 ± 0,4	0,9 ± 0,5	0,3 ± 0,2	0,8 ± 0,2	0,9 ± 0,4
IL-6	*control*	19,5 ± 5,7	34,3 ± 6,3	29,8 ± 7,5	19,4 ± 3,7	30,9 ± 10,1	22,7 ± 5,7
	exposed	27,9 ± 5,2	30,3 ± 4,5	39,6 ± 14,3	19,2 ± 6,0	25,5 ± 3,4	29,9 ± 6,7
IL-8	*control*	5815,4 ± 610,4	6183,4 ± 530,5	6236,1 ± 664,7	4718,9 ± 483,6	6163,3 ± 540,2	5530,7 ± 692,7
	exposed	4905,1 ± 753,8	5218,3 ± 681,0	4908,2 ± 672,8	4866,5 ± 806,9	5092,0 ± 596,0	4905,1 ± 784,7
TNF-α	*control*	4,0 ± 1,7	3,9 ± 0,4	10,3 ± 2,9	2,9 ± 0,7	4,6 ± 0,8	11,7 ± 2,8
	exposed	4,0 ± 1,4	6,2 ± 1,1	6,1 ± 0,9	3,1 ± 1,3	6,4 ± 1,6	8,0 ± 1,7

B **Cytokines panel**

Cytokine		80 ng/cm²									240 ng/cm²								
		6h			24h			48h			6h			24h			48h		
GM-CSF	*control*	10,9	±	2,7	23,7	±	1,4	81,0	±	12,8	6,8	±	1,5	23,9	±	2,5	82,4	±	5,2
	exposed	6,3	±	1,5	24,6	±	4,0	78,2	±	12,6	23,0	±	16,6	23,4	±	2,5	83,7	±	10,4
IL-12p40	*control*	1,3	±	0,8	2,3	±	0,7	3,6	±	1,9	1,0	±	0,3	2,0	±	0,3	2,6	±	0,8
	exposed	1,2	±	0,3	2,0	±	1,0	3,0	±	0,6	0,8	±	0,2	1,1	±	0,3	1,9	±	0,5
IL-15	*control*	1,3	±	0,5	3,3	±	0,4	7,0	±	1,0	0,8	±	0,1	3,1	±	0,4	5,8	±	1,0
	exposed	0,7	±	0,2	3,0	±	0,8	5,8	±	1,4	1,6	±	0,8	2,7	±	0,4	5,2	±	1,0
IL-16	*control*	5,5	±	1,3	22,6	±	4,2	28,4	±	6,6	8,8	±	3,8	17,3	±	3,1	27,9	±	7,8
	exposed	9,2	±	1,9	17,6	±	5,1	38,2	±	6,1	6,0	±	1,3	15,5	±	3,5	30,4	±	4,3
IL-17	*control*	**Not detectable under assay conditions**									**Not detectable under assay conditions**								
	exposed																		
IL-1α	*control*	0,9	±	0,2	7,0	±	4,1	7,1	±	2,3	19,9	±	19,0	2,2	±	0,3	8,5	±	2,8
	exposed	1,5	±	0,2	2,7	±	0,6	6,6	±	2,1	1,0	±	0,2	3,0	±	0,4	7,4	±	2,0
IL-5	*control*	**Not detectable under assay conditions**									**Not detectable under assay conditions**								
	exposed																		
IL-7	*control*	0,3	±	0,1	1,4	±	0,2	2,0	±	0,4	0,6	±	0,3	1,3	±	0,2	2,3	±	0,7
	exposed	0,6	±	0,2	1,0	±	0,3	2,7	±	0,6	0,3	±	0,1	1,0	±	0,3	2,2	±	0,5
TNF-β	*control*	0,0	±	0,0	0,0	±	0,0	0,0	±	0,0	0,0	±	0,0	0,1	±	0,0	0,0	±	0,0
	exposed	0,1	±	0,0	0,1	±	0,0	0,0	±	0,0	0,1	±	0,0	0,1	±	0,0	0,0	±	0,0
VEGF	*control*	29,3	±	4,5	125,5	±	17,2	357,3	±	38,9	113,4	±	76,2	110,1	±	21,5	376,0	±	52,2
	exposed	51,7	±	18,2	114,2	±	18,3	329,7	±	55,0	39,1	±	5,5	107,3	±	12,4	330,2	±	44,3

C **Chemokines panel**

Cytokine		80 ng/cm²									240 ng/cm²								
		6h			24h			48h			6h			24h			48h		
Eotaxin	*control*	41,1	±	18,6	13,7	±	5,2	35,5	±	19,6	41,1	±	18,6	23,9	±	3,9	35,2	±	16,4
	exposed	20,9	±	6,9	24,1	±	8,2	30,5	±	8,1	13,4	±	4,6	19,1	±	5,6	78,3	±	26,4
Eotaxin3	*control*	6,4	±	2,6	9,8	±	3,3	11,5	±	4,0	4,6	±	0,7	5,8	±	0,8	18,1	±	6,0
	exposed	9,5	±	3,2	7,0	±	4,0	9,4	±	1,3	9,5	±	3,2	7,8	±	1,8	17,1	±	4,9
IP-10	*control*	16,4	±	6,9	46,9	±	14,7	170,2	±	29,1	16,4	±	5,4	44,2	±	8,4	165,3	±	16,8
	exposed	16,0	±	4,0	57,0	±	18,6	214,7	±	76,4	16,0	±	4,0	44,0	±	11,1	164,5	±	11,7
MCP-1	*control*	4832,0	±	1181,5	6000,2	±	1189,1	10545,1	±	1307,9	4832,0	±	1181,5	7428,2	±	1087,1	8985,3	±	942,1
	exposed	4696,7	±	1186,7	7813,6	±	492,7	8708,3	±	1186,8	4314,5	±	620,7	6973,6	±	472,9	8391,9	±	1128,5
MCP-4	*control*	14,5	±	6,0	14,0	±	2,5	19,4	±	2,9	12,8	±	4,4	20,2	±	3,6	20,1	±	3,4
	exposed	12,7	±	2,7	11,8	±	1,5	24,8	±	5,5	12,7	±	2,7	16,8	±	3,4	22,7	±	2,3
MDC	*control*	192,2	±	53,3	269,8	±	64,0	452,2	±	98,0	192,2	±	53,3	280,1	±	65,1	461,2	±	69,1
	exposed	218,6	±	97,3	284,2	±	76,9	439,8	±	108,4	185,8	±	61,6	270,1	±	59,6	415,2	±	50,1
MIP1a	*control*	201,6	±	134,2	83,3	±	29,8	56,5	±	18,7	134,9	±	66,3	115,8	±	47,0	61,6	±	18,2
	exposed	260,7	±	154,1	103,3	±	44,7	62,6	±	21,9	260,7	±	154,1	130,6	±	62,1	45,1	±	7,6
MIP1b	*control*	158,4	±	42,5	129,4	±	17,5	87,6	±	35,4	158,4	±	42,5	129,6	±	19,5	117,9	±	17,1
	exposed	184,3	±	63,3	142,8	±	29,6	82,4	±	18,7	118,7	±	39,2	216,3	±	35,5	75,7	±	23,4
TARC	*control*	70,2	±	46,3	147,1	±	48,0	82,2	±	32,1	51,2	±	24,5	116,5	±	48,9	80,6	±	50,5
	exposed	62,9	±	29,6	108,2	±	71,6	102,2	±	46,9	62,9	±	29,6	49,1	±	17,4	86,7	±	32,4

3.2.4. UPREGULATION OF *HSP70* mRNA AS AN INDICATOR OF CELLULAR STRESS IN THE ENDOTHELIAL PART OF THE TETRACULTURE AFTER EXPOSURE TO DEPM

The heat shock protein 70 (HSP70) is a part of the chaperon system, which is present in almost all organisms. Heat shock proteins play an important role for the quality control of the protein biosynthesis to avoid accumulation of misfolded proteins. These enzymes become induced in response to heat stress, toxicants and also as a response to DEPM [294]. The upregulation of the chaperon HSP70 is suspected to be implicated in the pathogenesis of vascular dysfunction and cardiovascular disease [294]. In addition, Kido et al. postulated that HSP70 possibly contributes to air-pollution-induced vascular dysfunction and cardiovascular diseases [294].

For the evaluation of the potential of DEPM to induce *HSP70* upregulation on the mRNA level in the *in vitro* model system, tetracultures were exposed to 80 ng/cm^2 or 240 ng/cm^2 of diesel exhaust particles. Total mRNA of the endothelial cells of the tetracultures was sampled at 6, 24 and 48 h after exposure, reversely transcribed and analyzed via qRT-PCR. Tetracultures that were kept in the aerosol chamber for the same exposure time but with the particle generator in standby mode served as control.

The endothelial part of the tetraculture showed a small but significant increase in the expression of *HSP70* mRNA at 24 h after the indirect exposure to 80 ng/cm^2 of DEPM (1.36 ± 0.05 fold), compared to the cells analyzed at 6 h after the exposure, which were at the same level as the control cells (0.99 ± 0.11 fold) ($P<0.05$) (Figure 41 A). 48 h after the indirect exposure, the expression level of *HSP70* mRNA in the endothelial cells was slightly lower than after 24 h (1.26 ± 0.09 fold) (not significant) (Figure 41 A).

Endothelial cells that were indirectly exposed to 240 ng/cm^2 showed no significant response after 6 h (0.98 ± 0.08 fold) and 24 h (1.31 ± 0.08 fold). Treated cells that were incubated for 48 h after exposure showed the highest response for the upregulation of *HSP70* mRNA with 1.5 ± 0.05 fold increase ($P<0.05$ compared to the cells after 6 h) (Figure 41 B).

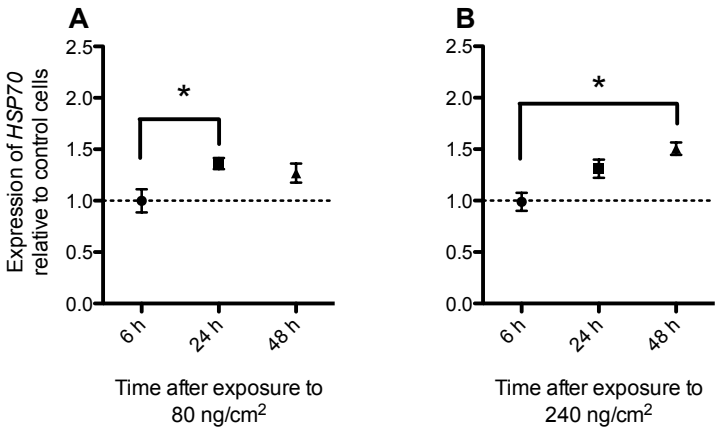

Figure 41: Impact of the exposure to different amounts of DEPM on the expression level of *HSP70* in the endothelial part of the tetraculture system at different time-points after exposure to DEPM. Tetracultures were exposed to 80 ng/cm^2 (**A**) or 240 ng/cm^2 (**B**) of diesel exhaust particles. Total mRNA of the endothelial cells of the tetracultures was sampled at 6, 24 and 48 h after exposure, reversely transcribed and analyzed via qRT-PCR. Tetracultures that were kept in the aerosol chamber for the same exposure time but with the particle generator in standby mode served as control.

Data represents the mean of at least four independent samples ± SEM. Asterisks indicate significant differences between the evaluated time-points (P<0.05). The dotted line indicates the level of expression of the control cells to which the results were normalized.

3.2.5. INFLUENCE OF RELEVANT DOSES OF DEPM ON THE EXPRESSION OF PRO-APOPTOTIC KEY GENES IN THE ENDOTHELIAL PART OF THE TETRACULTURE

The programmed cell death, apoptosis, is an important cellular mechanism to eliminate infected cells or cells that show abnormal behavior. Some chemicals and also environmental particles were shown to possess the potential to interfere with the programmed cell death and to induce key enzymes and genes disturbing this pathway, which may result in an unintended apoptotic activity of otherwise healthy cells and tissue. DEPM are also expected to potentially induce the apoptotic machinery [134, 162, 176].

In this experiment a potential upregulation of the pro-apoptotic key genes *FAS* and *CASP7* was evaluated. The *FAS* gene encodes for a protein that is important for the activation of the

apoptosis pathway. The *CASP7* gene encodes for a protein that is part of caspase family and necessary to execute the apoptotic process.

For the evaluation of the potential of DEPM to induce *FAS* and *CASP7* upregulation on the mRNA level in the *in vitro* model system, tetracultures were exposed to 80 ng/cm^2 or 240 ng/cm^2 of diesel exhaust particles. Total mRNA of the endothelial cells of the tetracultures was sampled at 6, 24 and 48 h after exposure, reversely transcribed and analyzed via qRT-PCR. Tetracultures that were kept in the aerosol chamber for the same exposure time but with the particle generator in standby mode served as control.

The endothelial part of the tetraculture showed no increase in the expression of *FAS* mRNA after the indirect exposure to 80 and 240 ng/cm^2 at any of the evaluated time-points (Figure 42).

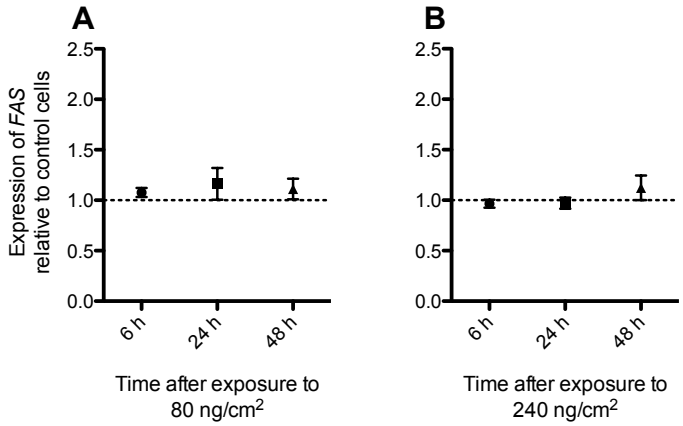

Figure 42: Impact of the exposure to different amounts of DEPM on the expression level of *FAS* in the endothelial part of the tetraculture system at different time-points after exposure to DEPM. Tetracultures were exposed to 80 ng/cm^2 (**A**) or 240 ng/cm^2 (**B**) of DEPM. Total mRNA of the endothelial cells of the tetracultures was sampled at 6, 24 and 48 h after exposure, reversely transcribed and analyzed via qRT-PCR. Tetracultures that were kept in the aerosol chamber for the same exposure time but with the particle generator in stand-by mode served as control.
Data represents the mean of at least four independent samples ± SEM. The dotted line indicates the level of expression of the control cells to which the results were normalized.

CASP7 mRNA was only significantly upregulated in endothelial cells that were indirectly exposed to 240 ng/cm^2 at 48 h after the exposure (1.2 ± 0.04; $P<0.05$ compared to the cells after 6 h and 24 h). The other samples were at the same level as the control cells (6 h: 0.95 ± 0.05; 24 h: 0.99 ± 0.05) (Figure 43).

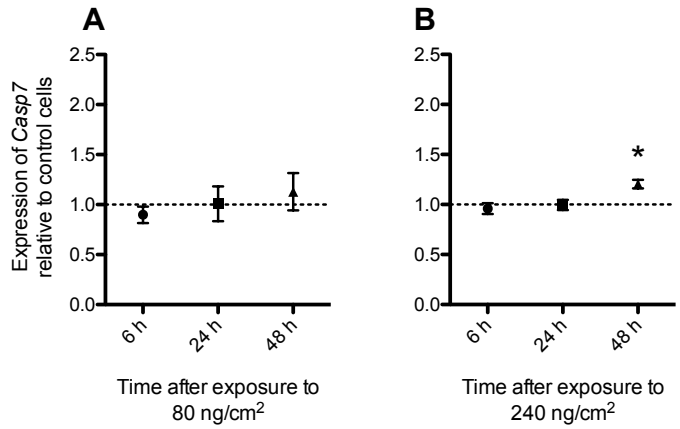

Figure 43: Impact of the exposure to different amounts of DEPM on the expression level of *Casp7* in the endothelial part of the tetraculture system at different time-points after exposure to DEPM. Tetracultures were exposed to 80 ng/cm^2 (**A**) or 240 ng/cm^2 (**B**) of diesel exhaust particles. Total mRNA of the endothelial cells of the tetracultures was sampled at 6, 24 and 48 h after exposure, reversely transcribed and analyzed via qRT-PCR. Tetracultures that were kept in the aerosol chamber for the same exposure time but with the particle generator in stand-by mode served as control.

Data represents the mean of at least four independent samples ± SEM. Asterisks indicate significant differences between the evaluated time-points (P<0.05). The dotted line indicates the level of expression of the control cells to which the results were normalized.

3.2.6. INDUCTION OF NRF2-REGULATED PATHWAYS IN THE ENDOTHLIAL PART OF THE TETRACULTURE AFTER DEPM EXPOSURE

The transcription factor Nrf2 plays an important role for the induction of the antioxidant defense in mammalian cells. Under basal conditions Nrf2 is bound to kelch-like ECH-associated protein 1 (Keap1) in the cytosol, and is continuously ubiquitinated by E3 ubiquitin ligase, and subsequently degraded by the 26S proteasome [295]. However, exposure to oxidative stress leads to the activation of Nrf2 and dissociation from Keap1. Nrf2 translocates to the nucleus resulting in enhanced transcription of a number of target antioxidant genes via the antioxidant response element (ARE). The activation of the ARE is necessary for cytoprotection [296]. In the lung, Nrf2 plays a protective role against oxidative

injury including hyperoxia, mechanical ventilation, and cigarette smoke. It was shown, that a lack of Nrf2 exacerbates lung inflammation [297].

3.2.6.1. NUCLEAR TRANSLOCATION OF THE TRANSCRIPTION FACTOR NRF2

In preliminary experiments with EA.hy 926 endothelial cells the potential of these cells to react to an oxidative stress with the nuclear translocation of the transcription factor Nrf2 was evaluated. EA.hy 926 endothelial cells in monoculture were incubated for 2 h with AAPH (20 mM). After the treatment, the cells were stained for the nucleus (Hoechst 33342) and Nrf2 (anti-Nrf2-antibody) and analyzed via CLSM. After 2 h of treatment, almost every cell was positive for the nuclear translocation of Nrf2 compared to the control cells (cells without AAPH) (Figure 44).

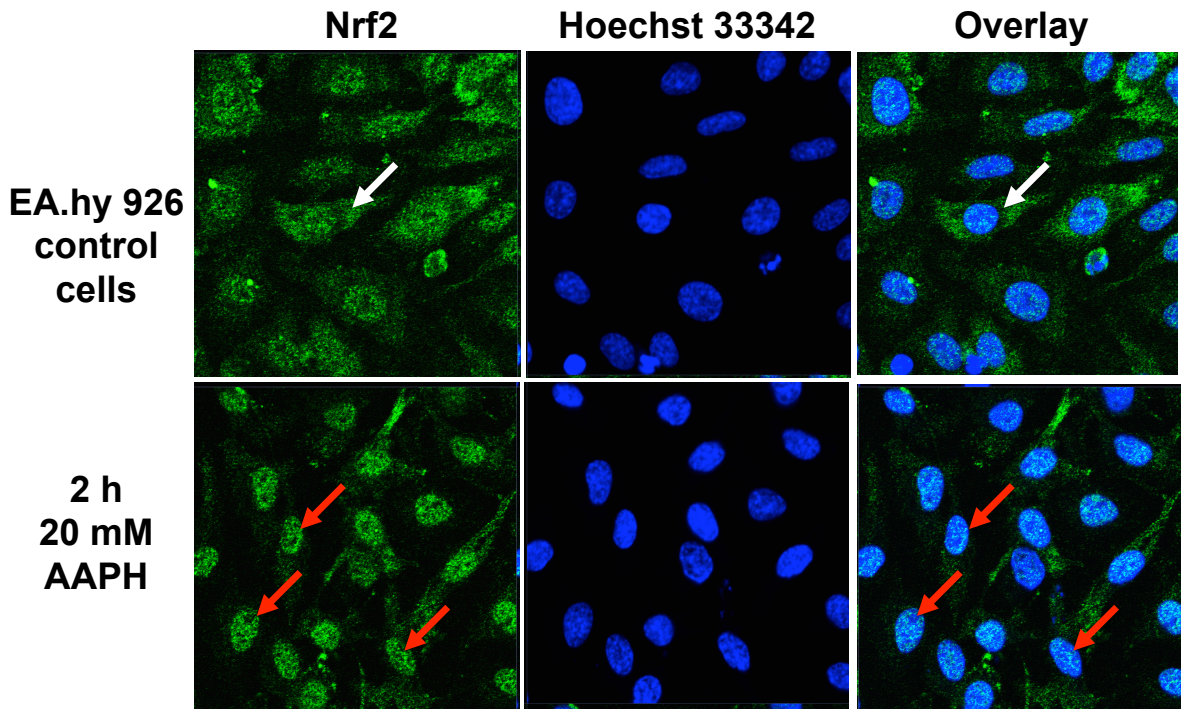

Figure 44: Nuclear translocation of Nrf2 in endothelial EA.hy 926 cells in monoculture after treatment with 20 mM AAPH for 2 h. EA.hy 926 cells were exposed to 20 mM AAPH in normal full cell culture medium for 2 h. Cells kept in normal medium without AAPH served as negative control. Nrf2 translocation was evaluated for 2 h after treatment. Cells were fixed and stained for Nucleus (Hoechst 33342) and anti-Nrf2 (green). Images were analyzed using a Zeiss LSM 510 META.
2 h after exposure almost every endothelial cells shows strong colocalization of Nrf2 with the nucleus (red arrows). In control EA.hy 926 cells, no nuclear translocation was observed (compare white arrows).

To evaluate the potential of DEPM to induce a similar nuclear translocation of the Nrf2, tetracultures were exposed to 240 ng/cm^2 of DEPM. Tetracultures that were kept in the aerosol chamber for the same exposure time but with the particle generator in standby mode served as control. The nuclear translocation of Nrf2 was evaluated for unexposed endothelial cells and for endothelial cells indirectly exposed to DEPM at 3, 4 and 5 h after the exposure. Cells were fixed and stained for nucleus (Hoechst 33342) and anti-Nrf2 (green) and subsequently analyzed using a Zeiss LSM 510 META.

At 3 h after exposure, first cells showed nuclear translocation (Figure 45, yellow arrow). At 4 h after the exposure, the nuclear translocation of Nrf2 could be detected in the majority of the cell population (Figure 45, orange arrows). Finally, at 5 h after the exposure almost every endothelial cell showed strong colocalization of Nrf2 with the nucleus (Figure 45, red arrows). In control EA.hy 926 cells, no nuclear translocation was observed at any time-point (Figure 45, white arrows in the representative control image).

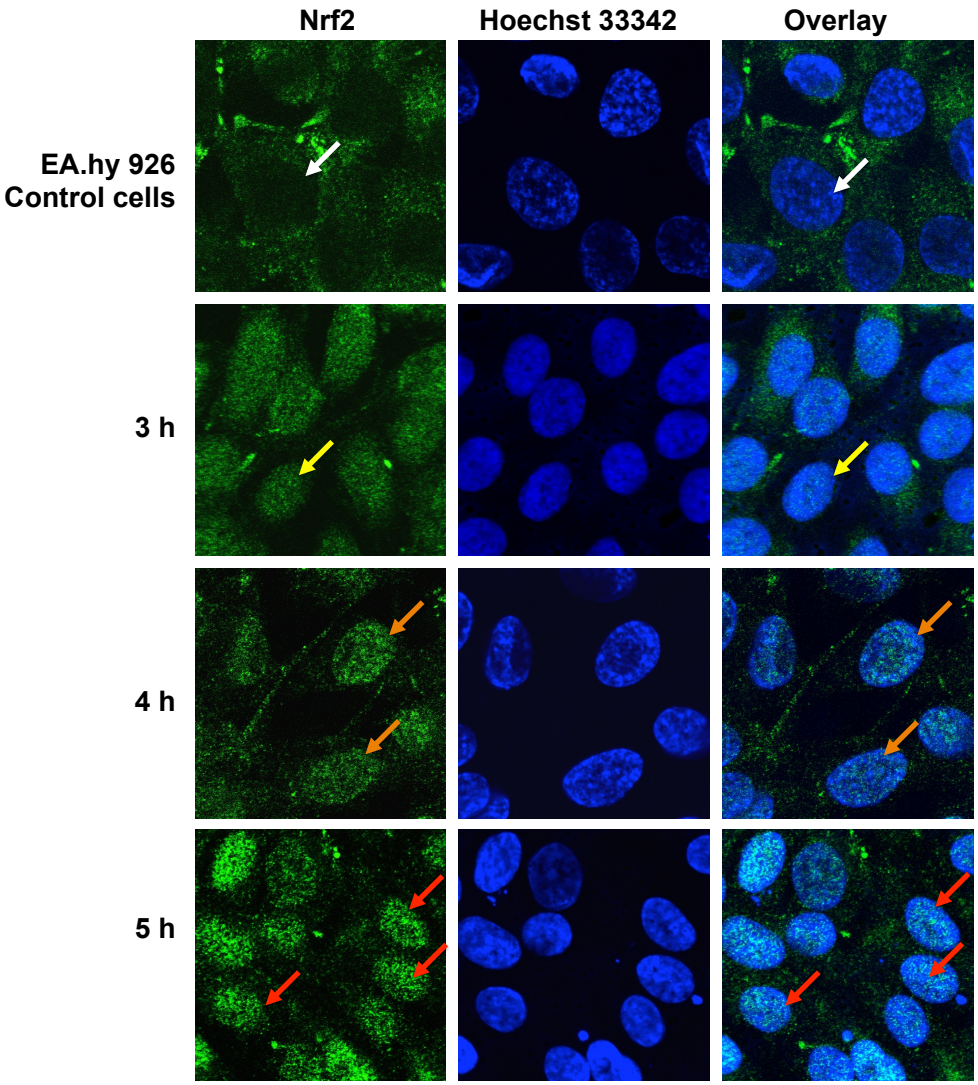

Figure 45: Potential of DEPM to induce nuclear translocation of the transcription factor Nrf2 at different time-points after the exposure. Tetracultures were exposed to 240 ng/cm^2 of DEPM. Tetracultures that were kept in the aerosol chamber for the same exposure time but with the particle generator in stand-by mode served as control. Nrf2 translocation was evaluated for unexposed cells and for cells indirectly exposed to diesel exhaust particles at 3, 4 and 5 h after exposure. Cells were fixed and stained for nucleus (Hoechst 33342) and anti-Nrf2 (green). Images were analyzed using a Zeiss LSM 510 META.

At 3 h after exposure, first cells showed nuclear translocation (Figure 45, yellow arrow). At 4 h after exposure, nuclear translocation was quite obvious in the majority of the cell population (compare orange arrows). At 5 h after exposure almost every endothelial cells showed strong colocalization of Nrf2 with the nucleus (red arrows). In control EA.hy 926 cells, no nuclear translocation was observed at any time-point (compare white arrows in the representative control image).

3.2.6.2. UPREGULATION OF TARGET GENS OF NRF2 RELEVANT FOR ANTIOXIDANT DEFENSE AT DIFFERENT TIME-POINTS AFTER INDIRECT EXPOSURE TO DEPM

The transcription factor Nrf2 regulates the expression of a number of key genes that are important for the cells to react to oxidative stress. In presence of oxidative stress, Nrf2 becomes activated and translocates into the nucleus of the cell where it activates the antioxidant response element (ARE). This leads to the transcription of important genes, like *NAD(P)H dehydrogenase quinone 1* (*NQO1*), *superoxide dismutase 1* (*SOD1*) and *HMOX1*. These genes play a very important role in deactivating and scavenging radicals to protect cellular components from oxidative damage. Among these genes, *HMOX1* is very versatile enzyme, which was described in literature to have high cytoprotective capacity. In addition, *HMOX1* was described to play a special role in the prevention of atherosclerosis and vascular inflammation [159].

Additionally to the genes already mentioned, we also evaluated potential changes in the expression level of the gene *nuclear erythroid factor 2* (*NEF2)*, which encodes for the transcription factor Nrf2, as well as for the gene *glutathione S-transferase* (*GST1*). Besides its role for phase II metabolism, *GST1* has also been described to be a target gene of Nrf2 and to be involved in the response of endothelial cells to DEPM [185].

To evaluate the response of the endothelial cells of the tetraculture on the mRNA level, tetracultures were exposed to 80 ng/cm^2 or 240 ng/cm^2 of diesel exhaust particles. Total mRNA of the endothelial cells was sampled at 6, 24 and 48 h after exposure, reversely transcribed and analyzed via qRT-PCR. Tetracultures that were kept in the aerosol chamber for the same exposure time but with the particle generator in standby mode served as control. None of the evaluated target genes showed a significant change in the expression level compared to the control cells (Table 8).

Table 8: Impact of the exposure to different amounts of DEPM on the expression level of Nrf2 target genes in the endothelial part of the tetraculture system at different time-points after exposure to DEPM.

Tetracultures were exposed to 80 ng/cm^2 or 240 ng/cm^2 of DEPM. Total mRNA of the endothelial cells of the tetracultures was sampled at 6, 24 and 48 h after exposure, reversely transcribed and analyzed via qRT-PCR. Tetracultures that were kept in the aerosol chamber for the same exposure time but with the particle generator in stand-by mode served as control.

Data represents the mean of at least four independent samples ± SEM. Results were normalized to the level of expression of the control cells.

	80 ng/cm^2			240 ng/cm^2		
Gene	**6 h**	**24 h**	**48 h**	**6 h**	**24 h**	**48 h**
NEF2	0,99 ± 0,05	1,01 ± 0,08	1,05 ± 0,04	1,00 ± 0,03	0,95 ± 0,03	1,20 ± 0,16
NQO1	1,01 ± 0,05	0,98 ± 0,02	1,01 ± 0,01	1,03 ± 0,01	1,01 ± 0,03	1,08 ± 0,01
GST1	1,03 ± 0,04	1,00 ± 0,06	0,97 ± 0,03	0,97 ± 0,02	0,92 ± 0,06	1,10 ± 0,05
HMOX1	1,09 ± 0,07	0,95 ± 0,03	0,93 ± 0,03	0,97 ± 0,04	0,97 ± 0,07	1,13 ± 0,11
HMOX2	1,14 ± 0,15	1,09 ± 0,02	1,03 ± 0,01	1,01 ± 0,04	1,09 ± 0,07	1,16 ± 0,15
SOD1	0,91 ± 0,10	0,98 ± 0,07	1,05 ± 0,04	0,98 ± 0,03	1,01 ± 0,05	1,06 ± 0,09

3.2.7. UPREGULATION OF *CYP1A1 mRNA* EXPRESSION IN THE ENDOTHELIAL PART OF THE TETRACULTURE AFTER DEPM EXPOSURE

DEPM were found to carry considerable amounts of xenobiotics on their outer shell. When respirated these xenobiotics can enter the respiratory system to finally reach the alveolar barrier. Due to the lack of clearance mechanisms, xenobiotics have the possibility to interact with cellular structures and to become metabolized, leading to sometimes more toxic and dangerous metabolites.

The cytochrome P450 enzyme family is a group of heme-thiolate mono-oxygenases important for the metabolism of various endogenous as well as exogenous compounds. Up to now, more than 481 different cytochrome P450, encoded by 74 gene families, could be identified [298]. Among these enzymes, The CYP1 family, which includes at least three enzymes, CYP1A1, CYP1A2, and CYP1B1, was found to be important for the metabolism of

xenobiotics, such as PAHs and heterocyclic amines in lung and other tissues [262]. The expression of these enzymes was shown to be inducible by compounds like TCDD. TCDD induces the transcription of CYP1 by activating the cytosolic AhR. This receptor becomes activated due to the interaction with a potential ligand, such as TCDD or B[a]P [299]. Here we evaluate the potential of DEPM to induce the nuclear translocation of the transcription factor AhR and the upregulation of the cytochrome *CYP1A1* on the mRNA level.

3.2.7.1. DEPM EXPOSURE AS POTENTIAL INDUCER OF AhR NUCLEAR TRANSLOCATION IN THE ENDOTHELIAL PART OF THE TETRACULTURE

To evaluate the potential of DEPM to induce a nuclear translocation of the AhR in the endothelial cells, tetracultures were exposed to 240 ng/cm^2 of DEPM. Tetracultures that were kept in the aerosol chamber for the same exposure time but with the particle generator in stand-by mode served as control. AhR translocation was evaluated for unexposed cells and for cells indirectly exposed to diesel exhaust particles at 3, 4 and 5 h after exposure. Cells were fixed and stained for Nucleus (Hoechst 33342) and anti-AhR (green). Images were analyzed using a Zeiss LSM 510 META.

At 3 h after exposure, first cells showed weak nuclear translocation (Figure 46, yellow arrow). At 4 h after exposure, nuclear translocation was almost at the same level as the control (Figure 46, orange arrows) and 5 h after exposure translocation of AhR was at the same level as the control (Figure 46, red arrows). In control EA.hy 926 cells, no nuclear translocation was observed at any time-point (Figure 46, white arrows in the representative control image). Overall, changes for the nuclear translocation of the AhR were weak and close to the detection limit.

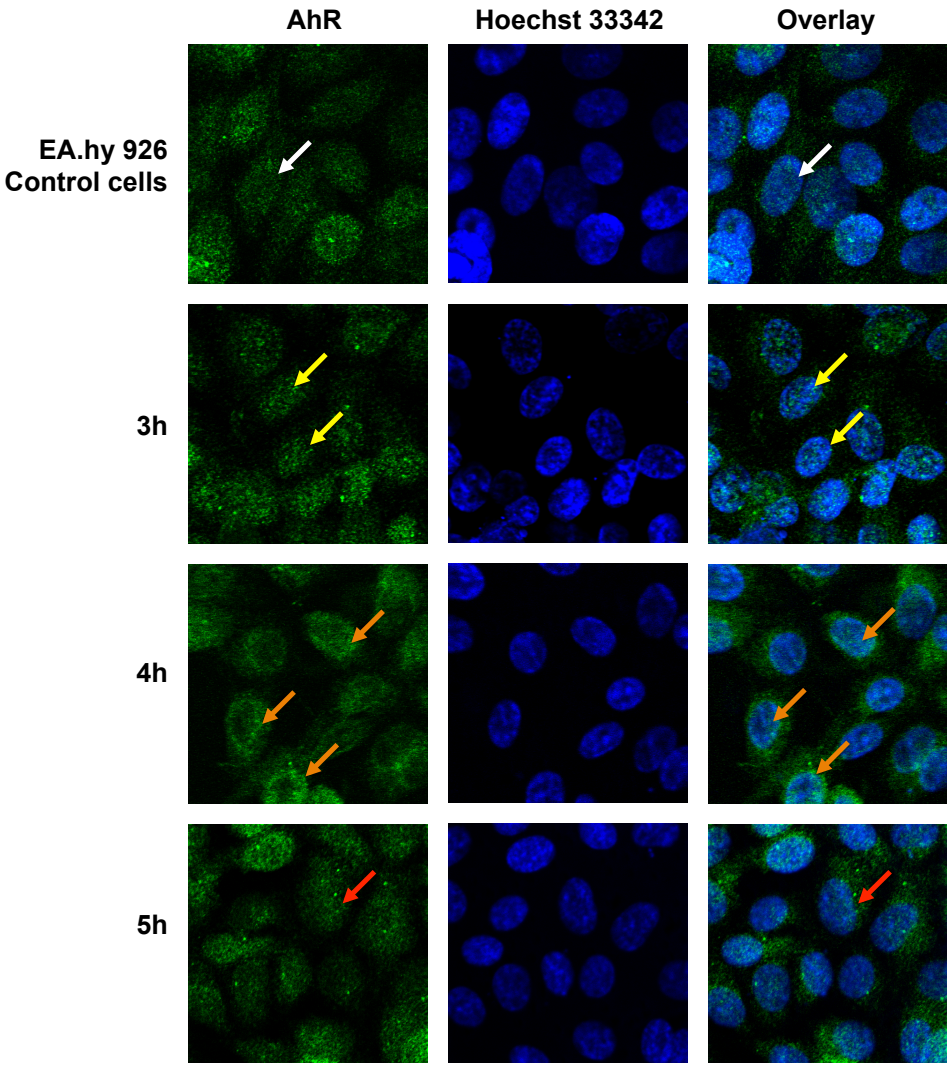

Figure 46: Potential of DEPM to induce nuclear translocation of the transcription factor AhR at different time-points after the exposure. Tetracultures were exposed to 240 ng/cm^2 of DEPM. Tetracultures that were kept in the aerosol chamber for the same exposure time but with the particle generator in stand-by mode served as control. AhR translocation was evaluated for unexposed cells and for cells indirectly exposed to diesel exhaust particles at 3, 4 and 5 h after exposure. Cells were fixed and stained for Nucleus (Hoechst 33342) and anti-AhR (green). Images were analyzed using a Zeiss LSM 510 META.

At 3 h after exposure, first cells showed weak nuclear translocation (yellow arrow). At 4 h after exposure, nuclear translocation was almost at the same level as the control (compare orange arrows). At 5 h after exposure translocation of AhR was at the same level as the control (red arrows). In control EA.hy 926 cells, no nuclear translocation was observed at any time point (compare white arrows in the representative control image).

3.2.7.2. *CYP1A1* mRNA EXPRESSION IN THE ENDOTHELIAL PART OF THE TETRACULTURE AFTER INDIRECT EXPOSURE TO DEPM

In order to evaluate if the nuclear translocation of the AhR receptor after the indirect exposure to DEPM lead to detectable changes in the transcription level of the mRNA for *CYP1A1*, tetracultures were exposed to 80 ng/cm^2 or 240 ng/cm^2 of diesel exhaust particles. Total mRNA of the endothelial cells of the tetracultures was sampled at 6, 24 and 48 h after exposure, reversely transcribed and analyzed via qRT-PCR. Tetracultures that were kept in the aerosol chamber for the same exposure time but with the particle generator in stand-by mode served as control.

The endothelial cells of the tetraculture showed a significant increase of 1.85 ± 0.37 fold (compared to the control cells) for *CYP1A1* mRNA 6 h after the indirect exposure to 80 ng/cm^2 of DEPM (P<0.05). Cells that were analyzed at 24 and 48 h after the indirect exposure showed lower expression for the *CYP1A1* mRNA than the control cells (24 h: 0.65 ± 0.03; 48 h: 0.56 ± 0.06) (Figure 47 A).

Similar results were obtained for cells that were indirectly exposed to 240 ng/cm^2 and analyzed at 6, 24 and 48 h after the exposure. The cells after 6 h showed the highest level of expression for the *CYP1A1* mRNA (1.34 ± 0.26 fold) compared to the control cells (not significant). Cells that were analyzed at 24 and 48 h after the indirect exposure showed lower expression level for the *CYP1A1* mRNA than the control cells (24 h: 0.83 ± 0.06; 48 h: 0.8 ± 0.16) (Figure 47 B). Exposure to 240 ng/cm^2 did not lead to significant upregulation of *CYP1A1* mRNA.

In addition to the experiment described above, the potential change in the expression level of the cytochrome *CYP1B1* mRNA was evaluated under similar conditions. However, the expression of *CYP1B1* mRNA was below the limit of detection in our experimental setup.

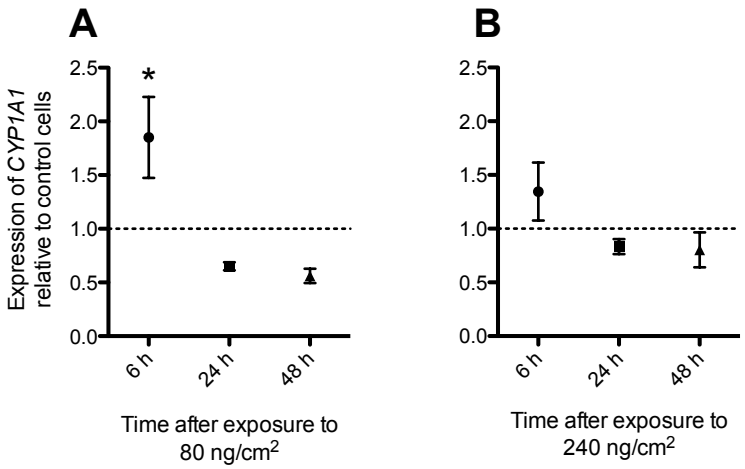

Figure 47: Impact of the exposure to different amounts of DEPM on the expression level of *CYP1A1* mRNA in the endothelial part of the tetraculture system at different time points after exposure to DEPM. Tetracultures were exposed to 80 ng/cm^2 (**A**) or 240 ng/cm^2 (**B**) of DEPM. Total mRNA of the endothelial cells of the tetracultures was sampled at 6, 24 and 48 h after exposure, reversely transcribed and analyzed via qRT-PCR. Tetracultures that were kept in the aerosol chamber for the same exposure time but with the particle generator in stand-by mode served as control.
Data represents the mean of at least four independent samples ± SEM. Asterisks indicate significant differences between the evaluated time-points (P<0.05). The dotted line indicates the level of expression of the control cells to which the results were normalized.

4. DISCUSSION

4.1. DIFFERENCES AND MODIFICATIONS OF THE *IN VITRO* MODEL COMPARED TO THE ORIGINAL VERSION OF THE TETRACULTURE ESTABLISHED BY ALFARO-MORENO ET AL.

The total number of *in vitro* approaches reported to be available for respiratory toxicology is relatively high. However, the majority of these *in vitro* systems are based on monocultures of cells derived from different regions of the lung [236]. For some scientific questions, such as the induction of endothelial inflammation by particles, the use of a monoculture is not appropriate, since the direct exposure of endothelial cells to particles is in most cases poorly justified [118]. The only possibility to address this issue is to use a multi-layered system, which combines epithelial cells, immune cells and endothelial cells together [292, 300]. Another limitation present in many systems currently used is the submerged exposure method that is not representing the *in vivo* situation. Such a system does not properly predict the hazard of the tested material, since it has been shown that the exposure route itself can have a crucial impact on the results [121].

In the original version of the system established by Alfaro-Moreno and coworkers [1], the triculture of A549, THP-1 and HMC-1 cells was located at the bottom of a cultivation well and endothelial cells were seeded in a Transwell™ insert in the same well [1]. Triculture and endothelial cells were physically separated by the microporous membrane and by cell culture medium, which does not resemble the histology of the tissue *in vivo*. In the modified version the triculture of A549, THP-1 and HMC-1 was shifted from the bottom of the multiwell plate into the Transwell™ insert and EA.hy 926 endothelial cells were moved from the inside of the Transwell™ insert to the basolateral side of the membrane in order to better reflect the *in vivo* anatomy of the alveolar region. The system contains differentiated THP-1 cells and HMC-1 cells as models for the innate immune system together with A549 epithelial cells and this allows the study of inflammatory mechanisms in the alveoli *in vitro*.

In the alveolar model presented in this publication, the seeding ratios are most likely not resembling the *in vivo* condition, as there might be an overrepresentation of monocytes and mast cells, compared to endothelial and epithelial cells. The rationale for this seeding ratio is mainly based on methodological arguments. Protocols to separate different cell types in the coculture after exposure in order to study the individual response require a higher number of cells. The same is true when applying -omic techniques, such as transcriptomics and proteomics that require higher quantities of cells. In order to reduce the technical complexity of such experiments, it was decided to increase the number of immune cells present in the system.

4.2. CHARACTERIZATION AND ESTABLISHMENT OF THE TETRACULTURE *IN VITRO* SYSTEM

4.2.1. ROLE OF THE PORE SIZE OF THE SUPPORTING TRANSWELL™ INSERT AND CELLULAR COMPOSITION FOR THE BARRIER QUALITIES OF THE IN VITRO SYSTEM

The Transwell™ insert itself is one of the key factors of an ALI exposure system. It allows growing the cells in contact to the ambient air from above and receiving nutrients from the medium below. These inserts are available with different pore sizes and densities, and these parameters can influence cellular growth and availability of nutrients as well as soluble second messengers.

Not all NPs can efficiently pass through a cell-free 0.4 µm Transwell™ insert [276]. In general, particles with a size below 100 nm should be able to pass a 400 nm pore easily; however, this depends not only on the size but rather on the surface chemistry of the NP, resulting in electrostatic changes and different hydrodynamic diameters [276, 301]. Therefore inserts of different pore sizes from the same supplier were tested in order to choose the most appropriate insert as a support for the 3D tetraculture system. Under assay conditions, the viability of cultures in 0.4 µm inserts was generally lower compared to

cultures grown in 1 and 3 µm inserts. For the cultivation of cells at the ALI it is mandatory to avoid the transfer of cell culture medium to the surface of the cell culture, which impairs ALI conditions. For the experiments with A549 cultures grown at the ALI in Transwell™ inserts with 3 µm pore size a considerable amount of liquid leached from the lower compartment into the upper compartment. A few hours after the start of the ALI cultivation the A549 cells in the inserts with 3 µm pore size were found to be again under submerged conditions, due to the leached cell culture medium from below. On the contrary, A549 cells grown in Transwell™ inserts with, 1 µm pore size the quantity of liquid appearing in the upper compartment was negligible.

The tightness of the epithelial barrier in the system was analyzed by adding a sodium fluorescein tracer-solution to the apical compartment after which the appearing fluorescence in the basolateral compartment was measured. An epithelium is considered to be efficiently sealed if the amount of leaked fluorescence within one hour is less than 1% of the initial concentration [276, 302]. In the experimental setup, Transwell™ inserts with 0.4 µm pores were significantly blocking the transport of tracer molecules across the membrane. This effect is larger than the ability of the different cultures to block and influence the liquid exchange. The tracer molecule used is small and is used as a reference for the passage of nutrients and second messengers through membranes. For 1 and 3 µm inserts the tetraculture system showed significantly higher barrier permeability than for other culture variations. Only the EA.hy 926 cells in monoculture in 1 µm inserts showed a higher amount of leached fluorescence. The accessibility of resazurin for the cells through the membrane in dependence on the pore size is consistent with the results observed for sodium-fluorescein.

The high permeability of endothelial cells can be explained by their *in vivo* function. Endothelial cells are found on the inner side of blood vessels (intima). Depending on the type of blood vessels, these cells have more or less tight and gap junctions resulting in different permeability [24]. In respect to these findings, Transwell™ inserts with 1 µm pore size were chosen, since they allow a stable cultivation of A549 cells at the ALI without affecting significantly the viability.

The presence of the model cells for the innate immune system was shown to have a significant impact on the behavior of A549 epithelial cells, which resulted in decreased transepithelial electrical resistance (TEER) [128]. The expression and presence of functional tight junctions is mainly responsible for high TEER values and primary cultures of AT-II cells can reach TEER values of more than 2000 Ω/cm^2 [303]. A TEER reduction can be considered to be followed by higher paracellular permeability [304]. The presence of functional tight junctions expressed by A549 cells, sealing the epithelium and allowing a high TEER is controversially discussed [236] and under the tested conditions, no significant differences in TEER were observed for freshly seeded cells compared to cultures of several days. Nevertheless, THP-1 and HMC-1 cells in the tetraculture seem to have an impact on the tightness of the cell layer, which resulted in a higher permeability of the tracer solution. Interestingly, a similar observation was described by Lehmann and coworkers in another coculture model of the alveolar barrier [128]. However, up to now it is not known if this increased paracellular permeability in the coculture systems is only restricted to the *in vitro* models or if it can be observed also *in vivo* for the alveolar barrier.

4.2.1.1. STRUCTURE AND DISTRIBUTION OF THE CELLULAR LAYERS IN THE TETRACULTURE SYSTEM

In vivo, the alveolar barrier is composed of a layer single layer of AT-I and AT-II cells, which is separated from the blood vessels and capillaries by the basement membrane [25]. In order to compare the cellular distribution of A549 cells and EA.hy 926 on the two sides of the Transwell™ membrane A549-EA.hy 926-cocultures were analyzed by CLSM. The results show a confluent monolayer of epithelial A549 cells in the apical compartment and a confluent monolayer of endothelial EA.hy 926 cells on the basolateral side of the membrane. Contrary to published reports [275], A549 cells did not form multi-layers even when cultured for several days.

The fate of particles in the alveolar region depends on their physico-chemical properties. Some kinds of NPs can be translocated through the epithelium and reach the bloodstream or other organs [46]. THP-1 cells are used as a surrogate for macrophage-like cells. Upon differentiation stimuli, they differentiate into mature macrophage-like cells and are known to show a considerable phagocytic activity [280].

The macrophage-like THP-1 cells showed the tendency to form colonies once seeded on top of the epithelial layer in coculture. During the differentiation of THP-1 in monoculture, cells did not form such colonies, but rather stayed attached as a single cell layer to the supporting material. A similar observation was made for HMC-1 cells. HMC-1 cells in monoculture, without stimulation floated and only a few cells attached to the support. In the tetraculture, almost all floating HMC-1 cells disappeared and attached to the epithelial layer. Furthermore it was observed that THP-1 and HMC-1 cells formed heterogeneous colonies on top of the A549 epithelial cells, which is not properly reflecting the *in vivo* situation. However, when the cultures were switched to the ALI conditions the colonies disappeared and the differentiated macrophage-like cells and the HMC-1 cells spread more equally on top of the A549 epithelial cells.

In vivo, a population of alveolar macrophages (AM) is efficiently ingesting bacteria and also intercepts particles. AMs are the key players in alveolar clearance and show generally a higher phagocytic activity than macrophages located in other tissues. *In vivo*, a population of alveolar macrophages (AM) is efficiently ingesting bacteria and also intercepts particles. AMs are the key players in alveolar clearance and show generally a higher phagocytic activity than macrophages located in other tissues [77, 78]. In order to evaluate if PMA-differentiated THP-1 cells to fulfill a similar task in the tetraculture system, the activity of these cells to act as particle-intercepting cells was studied under submerged conditions and at the ALI. In the experimental setup 50 nm SiO_2-Rhodamine particles were used that are known to enter both macrophage and epithelial cells in monoculture within relatively short time (data not shown). Principally a single 50 nm SiO_2-Rhodamine particle would be far beyond the detection range of any confocal microscope. However, by the use of CLSM

together with digital image restoration technologies even weak intracellular signals of NPs could be detected [305].

Because of the higher phagocytic activity of the differentiated THP-1 cells compared to the A549 cells, it was expected to find the majority of particles inside of THP-1 cells. However, in A549 cells, no particles were detectable and signals for internalized SiO_2-Rhodamine nanoparticles could be only detected in the THP-1 cells in significant amounts. The signals detected in THP-1 cells were likely the result of a high number of internalized particles that are stored as agglomerates in subcellular compartments, possibly endosomes or lysosomes [306]. This is in line with published results from submerged experiments showing that in a coculture system, the majority of particles can be detected in phagocytically active cells, such as macrophages and dendritic cells [305]. Up to now, the activity of phagocytes to internalize nanomaterials *in vitro* has only been studied under submerged conditions [224, 305, 307, 308]. The presented results demonstrate, that the macrophage-like THP-1 cells in tetraculture model system of the alveolar barrier are fully functional as particle intercepting cells under submerged conditions and at the ALI. Moreover, the use of aerosol exposure systems is more relevant than the exposure under submerged conditions: interactions of particles with molecules present in cell culture media can alter their properties [220], potentially leading to a misevaluation of the hazard of these particles. In addition, it was shown recently that the route of exposure influences the toxicity of particles, leading to a potential underestimation of effects in submerged exposure [309].

4.2.1.2. XENOBIOTIC METABOLISM IN THE DIFFERENT CELL LINES OF THE TETRACULTURE

Exposure to environmental pollutants and chemicals is considered to be the major route by which the human body encounters gases together with aerosolized particles or chemicals [262]. Among the substances to which we are exposed to every day via the ambient air, there are chemicals that pose a considerable risk to the lung, but also to other parts of the

human body, such as the circulatory system [94, 113, 135, 151, 310-312]. Some examples for such hazardous organic chemicals to which humans are accidentally or occupationally exposed by inhalation include PAHs, aromatic amines, aliphatic compounds, aldehydes, etc. [262]. Several of these chemicals can be found in the environment adsorbed to the outer shell of DEPM.

One aim of this PhD work was to develop an *in vitro* system that is able to mimic and to represent most of the characteristics of the barrier *in vivo*. The possibility to exhibit metabolic activity in response to xenobiotics is an important characteristic of such a system. Immune-histochemical analysis from human lungs confirmed the expression of P450 enzymes in alveolar type I and type II cells [313]. To represent the alveolar lining cells, the AT-II cell line A549 was chosen [259]. The potential of A549 cells to show xenobiotic activity is controversially discussed and seems to depend on the experimental setup [261, 262, 314, 315]. A549 were reported to possess xenobiotic activity that was comparable to the activity found in human lung tissue [261], whereas other investigators reported about phase I and phase II metabolic activity to be on a much lower level than in primary tissue samples [262, 315]. In respect to the variable performance of A549 cells in response to xenobiotic compounds, the xenobiotic potential of the cellular batch was characterized, using B[a]P and TCDD as model compounds to evaluate the expression level of *CYP1A1* and *CYP1B1* mRNA.

The basal level of *CYP1A1* mRNA was found to be close to the limit of detection, whereas *CYP1B1* mRNA was clearly detectable in DMSO-treated A549 cells. This is in line with a study, where A549 cells were compared to primary lung tissue [262]. The expression of *CYP1A1* in A549 cells was found to be about 16 times lower than in primary tissue samples. According to this study, the level of *CYP1B1* mRNA in A549 cells under non-induced conditions was already higher than in the analyzed primary tissue samples [262].

When treated with B[a]P, the A549 cells showed a high responsiveness resulting in a fold increase for *CYP1A1* mRNA of more than 400 fold after 48 h. In contrast to *CYP1A1*, *CYP1B1* mRNA was found to be much less inducible with a fold increase of 16 after 48 h of

treatment. Also these results are comparable to already published data with A549 cells [314].

In the literature different results can be found for the activity of CYP1 enzymes in A549 cells [261, 262, 314, 315]. As lung cells, these cells possess per se a considerably low xenobiotic activity compared to the liver [316]. Due to overlapping substrate specificity of CYP1 enzymes, such as CYP1A1, CYP1A2 and CYP1B1 [317], the direct evaluation of an increase of the specific activity of CYP1A1 is difficult and would need a well defined set of specific inhibitors. In order to evaluate if the observed response on the mRNA level was translated into an increase of CYP1 enzyme activity the metabolic activity of A549 cells treated with B[a]P or TCDD for different 24 and 48 h was analyzed in the EROD assay (as described by [241]). In respect to the expected low activity the EROD protocol was modified in order to assure the maximum of sensitivity. However, still no signal could be detected for the enzyme activity. A possibility to explain the missing signal for the EROD activity could be the high level of phase II metabolism in A549 cells [316]. The produced resorufin from the EROD assay could immediately be glucoronidated, and would thereby not be available for the fluorescence measurement [261]. In order to evaluate this possibility, aliquots of supernatants from induced cells were incubated with β-glucoronidase. However, even with the modified protocols the presence of CYP1 enzymatic activity could not be confirmed in the conditions of the presented system.

It is conceivable that the increase for *CYP1A1* and *CYP1B1* mRNA is not necessarily translated into elevated protein levels of both enzymes since *in vitro* studies with HepG2 cells demonstrated that *CYP1A1* mRNA is rapidly degraded due to a loss in poly-A tail [318]. In addition there are several cell-type-specific alternative processing variants for *CYP1B1* mRNA, which may regulate the stability and lifetime of the final transcript [319]. An alternative way besides the EROD assay to confirm CYP1 metabolic activity in A549 cells could be the direct quantification of metabolites from B[a]P metabolism such as 3-hydroxybenzo[a]pyrene [320].

Currently, the A549 cell line is the only cell line with alveolar characteristics that is available. These cells are often compared to normal human bronchial epithelial (NHBE) cells, which are reported to have higher induction levels of CYP1A1 and a considerable enzymatic activity [286]. However, A549 cells and NHBE cells originate from different regions of the lung namely the alveoli (A549) and the bronchi (NHBE).

80% of the PAHs deposited in the alveolar region are rapidly absorbed and transferred into the bloodstream with only little influence from alveolar local metabolism [321]. Only a small fraction of the inhaled PAHs (10 to 20%) remains in the alveoli for a longer time and will be slowly absorbed. As a result of the slow clearance of this fraction the PAHs become extensively metabolized in the airway epithelium despite the low absolute capacity of lung cells for metabolic reactions. A good indicator for this extensive metabolization and creation of reactive intermediates such as various metabolites but also ROS is the high incidence of alveolar tumors (adenocarcinoma) [316]. Interestingly, adenocarcinomas are particularly predominant for individuals living in countries with high levels of air pollution, such as Japan (72% of al lung cancers), Korea (65% of all lung cancers) or China (61% of all lung cancers) [322].

The inducibility of *CYP1A1* and *CYP1B1* mRNA was also evaluated for THP-1 cells, HMC-1 cells and the EA.hy 926 endothelial cells. Unstimulated THP-1 cells were reported to have only low levels of *CYP1A1* and *CYP1B1* together with limited potential to induce these genes by treating the cells with compounds such as B[a]P or TCDD [287, 323]. This is also in line with our results for undifferentiated THP-1 cells.

The differentiated THP-1 cells are responding differently after treatment with B[a]P or TCDD compared to the non-differentiated THP-1 cells. After the differentiation, THP-1 cells responded to the xenobiotic model compounds by upregulating *CYP1A1* and *CYP1B1* mRNA compared to the DMSO-treated control cells. A similar observation was recently described, where the activation of the vitamin D3 receptor enhanced the metabolism of B[a]P via CYP1A1 in THP-1 cells [323]. The activation of the vitamin D3 receptor induces differentiation in THP-1 cells, similar to the differentiation with PMA, where the potential of

THP-1 cells to xenobiotics respond to with an upregulation of *CYP1A1* and *CYP1B1* mRNA becomes increased [264].

Informations about the potential of human mast cells, here represented by the HMC-1 cells, to respond to xenobiotics do to the best of our knowledge not exist. In contrast to the undifferentiated THP-1 cells, HMC-1 cells were able to respond to B[a]P and TCDD exposure with upregulation of *CYP1A1* mRNA. The level of *CYP1B1* mRNA remained constant in HMC-1 cells during treatment with B[a]P and TCDD and did not change significantly compared to the control cells.

Similar to the other tested cell lines, EA.hy 926 were found to exhibit a significant upregulation of *CYP1A1* mRNA after 24 h of treatment compared to the control cells. In contrast to the other cell lines that were used to establish the tetraculture *in vitro* system the level of *CYP1B1* mRNA was below the limit of detection in EA.hy 926 cells. Studies with primary endothelial cells have shown that these cells express *CYP1B1* mRNA and this expression can be even further upregulated by applying shear stress to the endothelium [324, 325]. The lack of the potential to express *CYP1B1* mRNA might be a consequence resulting from the initial establishment of this cell line. EA.hy 926 cells have not been directly isolated as a cell line itself but are somatic cell hybrids between A549 cells and umbilical vein cells that were fused. EA.hy 926 share many characteristics with primary endothelial cells such as shape or expression of endothelial markers like the van Willebrand Factor (vWF) [266], but might have lost certain abilities during the fusion with the A549 cells. The role of CYP1A1 and CYP1B1 for the response of the endothelial cells to DEPM will be discussed in section 4.3.2.1. All cells were able to respond to the xenobiotic model compounds B[a]P and TCDD by showing an upregulation of at least *CYP1A1* mRNA.

4.3. RESPONSE OF THE ENDOTHELIAL PART OF A 3D TETRACULTURE *IN VITRO* MODEL IN A DOSE-CONTROLLED EXPOSURE SCENARIO TO DIESEL EXHAUST PARTICULATE MATTER AT THE AIR-LIQUID-INTERFACE (ALI)

DEPM is suspected to contribute significantly to cardiovascular diseases, such as atherosclerosis, and to exhibit an adverse potential on human health [213]. However, representative model systems to evaluate the hazard of DEPM on the human alveolar barrier were still missing. In this part of the PhD work the question if *in vivo* relevant doses of DEPM can elicit a response in the endothelial cells of the tetraculture model system relevant for the alveolar barrier was investigated.

Many studies that were focusing on the evaluation of the adverse effects of DEPM on human lung *in vitro* used DEPM in extremely high doses between 10 and 100 µg/mL [115, 121, 127, 169, 185, 213, 326, 327]. In respect to the considerations of *in vivo* relevant doses given in the materials and methods part these concentrations are around 100 times higher than what a human would aspirate in a very extreme exposure scenario. When assuming that the dose of a test substance that reaches 1 cm^2 of cell culture area corresponds to 1 cm^2 of 140 m^2 of the inner lung surface, concentrations of up to 10 µg per cm^2 will already represent pulmonary overload [221, 328].

This discrepancy between the applied doses *in vitro* and the *in vivo* relevant range may lead to an overestimation of certain effects whereas small changes in the cells might be overlooked. Regarding the studies mentioned above a missing consensus about how to express the applied dose seems to be an additional drawback within current inhalation toxicology. In submerged experiments, cells are exposed to particles or chemicals in suspension, which results then in a dose given as x µg/mL, assuming an almost equal distribution of the compound in the cell culture medium. However, in ALI experiments, values are frequently given as the particle concentration per m^3 of air and the flow rate per min. In order to make submerged exposure and ALI exposure more comparable, the deposited mass per surface area needs to be known. A commercial aerosol exposure system from

Vitrocell™ was used in the experiments of the thesis [309]. Up to now, the aerosol exposure system from Vitrocell™ is the only system that has proven its performance in several toxicological studies in different laboratories to achieve maximal uniformity during exposure [226, 233-235, 279, 329, 330]. With this system cells can be exposed to any liquid or powder that can be aerosolized. In addition, it is also possible to evaluate the deposition rate of an ALI experiment using quartz crystal microbalances (QCMs). These balances can measure down to 5 ng/cm^2. However, in the preliminary experiments the QCMs were not able to detect correctly the DEPM. This might be a result of the fact that these particles are electrostatically charged and may interfere with the quartz crystal. As a consequence, another method to evaluate the deposition rate of the DEPM was established. In contrast to the QCMs, this method does not allow a real-time evaluation of the deposited mass during the experiments, but can only measure the total amount deposited at the end of the exposure time. However, it is the only method available that can be used for an ALI exposure scenario with DEPM and the device from Vitrocell™.

The method is based on the findings from Rudd and Strom [291]. A standard curve of known DEPM concentrations has to be prepared and to be evaluated using a spectrophotometer. To this standard curves, the deposited amounts at different time-points were compared. The spectrophotometric method delivered reproducible and sensitive results for the deposition of DEPM. Even though the method does not allow real-time dosimetry, it is precise enough to allow a proper dosimetric approach in the relevant range for DEPM.

4.3.1. THE POTENTIAL OF DEPM TO TRIGGER AN NRF2-ORCHESTRATED RESPONSE *IN VITRO* IN THE ENDOTHELIAL PART OF THE TETRACULTURE

The endothelium can be described as a layer of cells separating all systemic organs from circulating xenobiotics [118]. The vascular endothelium is now gaining increasing attention as a major target of toxicants, especially for inhalable compounds or particles. Impaired

function of endothelial cell, such as endothelial dysfunction, can lead to severe diseases, like atherosclerosis and myocardial infarction. An impaired endothelial cell function is characterized by reduced dilatory properties and the increased expression of, surface adhesion molecules critical to inflammation, which are critical for the beginning of a site directed inflammation. Exposures to a variety of air pollutants has been shown to negatively impact endothelial function due to the production of radicals resulting in oxidative stress. The transcription factor Nrf2, which belongs to the group of bZip transcription factors [331] plays an important role for the cellular antioxidant defense. Nrf2 orchestrates cellular defense to electrophiles and oxidants by binding to the antioxidant response element in the promoter regions of cytoprotective genes [332]. In endothelial cells, the Nrf2-mediated response after contact to an oxidative stimulus is expected to be important to maintain the function of the endothelium and to prevent atherosclerosis. One key factor of this defense cascade under the control of Nrf2 is the gene *HMOX1*, which encodes for the enzyme heme oxygenase 1. This enzyme was shown to possess high cytoprotective potential, by scavenging radicals and neutralizing oxidants by the production of heme [157, 333]. In this experiment the potential of DEPM to induce an anti-oxidant response mediated by Nrf2 target gene expression and nuclear translocation of Nrf2 in the endothelial cells of the tetraculture was evaluated. Special attention was paid to the expression level of *HMOX1* mRNA, since its induction was claimed to contribute significantly to cellular redox homeostasis and cytoprotection against radicals [157, 334, 335]. The tetraculture *in vitro* system was exposed to *in vivo* relevant doses of DEPM in order to evaluate the response of the endothelial cells following indirect contact to these particles. Up to now, *in vitro* studies that were focusing on the evaluation of the adverse potential of DEPM on the endothelium, were mostly using DEPM extracts or suspended DEPM (reviewed in [213]). Regarding the anatomy of the human alveolar tract, the direct exposure of endothelial cells to high amounts of DEPM is far from representing the *in vivo* situation and poorly justified [118]. In addition studies that are using extracts from DEPM are not reflecting the full range of the hazard of DEPM since they are not taking into account the role of the carbon core of the particles. With the aerosol

exposure system from Vitrocell™ in combination with the tetraculture *in vitro* system the problems of direct exposure and low relevance of the exposure route can be overcome.

As a first step for the evaluation of the impact of the different doses on the tetraculture *in vitro* system, tetracultures were exposed to considerably low amounts (40 ng/cm^2, 80 ng/cm^2, and 240 ng/cm^2) of DEPM and the changes in cellular viability were monitored at 6, 24 and 48 h after exposure. As expected, the applied doses were not high enough to affect significantly the cellular viability of the DEPM-exposed cells compared to the controls. The results for cellular viability are in line with those of a recently published study where the effects of catalyzed and non-catalyzed diesel on lung cells exposed at the ALI was evaluated [134]. Similar to these findings, the diesel exhaust particles had almost no effect on cellular viability.

Regarding the concept of the hierarchical oxidative stress response, a strong effect of DEPM on cellular viability is not expected in *tier 1* and *tier 2* in contrast to *tier 3*, where extensive apoptosis and necrosis take place [160]. In order to further investigate the cellular response in the tetraculture model system, samples of the undernatant were taken at the same time-points as for the viability testing and the potential secretion of second messengers was analyzed, using a 3 x 10 multiplexed assay. As expected, no significant change in the secretion of any of the evaluated second messengers compared to the control cells was detected. Regarding the results of an ALI exposure study published by Steiner and coworkers, DEPM exposure may even lead to a reduction of the production of pro-inflammatory cytokines [134]. In contrast to the ALI exposure, cells in submerged exposure showed significant increase in the production of pro-inflammatory second messengers, such as IL-8 [115, 117, 162, 175]. However, also in submerged exposure DEPM was found to interfere with the cytokine secretion in macrophage cells [336]. Overall differences in the applied doses need to be considered when comparing the effects.

The differences of the results from ALI exposure and submerged exposure could be explained by two main facts: First, the doses used for ALI exposure experiments were several orders of magnitude lower than those applied for submerged exposure. Second, for

submerged exposure, DEPM suspensions and extracts with organic solvents are frequently used [213]. These extracts increase dramatically the availability of PAHs that are normally bound to the DEPM particle and may even not be at the surface. The higher dose range together with increased availability of PAHs may then result in an overestimation of the observed pro-inflammatory potential.

The same might be true for *in vivo* experiments using pulmonary instillation. Also for these experiments, particle suspensions are generated and afterwards instilled into the airways of the laboratory animal, which might lead to a kind of leaching of PAHs into the solvent and a potential misevaluation of the hazardous potential of DEPM.

Up to now results from the exposure of lung cells and coculture models to DEPM at the ALI are extremely limited and due to the lack of harmonized exposure rate definitions, the results are difficult to compare to each other. In addition, it was shown, that the outcome of experiments with DEPM differs depending on the exposure method [218].

In respect to the results obtained for cellular viability and the secretion of second messengers, the coculture system was still in the state of *tier 1* of the hierarchical oxidative stress response [160] after the exposure to DEPM. This matches also with the data for the evaluation of important marker genes for antioxidant defense and endothelial inflammation that were analyzed for the endothelial part of the tetraculture system at 6, 24 and 48 h after exposure. For the evaluated time-points no significant change for the marker genes, such as *HMOX1, NQO1, ICAM-1* or *VCAM1* could be detected. Besides the evaluation of the marker genes for cellular antioxidant defense and endothelial inflammation, the upregulation the transcription factor NF_kB was analyzed. This transcription factor is known to be involved in the upregulation of cytokines and the transcription of cellular adhesion molecules, such as ICAM-1 and VCAM1 at the beginning of an inflammation [337]. In *tier 2* of the oxidative stress response, the pathways mediated by NF_kB play a major role in antioxidant defense, which involves the production of chemokines, cytokines and adhesion molecules [160]. Data from i*n vivo* from experiments with rodents suggest that NF_kB plays a central role in inflammatory vascular diseases, such as atherosclerosis. It was shown, that the animals in

these studies had enhanced mRNA levels of *NF_kB* enhanced in the endothelium [338, 339]. In order to analyze if the endothelial cells of the tetraculture were able to react in a similar way to the applied DEPM, tetracultures were exposed different doses of DEPM. For the endothelial cells indirectly exposed to 240 ng/cm^2 of DEPM, a significant increase of *NF_kB* mRNA was detected 48 h after the exposure. The increase in *NF_kB* mRNA in endothelial cells at 48 h after the exposure might be the first sign of the beginning of a stress response in the endothelial cells, shifting cellular homeostasis towards *tier 2*. Another indicator to support this hypothesis is the upregulation of *HSP70* mRNA that was significantly increased after 48 h in endothelial cells indirectly exposed to 240 ng/cm^2. HSP70 is a member of the chaperon family and its normal function is to assist the refolding of misfolded proteins [340]. However, under stress, cells start to produce and to release HSP70 [341] and it was shown that organic compounds, such as B[a]P that can also be found in the outer shell of DEPM, were able to induce *HSP70* mRNA expression in lung cells [342]. *In vivo* experiments with rodents demonstrated that HSP70 contributed to endothelial dysfunction and cardiovascular disease [294]. In contrast to the presented results direct exposure of EA.hy 926 cells to DEPM under submerged conditions was not followed by enhanced *NF_kB* mRNA expression [140] but lead to an increased level of *HSP72* mRNA already after 6 h in rodent endothelial cells [124].

The late response for the upregulation of *HSP70* mRNA might be due to the fact that the endothelial cells in the tetraculture have no direct contact to the deposited DEPM. DEPM components, such as B[a]P, need to leach and to diffuse to access the endothelial cells or need to be metabolized by other cell types of the tetraculture to produce second messenger or metabolites that induce the stress response in the endothelial cells. Regarding the results for the metabolic competence of A549 cells, the overall competence of the system is probably very low. As a result potentially produced metabolites are not readily available to affect the endothelial part, but rather need a while to accumulate. This theory is in line with already published results, where A549 cells were exposed to relatively low doses of DEPM.

In these experiments, the protein level of HSP70 was found to be upregulated only at 72 h after the exposure [342].

Overall, the time between exposure and measurement was probably contributing to the fact that no strong cellular reaction could be observed. This might also explain the missing target gene expression for the antioxidant defense genes and the inflammatory marker genes in the endothelial cells of the tetraculture system. The results for *NF_kB* and *HSP70* point towards a cellular reaction after the exposure to 240 ng/cm^2, which takes more time than 48 h to trigger a measurable effect in the cells. However, the increased mRNA level of *HSP70* is not necessarily translated into elevated protein. The translation of increased HSP70 mRNA levels into elevated protein level needs to be confirmed by e.g. western blotting. This should be used as a starting point for future experiments, e.g. to confirm the upregulation of HSP70 protein and the activation of NF_kB-pathway.

HMOX1, *NQO1* and *SOD1* are known to be under the transcriptional control of the ARE together with Nrf2 as important transcription factor [159, 343]. In order to investigate if a missing translocation of Nrf2 in the endothelial cells of the tetraculture could explain the lack of target gene expression, cells were exposed under identical conditions as for the gene expression. The nuclear translocation of Nrf2 in the endothelial cells of the tetraculture was evaluated at 3, 4 and 5 h after the exposure via CLSM. Nuclear translocation could already be detected in cells 3 h after the exposure and reached its maximum 4 h after exposure. Even though the endothelial cells had no direct contact to the DEPM, the indirect exposure lead to a strong nuclear translocation of Nrf2. Compared to a study where bronchial cells were directly treated with DEPM suspensions, the nuclear translocation of Nrf2 in the present study was even higher and comparable to the signal that was observed for direct B[a]P treatment in 16HBE cells [344].

In addition, the translocation efficiency was comparable to EA.hy 926 cells that were exposed to an oxidative stress inducer (AAPH 20 mM for 2 h in monoculture), where all cells showed a positive response after 2 h of exposure.

Experiments with fluorescent NPs have shown, that even 50 nm particles were not able to cross the triculture in the upper part of the *in vitro* system and did not reach the endothelial layer in significant amounts. Therefore, direct contact of the endothelial EA.hy 926 cells to DEPM is very unlikely. It is more reasonable to assume that the cellular response is mediated by some of the components from the outer shell of the DEPM, such as PAHs, that probably leached and were able to reach the endothelial layer to trigger a response [167]. In addition, it seems also reasonable to assume, that in the tetraculture *in vitro* system a kind of cellular crosstalk exists. As a result of this, the direct exposure of the triculture composed of A549, THP-1 and HMC-1 cells may lead to the production of second messengers, which are then able to trigger a response in the endothelial part of the tetraculture without the need of direct contact to DEPM [292].

Despite the clear nuclear signal of Nrf2, no significant change for the expression of target genes was detected under assay conditions. To the best of our knowledge no other group has described a similar observation for Nrf2 and its target genes. One possible explanation could be that the endothelial EA.hy 926 cells might lack an important key factor, linking the nuclear translocation of Nrf2 and the target gene expression of genes under the transcriptional control of the ARE. In general, Nrf2 is activated by phosphorylational modification leading to Keap1/Nrf2 dissociation, nuclear Nrf2 translocation, and finally ARE responsiveness. Recent research has focused on the regulatory mechanisms of Keap1-dependent turnover and translocation of Nrf2 [334]. Under normal cell conditions Keap1 prevents the nuclear accumulation of Nrf2 but some investigators also proposed a stabilization of Nrf2 [345, 346]. After nuclear translocation Nrf2 must interact with other factors such as small Maf, the proto-oncogenes c-Jun and c-Fos, activating transcription factor (ATF)-4 or Fra-1 to be able to bind to the ARE and to induce target gene expression [332, 347-349]. EA.hy 926 cells may have lost one of the above-mentioned factors which are crucial for the target gene expression of ARE genes due to their origin. However, this does not fit to the fact that ARE target gene expression in these cells was recently described [350, 351].

A second possibility to explain the missing target gene expression and the strong nuclear signal of Nrf2 is based on the interaction of DEPM and cellular components. These particles have been described to interfere with parts of the cytoskeleton leading to cytoskeletal dysfunction [352-354]. Up to now it is not clear if the DEPM particles need to interact directly with the cells or if the leaching of PAHs or other components are responsible for the effect on the cytoskeleton. The production of radicals by PAHs can also lead to the disruption of actin filaments [355]. These cytoskeletal filaments are essential for the regulatory role of Keap1 and a disruption has been suggested to be required for nuclear accumulation of Nrf2 [356]. Nrf2 is known to be a nuclear protein and the activity of Keap1 is required for nuclear-cytosolic shuttling to avoid accumulation of Nrf2 in the nucleus [334, 357]. Interestingly, Keap1 has also been found in the nucleus forming a complex together with Nrf2 after stimulation [358]. The potentially leached PAHs could trigger nuclear accumulation of Nrf2 together with Keap1 due to a deregulation of its inhibitor. Due to the inhibitory effect of Keap1 on Nrf2 the ARE would then not be activated. However, this hypothesis needs to be confirmed by additional experiments, together with a well-defined positive control that is suitable for aerosol exposure.

4.3.2. DEPM AS POTENTIAL INDUCER OF AHR NUCLEAR TRANSLOCATION

Besides the alveolar epithelium the endothelial cell layer needs to be considered as an important target for air pollutants and inhaled xenobiotics [118]. DEPM particles carry PAHs on their outer shell and these compounds can be released upon contact with alveolar cells or lining fluids. These leached components could then reach the circulation [167]. The systemic availability of PAHs may potentially affect the endothelium and lead to an upregulation of xenobiotic metabolizing enzymes, such as CYP1A1 and CYP1B1. The gene expression of CYP enzymes can be modulated in response to the activation of key transcription factors by specific substrates. In the lung and the alveolar epithelium, the

activation of AhR by PAHs induces the transcription of *CYP1A1* and *CYP1B1* mRNA [359, 360].

The potential of DEPM and its components to induce the nuclear translocation of the AhR and target gene expression of *CYP1A1* and *CYP1B1* in the endothelial part of the tetraculture after indirect exposure need a thorough discussion. Cells were exposed under similar conditions as for the evaluation of Nrf2 target gene expression and nuclear translocation. Extracts from DEPM or whole DEPM suspensions were used to "simulate" the leaching process and the systemic availability of DEPM-bound PAHs on the endothelium [118]. The majority of the literature focuses on the oxidant effects of DEPM on the endothelium and only little information is available on the susceptibility of endothelial cells to xenobiotics [361]. The oxidative potential of DEPM particles may be a result of the metabolization of the adsorbed PAHs by enzymes of the CYP450 family. In this respect it seems necessary to evaluate the potential of DEPM to induce an upregulation of CYP450 enzymes in the endothelial cells.

The EA.hy 926 cells showed weak translocation efficiency for AhR compared to the signals that was detected for Nrf2 and the AhR signal disappeared at 5 h after the exposure. Regarding the datasheet provided from NIST for the SRM2975 DEPM reference material, the concentration of PAHs in the DEPM powder is extremely low. DEPM powder contains 0.599 mg of B[a]P per kg DEPM. Transferring this value to the experimental setup, where 1.008 µg of DEPM was deposited per Transwell™ at the highest dose of 240 ng/cm^2, the total quantity of B[a]P was only around 5.99 x 10^{-10} mg. The values for the dry weights of other PAHs, such as benzo[*j*]fluoranthene, dibenz[*a,h* + *a,c*]anthracene or picene, that can be found in the DEPM particles, are all similar. Furthermore the endothelial layer is covered by a layer consistent of three other cell types (A549, THP-1 and HMC-1 cells). In this respect, the low translocation efficiency of the AhR after the indirect exposure to DEPM seems not surprising but rather demonstrates the sensitivity of EA.hy 926 cells to detect very low amounts of xenobiotics. Indeed the sensitivity of these endothelial cells compared to other endothelial cell lines has also been confirmed by others [361]. The expression of

CYP1A1 and *CYP1B1* mRNA was evaluated at different time-points following the exposure, in order to analyze if the nuclear translocation of AhR lead to the expression of xenobiotic metabolizing genes. EA.hy 926 showed a significant increase for the expression of *CYP1A1* mRNA at 6 h after exposure but no expression of *CYP1B1* mRNA. The absence of detectable CYP1B1 expression in the endothelial cells was not surprising as they are known to express only a limited set of CYP450 enzymes [316]. Phase I metabolism in endothelial cells is mainly dependent on CYP2J2, which is highly expressed in the human pulmonary endothelium [362]. This enzyme is primarily involved in arachidonic acid metabolism, but was also described to be important for the metabolization of some xenobiotic drugs, such as diclofenac and bufuralol [363]. Regarding the expression of CYP1A1 in human lungs, the expression is mainly restricted to bronchiolar, terminal bronchiolar, and alveolar epithelium [316], but was also found in the respiratory endothelium [364]. The induction of CYP1A1 may be a precondition for the development of peripheral lung cancer in smokers. This assumption is underlined by *in vivo* studies where all individuals that were suffering from lung cancer had induced levels of CYP1A1 in their lungs [42, 364]. Interestingly, EA.hy 926 cells that were exposed in monoculture to 5 µM B[a]P for 24 h showed “just” a 50% higher response for *CYP1A1* mRNA levels. However, these experiments are hardly comparable because of the different exposure times, media conditions and route of exposure. The upregulation of *CYP1A1* mRNA can be explained in two ways: First, the low quantities of PAHs that can be found on the surface of the DEPM particles may be sufficient to induce a measurable response in the endothelial part of the tetraculture already at 6 h after exposure on the transcriptional level leading to the expression of *CYP1A1* mRNA. The second possibility is based on a potential cellular crosstalk between the upper compartment of the tetraculture that comprises the A549, THP-1 and HMC-1 cells and the basolateral compartment with the EA.hy 926 cells. It was shown, that DEPM trigger the production and the release of secondary products, such as arachidonic acid metabolites, in lung epithelial cells and macrophages [365-368]. Arachidonic acid derivatives, such as prostaglandin e2 (PGE2) were described as AhR ligands, inducing *CYP1A1* transcription [369]. It seems

reasonable to assume, that the DEPM deposited in the upper compartment of the tetraculture may have induced the production and the release of arachidonic acid compounds that finally reached the endothelial cells and lead to the upregulation of *CYP1A1* mRNA by binding to the AhR.

Nevertheless, the finding that *in vivo* relevant doses of DEPM particles are able to induce *CYP1A1* mRNA in the endothelial cells of the tetraculture needs to be considered as an important starting point for further mechanistic studies in order to study the cellular cross talk between the different cell types in the tetraculture system.

5. CONCLUDING REMARKS

An improved tetraculture system representing the alveolar barrier has been carefully characterized and adapted for native aerosol exposure. The cultivation of cells at the ALI is a prerequisite for the administration of PM and NPs via aerosol. Resembling the *in vivo* histology of the alveolar barrier the endothelial cells are grown on the basolateral side of the microporous membrane epithelial cells and the model cells for the innate immune system are grown within the Transwell™ insert. This setup ensures a 3D-orientation similar to the organization of the alveoli *in vivo*. Inserts with pores of 1 µm were found to be the most appropriate support for the 3D model system, since they ensure the optimal exchange of nutrients between compartments. Submerged cultures showed elevated levels in ROS production compared to ALI cultures when treated with an oxidative stress inducer, such as AAPH. The macrophage-like THP-1 cells act as particle-intercepting cells and form heterogeneous colonies with mast cells (HMC-1) in the *in vitro* system as shown by CLSM. Overall the results demonstrate that the proposed system is behaving in a physiological way and has characteristics that resemble the *in vivo* organization of the alveolar region. The macrophages are active and efficiently intercept particles in submerged conditions and exposed to an aerosol at the air-liquid-interface.

The system proved its functionality in a low dose real world exposure scenario with native DEPM particles. A method, which allows to determine the deposited dose of DEPM per cm^2 of cell culture area has been established.

The doses that were used for DEPM exposure are in contrast with many published studies in the relevant range for human health. The results indicate that the applied doses of DEPM particles trigger the nuclear translocation of the transcription factor Nrf2 that is important to activate transcription of target genes for antioxidant defense in the endothelial part of the tetraculture. Despite the clear nuclear accumulation of Nrf2, no target gene expression could be detected.

In contrast to the results for Nrf2 indirect DEPM exposure of the tetraculture system at the ALI lead to significant upregulation of *CYP1A1* mRNA and nuclear translocation of AhR. Regarding the low amounts of potential AhR ligands and inducer for *CYP1A1* the tetraculture system seems to possess high sensitivity to detect xenobiotic compounds.

DEPM particles were exhibiting a measurable effect on the endothelial part of the *in vitro* tetraculture system in this real life exposure scenario and the findings may help to design even more realistic *in vitro* exposure scenarios. Overall, the use of the tetraculture system may lead to a more realistic judgment regarding the hazard of new compounds in the future.

6. EMERGING CHALLENGES AND FUTURE PERSPECTIVES

Regarding the results from the characterization of the tetraculture system, it is still not fully clear if A549 cells possess a CYP1 activity or not. Since CYP1 metabolism is important for the activation of xenobiotics, which can also be found as parts of DEPM, the question about the metabolic competence of A549 cells but also of the tetraculture system should be further evaluated. For future experiments, the direct evaluation of metabolites from B[a]P metabolism could be used as a possibility to confirm the presence of CYP1 activity and to compare the potency to other well-characterized cell lines and coculture models.

An additional challenge that needs to be addressed for future experiments is the general lack of well-defined positive controls for ALI exposure experiments. A proper positive control would contribute significantly to improve the design of future studies, allowing better comparisons between different studies and between different laboratories. Such positive control particles are under development for experiments with NPs, but still not commercially available for use in other laboratories.

Within this context, the reason for the clear nuclear translocation but missing target gene expression should be addressed, using a well-defined positive control to trigger the expression of Nrf2 target genes in the endothelial cells in order to prove the functionality of the Nrf2 pathway in the EA.hy 926 cells.

Together with the implementation of robust positive controls, the results from the experiments regarding the potential activation of Nrf2-related pathways by DEPM should be used as a starting point to further investigate the indirect effects of low DEPM doses on the endothelium. Since first responses for the target gene expression appeared after 48 h after the exposure, it seems reasonable to increase the time after exposure to 72 h and to evaluate the cellular response.

Combining the exposure experiments with a next generation sequencing approach for the endothelial part of the tetraculture system may lead to a deeper understanding of the pathways that are involved in linking air pollution and cardiovascular disease.

Probably the most interesting but also most challenging future perspective will be the implementation of protocols that allow the separation of A549, HMC-1 and THP-1 cells from the triculture in the upper compartment. The separation the different cell lines after the exposure will offer the possibility to study the response of the cell types from the coculture system to DEPM while being in physical contact to other cell types. The separation could be achieved by using magnetic beads that are coupled to antibodies, which are specific for surface molecules that can be found on top of the different cell types. After the separation, the cells could be used for qRT-PCR experiments and/or a proteomic approach. This would allow studying the response in each cell line after being exposed to DEPM and in close contact to the other cell lines.

Therefore, future research efforts could involve the following aspects:

- Evaluation of representative metabolites from B[a]P metabolism in A549 cells and the tetraculture system to evaluate their potential for metabolizing xenobiotics
- Implementing a positive control suitable for ALI exposure experiments with DEPM and nanomaterials
- Using the potential positive control to proof the functionality of the Nrf2 pathway in EA.hy 926 endothelial cells
- Further investigation of the indirect effects of low doses of DEPM on the endothelium using a next generation sequencing approach
- Evaluation of the response of the endothelial cells of the tetraculture system at 72 h after the exposure
- Implementation of protocols to allow the separation of the different cell lines of the triculture system after the exposure to DEPM in order to evaluate the different responses of the different cell types of the triculture from the upper compartment

REFERENCES

1. Alfaro-Moreno E, Nawrot TS, Vanaudenaerde BM, Hoylaerts MF, Vanoirbeek JA, Nemery B, Hoet PH: **Co-cultures of multiple cell types mimic pulmonary cell communication in response to urban PM10.** *Eur Respir J* 2008, **32:**1184-1194.
2. Buzea C, Pacheco II, Robbie K: **Nanomaterials and nanoparticles: sources and toxicity.** *Biointerphases* 2007, **2:**MR17-172.
3. Taylor DA: **Dust in the wind.** *Environ Health Perspect* 2002, **110:**A80-87.
4. Akimoto H: **Global air quality and pollution.** *Science* 2003, **302:**1716-1719.
5. Krzyzanowski M: **WHO Air Quality Guidelines for Europe.** *J Toxicol Environ Health A* 2008, **71:**47-50.
6. Gutleb AC: **Potential of in vitro methods for mechanistic studies of particulate matter-induced cardiopulmonary toxicity.** *Crit Rev Environ Sci Technol* 2011, **41:**1971-2002.
7. Logan WP: **Mortality in the London fog incident, 1952.** *Lancet* 1953, **1:**336-338.
8. Bell ML, Davis DL, Fletcher T: **A retrospective assessment of mortality from the London smog episode of 1952: the role of influenza and pollution.** *Environ Health Perspect* 2004, **112:**6-8.
9. Krein A, Udelhoven T, Audinot JN, Hissler C, Guignard C, Pfister L, Migeon HN, Hoffmann L: **Imaging chemical patches on near-surface atmospheric dust particles with NanoSIMS 50 to identify material sources.** *Water, Air, & Soil Pollution: Focus* 2008, **8:**495-503.
10. Buchholz S, Krein A, Junk J, Gutleb AC, Pfister L, Hoffmann L: **Modeling,measuring, and characterizing airborne particles: case studies from southwestern Luxembourg.** *Crit Rev Environ Sci Technol* 2011, **41:**2077-2096.
11. Meesters JA, Veltman K, Hendriks AJ, van de Meent D: **Environmental exposure assessment of engineered nanoparticles: why REACH needs adjustment.** *Integr Environ Assess Manag* 2013, **9:**e15-26.
12. Borm PJ, Robbins D, Haubold S, Kuhlbusch T, Fissan H, Donaldson K, Schins R, Stone V, Kreyling W, Lademann J, et al: **The potential risks of nanomaterials: a review carried out for ECETOC.** *Part Fibre Toxicol* 2006, **3**.
13. Möller W, Felten K, Sommerer K, Scheuch G, Meyer G, Meyer P, Haussinger K, Kreyling WG: **Deposition, retention, and translocation of ultrafine particles from the central airways and lung periphery.** *Am J Respir Crit Care Med* 2008, **177:**426-432.
14. Nemmar A, Hoylaerts MF, Hoet PHM, Nemery B: **Possible mechanisms of the cardiovascular effects of inhaled particles: systemic translocation and prothrombotic effects.** *Toxicol Lett* 2004, **149:**243-253.
15. Schulz H, Harder V, Ibald-Mulli A, Khandoga A, Koenig W, Krombach F, Radykewicz R, Stampfl A, Thorand B, Peters A: **Cardiovascular effects of fine and ultrafine particles.** *J Aerosol Med* 2005, **18:**1-22.
16. Oberdörster G, Oberdörster E, Oberdörster J: **Nanotoxicology: an emerging discipline evolving from studies of ultrafine particles.** *Environ Health Perspect* 2005, **113:**823-839.
17. Choi HS, Ashitate Y, Lee JH, Kim SH, Matsui A, Insin N, Bawendi MG, Semmler-Behnke M, Frangioni JV, Tsuda A: **Rapid translocation of nanoparticles from the lung airspaces to the body.** *Nat Biotechnol* 2010, **28:**1300-1303.
18. Oberdörster G, Sharp Z, Atudorei V, Elder A, Gelein R, Kreyling W, Cox C: **Translocation of inhaled ultrafine particles to the brain.** *Inhal Toxicol* 2004, **16:**437-445.
19. Wang J, Liu Y, Jiao F, Lao F, Li W, Gu Y, Li Y, Ge C, Zhou G, Li B, et al: **Time-dependent translocation and potential impairment on central nervous system by intranasally instilled TiO(2) nanoparticles.** *Toxicology* 2008, **254:**82-90.
20. Tyler WS: **Comparative subgross anatomy of lungs. Pleuras, interlobular septa, and distal airways.** *Am Rev Respir Dis* 1983, **128:**32-36.

21. Mann-Jong M, Shih L, Wu R: **Pulmonary Epithelium: Cell Types and Functions.** In *The Pulmonary Epithelium in Health and Disease.* Edited by Proud M. West Sussex: John Wiley & Sons Ltd; 2008

22. Magno MG, Fishman AP: **Origin, distribution, and blood flow of bronchial circulation in anesthetized sheep.** *J Appl Physiol* 1982, **53:**272-279.

23. BéruBé K, Prytherch Z, Job C, Hughes T: **Human primary bronchial lung cell constructs: The new respiratory models.** *Toxicology* 2010, **278:**311-318.

24. Leonhardt H: *Histologie, Zytologie und Mikroanatomie des Menschen.* Stuttgart: Georg Thieme Verlag; 1990.

25. Mühlfeld C, Ochs M: **Functional Aspects of Lung Structure as Related to Interaction with Particles.** In *Particle-Lung Interactions - Second Edition.* Edited by Gehr P, Mühlfeld C, Rothen-Rutishauser B, Blank F. New York: Informa Healthcare USA, Inc.; 2010

26. Proud D: *The Pulmonary Epithelium in Health and Disease.*: John Wiley and sons Ltd.; 2008.

27. Sorokin SP: **The cells of the lungs.** In *Morphology of Experimental Respiratory Carcinogenesis.* Edited by Nettesheim P, Hannar MG, Deatherage JW: Atomic Energy Commission, Division of Technical Information; 1970: 40: *21 AEX Symosium Series*].

28. Breeze RG, Wheeldon EB: **The cells of the pulmonary airways.** *Am Rev Respir Dis* 1977, **116:**705-777.

29. Ochs M, Weibel ER: **Functional Design of the Human Lung for Gas Exchange.** In *Fishman's Pulmonary Diseases and Disorders. Volume* 1 & 2. Edited by Fishman AP: McGray-Hill Medical; 2008

30. Topinka J, Schwarz LR, Wiebel FJ, Cerna M, Wolff T: **Genotoxicity of urban air pollutants in the Czech Republic. Part II. DNA adduct formation in mammalian cells by extractable organic matter.** *Mutat Res* 2000, **469:**83-93.

31. Binkova B, Sram RJ: **The genotoxic effect of carcinogenic PAHs, their artificial and environmental mixtures (EOM) on human diploid lung fibroblasts.** *Mutat Res* 2004, **547:**109-121.

32. Binkova B, Vesely D, Vesela D, Jelinek R, Sram RJ: **Genotoxicity and embryotoxicity of urban air particulate matter collected during winter and summer period in two different districts of the Czech Republic.** *Mutat Res* 1999, **440:**45-58.

33. Marshall MV, McLemore TL, Martin RR, Wray NP, Busbee DL, Cantrell ET: **Benzo(a)pyrene activation and detoxification by human pulmonary alveolar macrophages and lymphocytes. Polynuclear aromatic hydrocarbons.** In *Polynuclear aromatic hydrocarbons Chemistry & biological effects.* Edited by Bjorseth A, Dennis AJ: Battelle Press; 1979

34. McLemore TL, Martin RR, Toppell KL, Busbee DL, Cantrell ET: **Comparison of aryl hydrocarbon hydroxylase induction in cultured blood lymphocytes and pulmonary macrophages.** *J Clin Invest* 1977, **60:**1017-1024.

35. McLemore TL, Martin RR: **In vitro induction of aryl hydrocarbon hydroxylase in human pulmonary alveolar macrophages by benzanthracene.** *Cancer Lett* 1977, **2:**327-333.

36. McLemore TL, Warr GA, Martin RR: **Induction of aryl hydrocarbon hydroxylase in human pulmonary alveolar macrophages and peripheral lymphocytes by cigarette tars.** *Cancer Lett* 1977, **2:**161-167.

37. Mersch-Sundermann V, Mochayedi S, Kevekordes S: **Genotoxicity of polycyclic aromatic hydrocarbons in Escherichia coli PQ37.** *Mutat Res* 1992, **278:**1-9.

38. International Agency for Research on Cancer (IARC): **Polynuclear Aromatic Compounds, Part I, Chemical, Environmental and Experimental Data.** Lyon: WHO; 1983.

39. Whitlock JP, Jr., Okino ST, Dong L, Ko HP, Clarke-Katzenberg R, Ma Q, Li H: **Cytochromes P450 5: induction of cytochrome P4501A1: a model for analyzing mammalian gene transcription.** *FASEB J* 1996, **10:**809-818.

40. Jones PB, Durrin LK, Galeazzi DR, Whitlock JP, Jr.: **Control of cytochrome P1-450 gene expression: analysis of a dioxin-responsive enhancer system.** *Proc Natl Acad Sci U S A* 1986, **83:**2802-2806.

41. Endo K, Uno S, Seki T, Ariga T, Kusumi Y, Mitsumata M, Yamada S, Makishima M: **Inhibition of aryl hydrocarbon receptor transactivation and DNA adduct formation by CYP1 isoform-selective metabolic deactivation of benzo[a]pyrene.** *Toxicol Appl Pharmacol* 2008, **230:**135-143.

42. Piipari R, Savela K, Nurminen T, Hukkanen J, Raunio H, Hakkola J, Mantyla T, Beaune P, Edwards RJ, Boobis AR, Anttila S: **Expression of CYP1A1, CYP1B1 and CYP3A, and polycyclic aromatic hydrocarbon-DNA adduct formation in bronchoalveolar macrophages of smokers and non-smokers.** *Int J Cancer* 2000, **86:**610-616.

43. Reyes H, Reisz-Porszasz S, Hankinson O: **Identification of the Ah receptor nuclear translocator protein (Arnt) as a component of the DNA binding form of the Ah receptor.** *Science* 1992, **256:**1193-1195.

44. Pinkus R, Weiner LM, Daniel V: **Role of quinone-mediated generation of hydroxyl radicals in the induction of glutathione S-transferase gene expression.** *Biochemistry* 1995, **34:**81-88.

45. Rushmore TH, Morton MR, Pickett CB: **The antioxidant responsive element. Activation by oxidative stress and identification of the DNA consensus sequence required for functional activity.** *J Biol Chem* 1991, **266:**11632-11639.

46. Hoet PHM, Brüske-Hohlfeld I, Salata OV: **Nanoparticles - known and unknown health risks.** *J Nanobiotechnol* 2004, **2**.

47. International Commission on Radiological Protection: **IRCP Publication 66: Human Respiratory Model For Radiological Protection.** In *Annals of the IRCP*, vol. 24. pp. 1-300; 1994:1-300.

48. Donaldson K, Stone V, Clouter A, Renwick L, MacNee W: **Ultrafine particles.** *Occup Environ Med* 2001, **58:**211-216, 199.

49. Solomon PA, Costa DL: **Ambient Tropospheric Particles.** In *Particle-Lung Interactions (2nd ed).* Edited by Gehr P, Mühlfeld C, Rothen-Rutishauser B, Blank F. Informa Healthcare USA, Inc.; 2010: 17-38

50. Möller W, Kreyling WG, Schmid O, Semmler-Behnke M, Schulz H: **Deposition, retention and clearance, and translocation of inhaled fine and nano-sized particles in the respiratory tract.** In *Particle-Lung Interactions (2nd ed).* Edited by Gehr P, Mühlfeld C, Rothen-Rutishauser B, Blank F: Informa Healthcare USA, Inc.; 2010: 79-108

51. Seinfeld JH, Pandis SN: *Atmospheric Chemistry and Physics from Air Pollution to Climate Change.* New York: John Wiley and Sons, Inc.; 1998.

52. Brooks AL, Wolff RK, Royer RE, Clark CR, Sanchez A, McClellan RO: **Deposition and biological availability of diesel particles and their associated mutagenic chemicals.** *Environ Int* 1981, **5:**263-267.

53. Yeates DB, Mayhugh M: **A phoswich multidetector probe for measuring tracheal mucus velocity.** *Clin Phys Physiol Meas* 1984, **5:**313-320.

54. Morgan L, Pearson M, de Iongh R, Mackey D, van der Wall H, Peters M, Rutland J: **Scintigraphic measurement of tracheal mucus velocity in vivo.** *Eur Respir J* 2004, **23:**518-522.

55. Chan TL, Lee PS, Hering WE: **Deposition and clearance of inhaled diesel exhaust particles in the respiratory tract of Fischer rats.** *J Appl Toxicol* 1981, **1:**77-82.

56. Geiser M, Casaulta M, Kupferschmid B, Schulz H, Semmler-Behnke M, Kreyling W: **The role of macrophages in the clearance of inhaled ultrafine titanium dioxide particles.** *Am J Respir Cell Mol Biol* 2008, **38:**371-376.

57. Crapo JD, Barry BE, Gehr P, Bachofen M, Weibel ER: **Cell number and cell characteristics of the normal human lung.** *Am Rev Respir Dis* 1982, **126:**332-337.

58. Crapo JD, Young SL, Fram EK, Pinkerton KE, Barry BE, Crapo RO: **Morphometric characteristics of cells in the alveolar region of mammalian lungs.** *Am Rev Respir Dis* 1983, **128:**42-46.

59. Bartels H: **The air-blood barrier in the human lung. A freeze-fracture study.** *Cell Tissue Res* 1979**:**269-285.

60. Evans MJ, Cabral LJ, Stephens RJ, Freeman G: **Transformation of alveolar type 2 cells to type 1 cells following exposure to NO2.** *Exp Mol Pathol* 1975, **22:**142-150.

61. Pison U, Max M, Neuendank A, Weissbach S, Pietschmann S: **Host defence capacities of pulmonary surfactant: evidence for 'non-surfactant' functions of the surfactant system.** *Eur J Clin Invest* 1994, **24:**586-599.

62. Wright JR: **Host defense functions of pulmonary surfactant.** *Biol Neonate* 2004, **85:**326-332.

63. Crouch EC: **Surfactant protein-D and pulmonary host defense.** *Respir Res* 2000, **1:**93-108.

64. Singh G, Katyal SL, Brown WE, Collins DL, Mason RJ: **Pulmonary lysozyme--a secretory protein of type II pneumocytes in the rat.** *Am Rev Respir Dis* 1988, **138:**1261-1267.

65. Haller EM, Shelley SA, Montgomery MR, Balis JU: **Immunocytochemical localization of lysozyme and surfactant protein A in rat type II cells and extracellular surfactant forms.** *J Histochem Cytochem* 1992, **40:**1491-1500.

66. Mason RJ, Williams MC: **Type II alveolar cell. Defender of the alveolus. .** *Am Rev Respir Dis* 1977**:**81-91.

67. Fehrenbach H: **Alveolar epithelial type II cell: defender of the alveolus revisited.** *Respir Res* 2001**:**33-46.

68. Finkelstein JN, Johnston C, Barrett T, Oberdorster G: **Particulate-cell interactions and pulmonary cytokine expression.** *Environ Health Perspect* 1997, **105 Suppl 5:**1179-1182.

69. O'Brien AD, Standiford TJ, Christensen PJ, Wilcoxen SE, Paine R, 3rd: **Chemotaxis of alveolar macrophages in response to signals derived from alveolar epithelial cells.** *J Lab Clin Med* 1998, **131:**417-424.

70. Blau H, Riklis S, Kravtsov V, Kalina M: **Secretion of cytokines by rat alveolar epithelial cells: possible regulatory role for SP-A.** *Am J Physiol* 1994, **266:**L148-155.

71. Christensen PJ, Armstrong LR, Fak JJ, Chen GH, McDonald RA, Toews GB, Paine R, 3rd: **Regulation of rat pulmonary dendritic cell immunostimulatory activity by alveolar epithelial cell-derived granulocyte macrophage colony-stimulating factor.** *Am J Respir Cell Mol Biol* 1995, **13:**426-433.

72. Worgall S, Singh R, Leopold PL, Kaner RJ, Hackett NR, Topf N, Moore MA, Crystal RG: **Selective expansion of alveolar macrophages in vivo by adenovirus-mediated transfer of the murine granulocyte-macrophage colony-stimulating factor cDNA.** *Blood* 1999, **93:**655-666.

73. Weissbach S, Neuendank A, Pettersson M, Schaberg T, Pison U: **Surfactant protein A modulates release of reactive oxygen species from alveolar macrophages.** *Am J Physiol* 1994, **267:**L660-666.

74. Stamme C, Walsh E, Wright JR: **Surfactant protein A differentially regulates IFN-gamma- and LPS-induced nitrite production by rat alveolar macrophages.** *Am J Respir Cell Mol Biol* 2000, **23:**772-779.

75. Little FF, Wilson KC, Berman JS, Center DM: **Lymphocyte- and Macrophage-Mediated Inflammation in the Lung.** In *Fishman's Pulmonary Diseases and Disorders - Fourth Edition. Volume* 1. Edited by Fishman AP: The McGraw-Hill Companies; 2008

76. Sibille Y, Reynolds HY: **Macrophages and polymorphonuclear neutrophils in lung defense and injury.** *Am Rev Respir Dis* 1990, **141:**471-501.

77. Geiser M, Baumann M, Cruz-Orive LM, Im Hof V, Waber U, Gehr P: **The effect of particle inhalation on macrophage number and phagocytic activity in the intrapulmonary conducting airways of hamsters.** *Am J Respir Cell Mol Biol* 1994, **10:**594-603.

78. Brain JD: **Lung macrophages: how many kinds are there? What do they do?** *Am Rev Respir Dis* 1988, **137:**507-509.

79. Chono S, Tauchi Y, Morimoto K: **Influence of particle size on the distributions of liposomes to atherosclerotic lesions in mice.** *Drug Dev Ind Pharm* 2006, **32:**125-135.

80. Oberdörster G, Ferin J, Lehnert BE: **Correlation between particle size, *in vivo* particle persistence, and lung injury.** *Environ Health Perspect* 1994, **102:**172-179.

81. Nel A, Xia T, Madler L, Li N: **Toxic potential of materials at the nanolevel.** *Science* 2006, **311:**622-627.

82. Robert MA, VanBergen S, Kleeman MJ, Jakober CA: **Size and composition distributions of particulate matter emissions: part 1--light-duty gasoline vehicles.** *J Air Waste Manag Assoc* 2007, **57:**1414-1428.

83. Valavanidis A, Fiotakis K, Vlachogianni T: **Airborne particulate matter and human health: toxicological assessment and importance of size and composition of particles for oxidative damage and carcinogenic mechanisms.** *J Environ Sci Health C Environ Carcinog Ecotoxicol Rev* 2008, **26:**339-362.

84. Turnbull AB, Harrison RM: **Major component contributions to PM10 composition in the UK atmosphere.** *Atmos Environ* 2000, **34:**3129-3137.

85. Zielinska B, Sagebiel J, McDonald JD, Whitney K, Lawson DR: **Emission rates and comparative chemical composition from selected in-use diesel and gasoline-fueled vehicles.** *J Air Waste Manag Assoc* 2004, **54:**1138-1150.

86. Sydbom A, Blomberg A, Parnia S, Stenfors N, Sandstrom T, Dahlen SE: **Health effects of diesel exhaust emissions.** *Eur Respir J* 2001, **17:**733-746.

87. Scheepers PT, Bos RP: **Combustion of diesel fuel from a toxicological perspective. I. Origin of incomplete combustion products.** *Int Arch Occup Environ Health* 1992, **64:**149-161.

88. Scheepers PT, Bos RP: **Combustion of diesel fuel from a toxicological perspective. II. Toxicity.** *Int Arch Occup Environ Health* 1992, **64:**163-177.

89. Heinrich J, Wichmann HE: **Traffic related pollutants in Europe and their effect on allergic disease.** *Curr Opin Allergy Clin Immunol* 2004, **4:**341-348.

90. Kagawa J: **Health effects of diesel exhaust emissions--a mixture of air pollutants of worldwide concern.** *Toxicology* 2002, **181-182:**349-353.

91. Mohan D, Thiyagarajan D, Murthy PB: **Toxicity of exhaust nanoparticles.** *African Journal of Pharmacy and Pharmacology* 2013, **7:**318-331.

92. WHO Office for Europe: **Air Quality Guidelines for Europe.** vol. European Series Volume 23. Copenhagen: World Health Organization Regional Publications.

93. McClellan RO, Hesterberg TW, Wall JC: **Evaluation of carcinogenic hazard of diesel engine exhaust needs to consider revolutionary changes in diesel technology.** *Regul Toxicol Pharmacol* 2012, **63:**225-258.

94. Pope CA, 3rd: **Respiratory disease associated with community air pollution and a steel mill, Utah Valley.** *Am J Public Health* 1989, **79:**623-628.

95. Schwartz J, Dockery DW: **Increased mortality in Philadelphia associated with daily air pollution concentrations.** *Am Rev Respir Dis* 1992, **145:**600-604.

96. Schwartz J, Dockery DW: **Particulate air pollution and daily mortality in Steubenville, Ohio.** *Am J Epidemiol* 1992, **135:**12-19; discussion 20-15.

97. Woolcock AJ, Peat JK: **Evidence for the increase in asthma worldwide.** *Ciba Found Symp* 1997, **206:**122-134; discussion 134-129, 157-129.

98. Ertle AR, London MR: **Insights into asthma prevalence in Oregon.** *J Asthma* 1998, **35:**281-289.

99. Crain EF, Weiss KB, Bijur PE, Hersh M, Westbrook L, Stein RE: **An estimate of the prevalence of asthma and wheezing among inner-city children.** *Pediatrics* 1994, **94:**356-362.

100. Persky VW, Slezak J, Contreras A, Becker L, Hernandez E, Ramakrishnan V, Piorkowski J: **Relationships of race and socioeconomic status with prevalence, severity, and symptoms of asthma in Chicago school children.** *Ann Allergy Asthma Immunol* 1998, **81:**266-271.

101. Senthilselvan A: **Prevalence of physician-diagnosed asthma in Saskatchewan, 1981 to 1990.** *Chest* 1998, **114:**388-392.

102. Mannino DM, Homa DM, Pertowski CA, Ashizawa A, Nixon LL, Johnson CA, Ball LB, Jack E, Kang DS: **Surveillance for asthma--United States, 1960-1995.** *MMWR CDC Surveill Summ* 1998, **47:**1-27.

103. World Health Organization: **Global surveillance, prevention and control of chronic respiratory diseases: a comprehensive approach.**; 2007.

104. International Program on Chemical Safety: **Environmental Health Criteria 171, Diesel Fuel and Exhaust Emissions.**; 1996.

105. Tian L, Lawrence DA: **Metal-induced modulation of nitric oxide production in vitro by murine macrophages: lead, nickel, and cobalt utilize different mechanisms.** *Toxicol Appl Pharmacol* 1996, **141:**540-547.

106. Mills NL, Tornqvist H, Robinson SD, Gonzalez M, Darnley K, MacNee W, Boon NA, Donaldson K, Blomberg A, Sandstrom T, Newby DE: **Diesel exhaust inhalation causes vascular dysfunction and impaired endogenous fibrinolysis.** *Circulation* 2005, **112:**3930-3936.

107. Heitzer T, Schlinzig T, Krohn K, Meinertz T, Munzel T: **Endothelial dysfunction, oxidative stress, and risk of cardiovascular events in patients with coronary artery disease.** *Circulation* 2001, **104:**2673-2678.

108. Okayama Y, Kuwahara M, Suzuki AK, Tsubone H: **Role of reactive oxygen species on diesel exhaust particle-induced cytotoxicity in rat cardiac myocytes.** *J Toxicol Environ Health A* 2006, **69:**1699-1710.

109. Stoeger T, Takenaka S, Frankenberger B, Ritter B, Karg E, Maier K, Schulz H, Schmid O: **Deducing in vivo toxicity of combustion-derived nanoparticles from a cell-free oxidative potency assay and metabolic activation of organic compounds.** *Environ Health Perspect* 2009, **117:**54-60.

110. Ikeda M, Shitashige M, Yamasaki H, Sagai M, Tomita T: **Oxidative modification of low density lipoprotein by diesel exhaust particles.** *Biol Pharm Bull* 1995, **18:**866-871.

111. Aam BB, Fonnum F: **Carbon black particles increase reactive oxygen species formation in rat alveolar macrophages in vitro.** *Arch Toxicol* 2007, **81:**441-446.

112. Miller MR, Borthwick SJ, Shaw CA, McLean SG, McClure D, Mills NL, Duffin R, Donaldson K, Megson IL, Hadoke PWF, Newby DE: **Direct Impairment of Vascular Function by Diesel Exhaust Particulate Through Reduced Bioavailability of Endothelium-Derived Nitric Oxide Induced by Superoxide Free Radicals.** *Environ Health Perspect* 2008.

113. Miller MR, Shaw CA, Langrish JP: **From particles to patients: oxidative stress and the cardiovascular effects of air pollution.** *Future Cardiology* 2012, **8:**577-602.

114. Aam BB, Fonnum F: **ROS scavenging effects of organic extract of diesel exhaust particles on human neutrophil granulocytes and rat alveolar macrophages.** *Toxicology* 2007, **230:**207-218.

115. Boland S, Baeza-Squiban A, Fournier T, Houcine O, Gendron MC, Chevrier M, Jouvenot G, Coste A, Aubier M, Marano F: **Diesel exhaust particles are taken up by human airway epithelial cells in vitro and alter cytokine production.** *Am J Physiol* 1999, **276:**L604-613.

116. van Berlo D, Hullmann M, Schins RPF: **Toxicology of Ambient Particulate Matter.** In *Molecular, Clinical and Environmental Toxicology. Volume* 101. Edited by Luch A. Basel: Springer Basel; 2012: 165-217

117. Abe S, Takizawa H, Sugawara I, Kudoh S: **Diesel exhaust (DE)-induced cytokine expression in human bronchial epithelial cells: a study with a new cell exposure system to freshly generated DE *in vitro*.** *Am J Respir Cell Mol Biol* 2000, **22:**296-303.

118. Campen MJ: **Vascular endothelium as a target of diesel particulate matter-associated toxicants.** *Arch Toxicol* 2012, **86:**517-518.

119. Chan RC, Wang M, Li N, Yanagawa Y, Onoe K, Lee JJ, Nel AE: **Pro-oxidative diesel exhaust particle chemicals inhibit LPS-induced dendritic cell responses involved in T-helper differentiation.** *J Allergy Clin Immunol* 2006, **118:**455-465.

120. Chaudhuri N, Paiva C, Donaldson K, Duffin R, Parker LC, Sabroe I: **Diesel exhaust particles override natural injury-limiting pathways in the lung.** *Am J Physiol Lung Cell Mol Physiol* 2010.

121. Cooney DJ, Hickey AJ: **Cellular response to the deposition of diesel exhaust particle aerosols onto human lung cells grown at the air-liquid interface by inertial impaction.** *Toxicol In Vitro* 2011, **25:**1953-1965.

122. Furuyama A, Hirano S, Koike E, Kobayashi T: **Induction of oxidative stress and inhibition of plasminogen activator inhibitor-1 production in endothelial cells following exposure to organic extracts of diesel exhaust particles and urban fine particles.** *Arch Toxicol* 2005, **80:**154-162.

123. Garshick E, Laden F, Hart JE, Rosner B, Smith TJ, Dockery DW, Speizer FE: **Lung Cancer in Railroad Workers Exposed to Diesel Exhaust.** *Environ Health Perspect* 2004, **112:**1539-1543.

124. Hirano S, Furuyama A, Koike E, Kobayashi T: **Oxidative-stress potency of organic extracts of diesel exhaust and urban fine particles in rat heart microvessel endothelial cells.** *Toxicology* 2003, **187:**161-170.

125. Hiura TS, Kaszubowski MP, Li N, Nel AE: **Chemicals in diesel exhaust particles generate reactive oxygen radicals and induce apoptosis in macrophages.** *The Journal of Immunology* 1999, **163:**5582-5591.

126. Iba MM, Shin M, Caccavale RJ: **Cytochromes P4501 (CYP1): Catalytic activities and inducibility by diesel exhaust particle extract and benzo[a]pyrene in intact human lung ex vivo.** *Toxicology* 2010, **273:**35-44.

127. Ikeda M, Watarai K, Suzuki M, Ito T, Yamasaki H, Sagai M, Tomita T: **Mechanism of pathophysiological effects of diesel exhaust particles on endothelial cells.** *Environ Toxicol Pharmacol* 1998, **6:**117-123.

128. Lehmann A, Blank F, Baum O, Gehr P, Rothen-Rutishauser B: **Diesel exhaust particles modulate the tight junction protein occludin in lung cells in vitro.** *Particle and Fibre Toxicology* 2009, **6**.

129. Lipsett M, Campleman S: **Occupational exposure to diesel exhaust and lung cancer: a meta-analysis.** *Am J Public Health* 1999, **89:**1009-1017.

130. Löndahl J, Swietlicki E, Rissler J, Bengtsson A, Boman C, Blomberg A, Sandström T: **Experimental determination of the respiratory tract deposition of diesel combustion particles in patients with chronic obstructive pulmonary disease.** *Age (yrs)* 2012, **30:**67-67.

131. Pandya RJ, Solomon G, Kinner A, Balmes JR: **Diesel exhaust and asthma: hypotheses and molecular mechanisms of action.** *Environ Health Perspect* 2002, **110 Suppl 1:**103-112.

132. Riedl M, Diaz-Sanchez D: **Biology of diesel exhaust effects on respiratory function.** *J Allergy Clin Immunol* 2005, **115:**221-228.

133. Salvi S, Blomberg A, Rudell B, Kelly F, Sandstrom T, Holgate ST, Frew A: **Acute inflammatory responses in the airways and peripheral blood after short-term exposure to diesel exhaust in healthy human volunteers.** *Am J Respir Crit Care Med* 1999, **159:**702-709.

134. Steiner S, Czerwinski J, Comte P, Müller LL, Heeb NV, Mayer A, Petri-Fink A, Rothen-Rutishauser B: **Reduction in (pro-)inflammatory responses of lung cells exposed in vitro to diesel exhaust treated with a non-catalyzed diesel particle filter.** *Atmos Environ* 2013, **81:**117-124.

135. Dockery DW, Pope CA, 3rd, Xu X, Spengler JD, Ware JH, Fay ME, Ferris BG, Jr., Speizer FE: **An association between air pollution and mortality in six U.S. cities.** *N Engl J Med* 1993, **329:**1753-1759.

136. Samet JM, Zeger SL, Dominici F, Curriero F, Coursac I, Dockery DW, Schwartz J, Zanobetti A: **The National Morbidity, Mortality, and Air Pollution Study. Part II: Morbidity and mortality from air pollution in the United States.** *Res Rep Health Eff Inst* 2000, **94:**5-70; discussion 71-79.

137. Glantz SA: **Air pollution as a cause of heart disease: Time for action.** *J Am Coll Cardiol* 2002, **39:**943-945.

138. Sun Q, Wang A, Jin X, Natanzon A, Duquaine D, Brook RD, Aguinaldo JG, Fayad ZA, Fuster V, Lippmann M, et al: **Long-term air pollution exposure and acceleration of atherosclerosis and vascular inflammation in an animal model.** *JAMA* 2005, **294:**3003-3010.

139. Nel AE, Diaz-Sanchez D, Ng D, Hiura T, Saxon A: **Enhancement of allergic inflammation by the interaction between diesel exhaust particles and the immune system.** *J Allergy Clin Immunol* 1998, **102:**539-554.

140. Han W, Dan W, Shuo Y, Fang Z, Wenjun D: **Oxidative stress induced by urban fine particles in cultured EA.hy926 cells.** *Hum Exp Toxicol* 2011, **30:**579-590.

141. Hussain S, Boland S, Baeza-Squiban A, Hamel R, Thomassen LC, Martens JA, Billon-Galland MA, Fleury-Feith J, Moisan F, Pairon JC, Marano F: **Oxidative stress and proinflammatory effects of carbon black and titanium dioxide nanoparticles: role of particle surface area and internalized amount.** *Toxicology* 2009, **260:**142-149.

142. Mazzoli-Rocha F, Fernandes S, Einicker-Lamas M, Zin W: **Roles of oxidative stress in signaling and inflammation induced by particulate matter.** *Cell Biol Toxicol* 2010, **26:**481-498.

143. Li N, Hao M, Phalen RF, Hinds WC, Nel AE: **Particulate air pollutants and asthma.** *Clin Immunol* 2003, **109:**250-265.

144. Cherng TW, Paffett ML, Jackson-Weaver O, Campen MJ, Walker BR, Kanagy NL: **Mechanisms of diesel-induced endothelial nitric oxide synthase dysfunction in coronary arterioles.** *Environ Health Perspect* 2011, **119:**98-103.

145. Gong KW, Zhao W, Li N, Barajas B, Kleinman M, Sioutas C, Horvath S, Lusis AJ, Nel A, Araujo JA: **Air-pollutant chemicals and oxidized lipids exhibit genome-wide synergistic effects on endothelial cells.** *Genome Biol* 2007, **8**.

146. Xia T, Korge P, Weiss JN, Li N, Venkatesen MI, Sioutas C, Nel A: **Quinones and aromatic chemical compounds in particulate matter induce mitochondrial dysfunction: implications for ultrafine particle toxicity.** *Environ Health Perspect* 2004, **112:**1347-1358.

147. Salonen RO, Halinen AI, Pennanen AS, Hirvonen MR, Sillanpaa M, Hillamo R, Shi T, Borm P, Sandell E, Koskentalo T, Aarnio P: **Chemical and in vitro toxicologic characterization of wintertime and springtime urban-air particles with an aerodynamic diameter below 10 microm in Helsinki.** *Scand J Work Environ Health* 2004, **30 Suppl 2:**80-90.

148. Lim HB, Ichinose T, Miyabara Y, Takano H, Kumagai Y, Shimojyo N, Devalia JL, Sagai M: **Involvement of superoxide and nitric oxide on airway inflammation and hyperresponsiveness induced by diesel exhaust particles in mice.** *Free Radic Biol Med* 1998, **25:**635-644.

149. Li N, Sioutas C, Cho A, Schmitz D, Misra C, Sempf J, Wang M, Oberley T, Froines J, Nel A: **Ultrafine particulate pollutants induce oxidative stress and mitochondrial damage.** *Environ Health Perspect* 2003, **111:**455-460.

150. Sagai M, Saito H, Ichinose T, Kodama M, Mori Y: **Biological effects of diesel exhaust particles. I. In vitro production of superoxide and in vivo toxicity in mouse.** *Free Radic Biol Med* 1993, **14:**37-47.

151. Brook RD, Rajagopalan S, Pope CA, 3rd, Brook JR, Bhatnagar A, Diez-Roux AV, Holguin F, Hong Y, Luepker RV, Mittleman MA, et al: **Particulate matter air pollution and cardiovascular disease: An update to the scientific statement from the American Heart Association.** *Circulation* 2010, **121:**2331-2378.

152. Bowler RP, Crapo JD: **Oxidative stress in allergic respiratory diseases.** *J Allergy Clin Immunol* 2002, **110:**349-356.

153. Xiao GG, Wang M, Li N, Loo JA, Nel AE: **Use of proteomics to demonstrate a hierarchical oxidative stress response to diesel exhaust particle chemicals in a macrophage cell line.** *J Biol Chem* 2003, **278:**50781-50790.

154. Li N, Venkatesan MI, Miguel A, Kaplan R, Gujuluva C, Alam J, Nel A: **Induction of heme oxygenase-1 expression in macrophages by diesel exhaust particle chemicals and quinones via the antioxidant-responsive element.** *The Journal of Immunology* 2000, **165:**3393-3401.

155. Maines MD: **Heme oxygenase: function, multiplicity, regulatory mechanisms, and clinical applications.** *FASEB J* 1988, **2:**2557-2568.

156. Maines MD: **The heme oxygenase system: a regulator of second messenger gases.** *Annu Rev Pharmacol Toxicol* 1997, **37:**517-554.

157. Choi AM, Alam J: **Heme oxygenase-1: function, regulation, and implication of a novel stress-inducible protein in oxidant-induced lung injury.** *Am J Respir Cell Mol Biol* 1996, **15:**9-19.

158. Romanoski CE, Che N, Yin F, Mai N, Pouldar D, Civelek M, Pan C, Lee S, Vakili L, Yang WP, et al: **Network for activation of human endothelial cells by oxidized phospholipids: a critical role of heme oxygenase 1.** *Circ Res* 2011, **109:**e27-41.

159. Araujo JA, Zhang M, Yin F: **Heme Oxygenase-1, Oxidation, Inflammation, and Atherosclerosis.** *Frontiers in Pharmacology* 2012, **3**.

160. Araujo JA, Nel AE: **Particulate matter and atherosclerosis: role of particle size, composition and oxidative stress.** *Particle and Fibre Toxicology* 2009, **6**.

161. Oberdörster G, Utell MJ: **Ultrafine particles in the urban air: to the respiratory tract--and beyond?** *Environ Health Perspect* 2002, **110:**A440-441.

162. Li N, Wang M, Oberley TD, Sempf JM, Nel AE: **Comparison of the pro-oxidative and proinflammatory effects of organic diesel exhaust particle chemicals in bronchial epithelial cells and macrophages.** *J Immunol* 2002, **169:**4531-4541.

163. Li N, Xia T, Nel AE: **The role of oxidative stress in ambient particulate matter-induced lung diseases and its implications in the toxicity of engineered nanoparticles.** *Free Radic Biol Med* 2008, **44:**1689-1699.

164. Vanhoutte PM, Shimokawa H, Tang EH, Feletou M: **Endothelial dysfunction and vascular disease.** *Acta Physiol (Oxf)* 2009, **196:**193-222.

165. Rocha M, Apostolova N, Hernandez-Mijares A, Herance R, Victor VM: **Oxidative stress and endothelial dysfunction in cardiovascular disease: mitochondria-targeted therapeutics.** *Curr Med Chem* 2010, **17:**3827-3841.

166. Burri PH: **Development and growth of the human lung.** In *Handbook of Physiology, Section 3, The Respiratory System.* Edited by ishman AP. Bethesda: Am. Physiol. Soc.; 1985

167. Gerde P, Muggenburg BA, Lundborg M, Tesfaigzi Y, Dahl AR: **Respiratory epithelial penetration and clearance of particle-borne benzo[a]pyrene.** *Res Rep Health Eff Inst* 2001**:**5-25; discussion 27-32.

168. Wallenborn JG, McGee JK, Schladweiler MC, Ledbetter AD, Kodavanti UP: **Systemic translocation of particulate matter-associated metals following a single intratracheal instillation in rats.** *Toxicol Sci* 2007, **98:**231-239.

169. Chao MW, Kozlosky J, Po IP, Strickland PO, Svoboda KK, Cooper K, Laumbach RJ, Gordon MK: **Diesel exhaust particle exposure causes redistribution of endothelial tube VE-cadherin.** *Toxicology* 2011, **279:**73-84.

170. Suwa T, Hogg JC, Quinlan KB, Ohgami A, Vincent R, van Eeden SF: **Particulate air pollution induces progression of atherosclerosis.** *J Am Coll Cardiol* 2002, **39:**935-942.

171. Lusis AJ: **Atherosclerosis.** *Nature* 2000, **407:**233-241.

172. Gargalovic PS, Gharavi NM, Clark MJ, Pagnon J, Yang WP, He A, Truong A, Baruch-Oren T, Berliner JA, Kirchgessner TG, Lusis AJ: **The unfolded protein response is an important regulator of inflammatory genes in endothelial cells.** *Arterioscler Thromb Vasc Biol* 2006, **26:**2490-2496.

173. Bai Y, Suzuki AK, Sagai M: **The cytotoxic effects of diesel exhaust particles on human pulmonary artery endothelial cells in vitro: role of active oxygen species.** *Free Radic Biol Med* 2001, **30:**555-562.

174. Li R, Ning Z, Cui J, Khalsa B, Ai L, Takabe W, Beebe T, Majumdar R, Sioutas C, Hsiai T: **Ultrafine particles from diesel engines induce vascular oxidative stress via JNK activation.** *Free Radic Biol Med* 2009, **46:**775-782.

175. Li R, Ning Z, Majumdar R, Cui J, Takabe W, Jen N, Sioutas C, Hsiai T: **Ultrafine particles from diesel vehicle emissions at different driving cycles induce differential vascular**

pro-inflammatory responses: implication of chemical components and NF-kappaB signaling. *Part Fibre Toxicol* 2010, **7:**6.

176. Montiel-Dávalos A, Ibarra-Sanchez MdJ, Ventura-Gallegos JL, Alfaro-Moreno E, López-Marure R: **Oxidative stress and apoptosis are induced in human endothelial cells exposed to urban particulate matter.** *Toxicol In Vitro* 2010, **24:**135-141.

177. Knuckles TL, Lund AK, Lucas SN, Campen MJ: **Diesel exhaust exposure enhances venoconstriction via uncoupling of eNOS.** *Toxicol Appl Pharmacol* 2008, **230:**346-351.

178. Nurkiewicz TR, Porter DW, Barger M, Millecchia L, Rao KM, Marvar PJ, Hubbs AF, Castranova V, Boegehold MA: **Systemic microvascular dysfunction and inflammation after pulmonary particulate matter exposure.** *Environ Health Perspect* 2006, **114:**412-419.

179. Kizu R, Okamura K, Toriba A, Mizokami A, Burnstein KL, Klinge CM, Hayakawa K: **Antiandrogenic activities of diesel exhaust particle extracts in PC3/AR human prostate carcinoma cells.** *Toxicol Sci* 2003, **76:**299-309.

180. Kizu R, Otsuki N, Kishida Y, Toriba A, Mizokami A, Burnstein KL, Klinge CM, Hayakawai K: **A new luciferase reporter gene assay for the detection of androgenic and antiandrogenic effects based on a human prostate specific antigen promoter and PC3/AR human prostate cancer cells.** *Anal Sci* 2004, **20:**55-59.

181. Okamura K, Kizu R, Toriba A, Klinge CM, Hayakawa K: **Antiestrogenic Activity of Extracts of Diesel Exhaust Particulate Matter in MCF-7 Human Breast Carcinoma Cells.** *Polycyclic Aromat Compd* 2002, **22:**747-759.

182. Okamura K, Kizu R, Toriba A, Murahashi T, Mizokami A, Burnstein KL, Klinge CM, Hayakawa K: **Antiandrogenic activity of extracts of diesel exhaust particles emitted from diesel-engine truck under different engine loads and speeds.** *Toxicology* 2004, **195:**243-254.

183. Mattingly KA, Klinge CM: **Diesel exhaust particulate extracts inhibit transcription of nuclear respiratory factor-1 and cell viability in human umbilical vein endothelial cells.** *Arch Toxicol* 2011, **86:**633-642.

184. Siow RCM, Li FYL, Rowlands DJ, de Winter P, Mann GE: **Cardiovascular targets for estrogens and phytoestrogens: Transcriptional regulation of nitric oxide synthase and antioxidant defense genes.** *Free Radic Biol Med* 2007, **42:**909-925.

185. Weldy CS, Wilkerson H-W, Larson TV, Stewart JA, Kavanagh TJ: **DIESEL particulate exposed macrophages alter endothelial cell expression of eNOS, iNOS, MCP1, and glutathione synthesis genes.** *Toxicol In Vitro* 2011, **25:**2064-2073.

186. Zhang K, Kaufman RJ: **Signaling the unfolded protein response from the endoplasmic reticulum.** *J Biol Chem* 2004, **279:**25935-25938.

187. Jung EJ, Avliyakulov NK, Boontheung P, Loo JA, Nel AE: **Pro-oxidative DEP chemicals induce heat shock proteins and an unfolding protein response in a bronchial epithelial cell line as determined by DIGE analysis.** *Proteomics* 2007, **7:**3906-3918.

188. Tabas I: **The role of endoplasmic reticulum stress in the progression of atherosclerosis.** *Circ Res* 2010, **107:**839-850.

189. Muranaka M, Suzuki S, Koizumi K, Takafuji S, Miyamoto T, Ikemori R, Tokiwa H: **Adjuvant activity of diesel-exhaust particulates for the production of IgE antibody in mice.** *J Allergy Clin Immunol* 1986, **77:**616-623.

190. Sadakane K, Ichinose T, Takano H, Yanagisawa R, Sagai M, Yoshikawa T, Shibamoto T: **Murine strain differences in airway inflammation induced by diesel exhaust particles and house dust mite allergen.** *Int Arch Allergy Immunol* 2002, **128:**220-228.

191. Ichinose T, Takano H, Miyabara Y, Sadakaneo K, Sagai M, Shibamoto T: **Enhancement of antigen-induced eosinophilic inflammation in the airways of mast-cell deficient mice by diesel exhaust particles.** *Toxicology* 2002, **180:**293-301.

192. Takano H, Ichinose T, Miyabara Y, Yoshikawa T, Sagai M: **Diesel exhaust particles enhance airway responsiveness following allergen exposure in mice.** *Immunopharmacol Immunotoxicol* 1998, **20:**329-336.

193. Diaz-Sanchez D, Tsien A, Fleming J, Saxon A: **Combined diesel exhaust particulate and ragweed allergen challenge markedly enhances human in vivo nasal ragweed-specific IgE and skews cytokine production to a T helper cell 2-type pattern.** *J Immunol* 1997, **158:**2406-2413.

194. Fujieda S, Diaz-Sanchez D, Saxon A: **Combined nasal challenge with diesel exhaust particles and allergen induces In vivo IgE isotype switching.** *Am J Respir Cell Mol Biol* 1998, **19:**507-512.

195. Peterson B, Saxon A: **Global increases in allergic respiratory disease: the possible role of diesel exhaust particles.** *Ann Allergy Asthma Immunol* 1996, **77:**263-268; quiz 269-270.

196. Takano H, Yoshikawa T, Ichinose T, Miyabara Y, Imaoka K, Sagai M: **Diesel exhaust particles enhance antigen-induced airway inflammation and local cytokine expression in mice.** *Am J Respir Crit Care Med* 1997, **156:**36-42.

197. van Zijverden M, van der Pijl A, Bol M, van Pinxteren FA, de Haar C, Penninks AH, van Loveren H, Pieters R: **Diesel exhaust, carbon black, and silica particles display distinct Th1/Th2 modulating activity.** *Toxicol Appl Pharmacol* 2000, **168:**131-139.

198. Diaz-Sanchez D, Garcia MP, Wang M, Jyrala M, Saxon A: **Nasal challenge with diesel exhaust particles can induce sensitization to a neoallergen in the human mucosa.** *J Allergy Clin Immunol* 1999, **104:**1183-1188.

199. Bjorksten B: **The environmental influence on childhood asthma.** *Allergy* 1999, **54 Suppl 49:**17-23.

200. Sanders SP, Zweier JL, Harrison SJ, Trush MA, Rembish SJ, Liu MC: **Spontaneous oxygen radical production at sites of antigen challenge in allergic subjects.** *Am J Respir Crit Care Med* 1995, **151:**1725-1733.

201. Stevens WH, Inman MD, Wattie J, O'Byrne PM: **Allergen-induced oxygen radical release from bronchoalveolar lavage cells and airway hyperresponsiveness in dogs.** *Am J Respir Crit Care Med* 1995, **151:**1526-1531.

202. Lansing MW, Ahmed A, Cortes A, Sielczak MW, Wanner A, Abraham WM: **Oxygen radicals contribute to antigen-induced airway hyperresponsiveness in conscious sheep.** *Am Rev Respir Dis* 1993, **147:**321-326.

203. Hulsmann AR, Raatgeep HR, den Hollander JC, Stijnen T, Saxena PR, Kerrebijn KF, de Jongste JC: **Oxidative epithelial damage produces hyperresponsiveness of human peripheral airways.** *Am J Respir Crit Care Med* 1994, **149:**519-525.

204. Sagai M, Furuyama A, Ichinose T: **Biological effects of diesel exhaust particles (DEP). III. Pathogenesis of asthma like symptoms in mice.** *Free Radic Biol Med* 1996, **21:**199-209.

205. Comhair SA, Bhathena PR, Farver C, Thunnissen FB, Erzurum SC: **Extracellular glutathione peroxidase induction in asthmatic lungs: evidence for redox regulation of expression in human airway epithelial cells.** *FASEB J* 2001, **15:**70-78.

206. Powell CV, Nash AA, Powers HJ, Primhak RA: **Antioxidant status in asthma.** *Pediatr Pulmonol* 1994, **18:**34-38.

207. Kinnula VL, Crapo JD: **Superoxide dismutases in the lung and human lung diseases.** *Am J Respir Crit Care Med* 2003, **167:**1600-1619.

208. Seed MJ, Cullinan P, Agius RM: **Methods for the prediction of low-molecular-weight occupational respiratory sensitizers.** *Curr Opin Allergy Clin Immunol* 2008, **8:**103-109.

209. Isola D, Kimber I, Sarlo K, Lalko J, Sipes IG: **Chemical respiratory allergy and occupational asthma: what are the key areas of uncertainty?** *J Appl Toxicol* 2008, **28:**249-253.

210. Scherer G: **Biomonitoring of inhaled complex mixtures--ambient air, diesel exhaust and cigarette smoke.** *Exp Toxicol Pathol* 2005, **57 Suppl 1:**75-110.

211. Birch ME, Cary RA: **Elemental carbon-based method for occupational monitoring of particulate diesel exhaust: methodology and exposure issues.** *Analyst* 1996, **121:**1183-1190.

212. Paul J, Gessner F, Wechsler JG, Kuhn K, Orth K, Ditschuneit H: **Increased incidence of gallstones and prior cholecystectomy in patients with large bowel cancer.** *Am J Gastroenterol* 1992, **87:**1120-1124.

213. Schwarze PE, Totlandsdal AI, Lag M, Refsnes M, Holme JA, Ovrevik J: **Inflammation-related effects of diesel engine exhaust particles: studies on lung cells in vitro.** *Biomed Res Int* 2013, **2013:**685142.

214. Ichinose T, Furuyama A, Sagai M: **Biological effects of diesel exhaust particles (DEP). II. Acute toxicity of DEP introduced into lung by intratracheal instillation.** *Toxicology* 1995, **99:**153-167.

215. Nagashima M, Kasai H, Yokota J, Nagamachi Y, Ichinose T, Sagai M: **Formation of an oxidative DNA damage, 8-hydroxydeoxyguanosine, in mouse lung DNA after intratracheal instillation of diesel exhaust particles and effects of high dietary fat and beta-carotene on this process.** *Carcinogenesis* 1995, **16:**1441-1445.

216. Nemmar A, Hoet PH, Dinsdale D, Vermylen J, Hoylaerts MF, Nemery B: **Diesel exhaust particles in lung acutely enhance experimental peripheral thrombosis.** *Circulation* 2003, **107:**1202-1208.

217. Fujimaki H, Nohara O, Ichinose T, Watanabe N, Saito S: **IL-4 production in mediastinal lymph node cells in mice intratracheally instilled with diesel exhaust particulates and antigen.** *Toxicology* 1994, **92:**261-268.

218. Holder AL, Lucas D, Goth-Goldstein R, Koshland CP: **Cellular Response to Diesel Exhaust Particles Strongly Depends on the Exposure Method.** *Toxicol Sci* 2007, **103:**108-115.

219. Oberdörster G: **Lung particle overload: implications for occupational exposures to particles.** *Regul Toxicol Pharmacol* 1995, **21:**123-135.

220. Lynch I, Cedervall T, Lundqvist M, Cabaleiro-Lago C, Linse S, Dawson KA: **The nanoparticle-protein complex as a biological entity; a complex fluids and surface science challenge for the 21st century.** *Adv Colloid Interface Sci* 2007, **134-135:**167-174.

221. Kroll A, Dierker C, Rommel C, Hahn D, Wohlleben W, Schulze-Isfort C, Gobbert C, Voetz M, Hardinghaus F, Schnekenburger J: **Cytotoxicity screening of 23 engineered nanomaterials using a test matrix of ten cell lines and three different assays.** *Part Fibre Toxicol* 2011, **8:**9.

222. Bihari P, Vippola M, Schultes S, Praetner M, Khandoga AG, Reichel CA, Coester C, Tuomi T, Rehberg M, Krombach F: **Optimized dispersion of nanoparticles for biological in vitro and in vivo studies.** *Part Fibre Toxicol* 2008, **5:**14.

223. Teeguarden JG, Hinderliter PM, Orr G, Thrall BD, Pounds JG: **Particokinetics in vitro: dosimetry considerations for in vitro nanoparticle toxicity assessments.** *Toxicol Sci* 2007, **95:**300-312.

224. Mühlfeld C, Rothen-Rutishauser B, Blank F, Vanhecke D, Ochs M, Gehr P: **Interactions of nanoparticles with pulmonary structures and cellular responses.** *Am J Physiol Lung Cell Mol Physiol* 2008, **294:**L817-L829.

225. Voisin C, Aerts C, Jakubczak E, Houdret JL, Tonnel TB: **Effects of nitrogen dioxide on alveolar macrophages surviving in the gas phase. A new experimental model for the study of in vitro cytotoxicity of toxic gases.** *Bull Eur Physiopathol Respir* 1977, **13:**137-144.

226. Aufderheide M, Knebel JW, Ritter D: **Novel approaches for studying pulmonary toxicity in vitro.** *Toxicol Lett* 2003, **140-141:**205-211.

227. Paur R, Mülhopt S, Weiss C, Diabaté S: ***In vitro* exposure systems and bioassays for the assessment of toxicity of nanoparticles to the human lung.** *J Verbr Lebensm* 2008, **3:**319-329.

228. Ross AJ, Dailey LA, Brighton LE, Devlin RB: **Transcriptional profiling of mucociliary differentiation in human airway epithelial cells.** *Am J RespirCell Mol Biol* 2007, **37:**169-185.

229. Rothen-Rutishauser B, Blank F, Mühlfeld C, Gehr P: ***In vitro* models of the human epithelial airway barrier to study the toxic potential of particulate matter.** *Expert Opin Drug Metab Toxicol* 2008, **4:**1075-1089.

230. Schürch S, Gehr P, Im HV, Geiser M, Green F: **Surfactant displaces particles toward the epithelium in airways and alveoli.** *RespirPhysiol* 1990, **80:**17-32.

231. Gehr P, Green FH, Geiser M, Im HV, Lee MM, Schurch S: **Airway surfactant, a primary defense barrier: mechanical and immunological aspects.** *J Aerosol Med* 1996, **9:**163-181.

232. Kaartinen L, Nettesheim P, Adler KB, Randell SH: **Rat tracheal epithelial cell differentiation *in vitro*.** *In Vitro Cell Dev Biol Anim* 1993, **29A:**481-492.

233. Aufderheide M: **An efficient direct exposure method for studying the effects of native atmospheres.** *Toxicol Lett* 2009, **189:**S63.

234. Aufderheide M: **Experimental *In Vitro* Exposure Methods for Studying the Effects of Inhalable Compounds.** In *Cigarette Smoke and Oxidative Stress.* Edited by Halliwell BB, Poulsen HE: Springer Berlin Heidelberg; 2006: 261-277

235. Aufderheide M, Mohr U: **CULTEX - An alternative technique for cultivation and exposure of cells of the respiratory tract to airborne pollutants at the air/liquid interface.** *Exp Toxicol Pathol* 2000, **52:**265-270.

236. Klein SG, Hennen J, Serchi T, Blömeke B, Gutleb AC: **Potential of coculture *in vitro* models to study inflammatory and sensitizing effects of particles on the lung.** *Toxicol In Vitro* 2011, **25:**1516-1534.

237. Müller L, Riediker M, Wick P, Mohr M, Gehr P, Rothen-Rutishauser B: **Oxidative stress and inflammation response after nanoparticle exposure: differences between human lung cell monocultures and an advanced three-dimensional model of the human epithelial airways.** *J R Soc Interface* 2010, **7 Suppl 1:**S27-40.

238. BéruBé K, Aufderheide M, Breheny D, Clothier R, Combes R, Duffin R, Forbes B, Gaca M, Gray A, Hall I, et al: ***In vitro* models of inhalation toxicity and disease. The report of a FRAME workshop.** *AlternLab Anim* 2009, **37:**89-141.

239. Kimber I, Agius R, Basketter DA, Corsini E, Cullinan P, Dearman RJ, Gimenez-Arnau E, Greenwell L, Hartung T, Kuper F, et al: **Chemical respiratory allergy: opportunities for hazard identification and characterisation. The report and recommendations of ECVAM workshop 60.** *Altern Lab Anim* 2007, **35:**243-265.

240. Hartung T, Balls M, Bardouille C, Blanck O, Coecke S, Gstraunthaler G, Lewis D: **Good Cell Culture Practice. ECVAM Good Cell Culture Practice Task Force Report 1.** *AlternLab Anim* 2002, **30:**407-414.

241. Bonifas J, Hennen J, Dierolf D, Kalmes M, Blömeke B: **Evaluation of cytochrome P450 1 (CYP1) and N-acetyltransferase 1 (NAT1) activities in HaCaT cells: implications for the development of *in vitro* techniques for predictive testing of contact sensitizers.** *Toxicol In Vitro* 2010, **24:**973-980.

242. Nelson S, Summer WR: **Innate immunity, cytokines, and pulmonary host defense.** *Infect Dis Clin North Am* 1998, **12:**555-567.

243. Reynolds HY: **Pulmonary Host Defenses.** *Chest* 1989, **95:**223-230.

244. Ozaki T, Maeda M, Hayashi H, Nakamura Y, Moriguchi H, Kamei T, Yasuoka S, Ogura T: **Role of alveolar macrophages in the neutrophil-dependent defense system against Pseudomonas aeruginosa infection in the lower respiratory tract. Amplifying effect of muramyl dipeptide analog.** *Am Rev Respir Dis* 1989, **140:**1595-1601.

245. Toews GB: **Determinants of bacterial clearance from the lower respiratory tract.** *Semin Respir Infect* 1986, **1:**68-78.

246. Ishii H, Hayashi S, Hogg JC, Fujii T, Goto Y, Sakamoto N, Mukae H, Vincent R, van Eeden SF: **Alveolar macrophage-epithelial cell interaction following exposure to atmospheric particles induces the release of mediators involved in monocyte mobilization and recruitment.** *Respir Res* 2005, **6**.

247. Becker S, Mundandhara S, Devlin RB, Madden M: **Regulation of cytokine production in human alveolar macrophages and airway epithelial cells in response to ambient air pollution particles: further mechanistic studies.** *Toxicol Appl Pharmacol* 2005, **207:**269-275.

248. Holt PG, Oliver J, Bilyk N, McMenamin C, McMenamin PG, Kraal G, Thepen T: **Downregulation of the antigen presenting cell function(s) of pulmonary dendritic cells *in vivo* by resident alveolar macrophages.** *J Exp Med* 1993, **177:**397-407.

249. Holt PG, Schon-Hegrad MA, Oliver J: **MHC class II antigen-bearing dendritic cells in pulmonary tissues of the rat. Regulation of antigen presentation activity by endogenous macrophage populations.** *J Exp Med* 1988, **167:**262-274.

250. Reynolds HY: **Advances in understanding pulmonary host defense mechanisms: dendritic cell function and immunomodulation.** *Curr Opin Pulm Med* 2000, **6:**209-216.

251. Mantovani A, Muzio M, Garlanda C, Sozzani S, Allavena P: **Macrophage control of inflammation: negative pathways of regulation of inflammatory cytokines.** *Novartis Found Symp* 2001, **234:**120-131; discussion 131-125.

252. Kuipers H, Lambrecht BN: **The interplay of dendritic cells, Th2 cells and regulatory T cells in asthma.** *Curr Opin Immunol* 2004, **16:**702-708.

253. Finkelstein JN, Barrett EG: **Alterations in Gene Expression in Pulmonary Cells Following Particle Interactions.** In *Particle-Lung Interactions. Volume* 143. Edited by Gehr P, Heyder J. New York: Marcel Dekker, Inc.; 2000

254. Liu Y, Gao W, Zhang D: **Effects of cigarette smoke extract on A549 cells and human lung fibroblasts treated with transforming growth factor-β1 in a coculture system.** *Clin Exp Med* 2010, **10:**159-167.

255. Crabbé A, Sarker SF, Van Houdt R, Ott CM, Leys N, Cornelis P, Nickerson CA: **Alveolar epithelium protects macrophages from quorum sensing-induced cytotoxicity in a three-dimensional co-culture model.** *Cell Microbiol* 2010, **13:**469-481.

256. Wottrich R, Diabaté S, Krug HF: **Biological effects of ultrafine model particles in human macrophages and epithelial cells in mono- and co-culture.** *Int J Hyg Environ Health* 2004, **207:**353-361.

257. Rothen-Rutishauser BM, Kiama SG, Gehr P: **A three-dimensional cellular model of the human respiratory tract to study the interaction with particles.** *Am J RespirCell Mol Biol* 2005, **32:**281-289.

258. Rubovitch V, Gershnabel S, Kalina M: **Lung epithelial cells modulate the inflammatory response of alveolar macrophages.** *Inflammation* 2007, **30:**236-243.

259. Lieber M, Smith B, Szakal A, Nelson-Rees W, Todaro G: **A continuous tumor-cell line from a human lung carcinoma with properties of type II alveolar epithelial cells.** *Int J Cancer* 1976, **17:**62-70.

260. Balis JU, Bumgarner SD, Paciga JE, Paterson JF, Shelley SA: **Synthesis of lung surfactant-associated glycoproteins by A549 cells: description of an *in vitro* model for human type II cell dysfunction.** *Exp Lung Res* 1984, **6:**197-213.

261. Foster KA, Oster CG, Mayer MM, Avery ML, Audus KL: **Characterization of the A549 Cell Line as a Type II Pulmonary Epithelial Cell Model for Drug Metabolism.** *Exp Cell Res* 1998, **243:**359-366.

262. Castell JV, Teresa Donato M, Gómez-Lechón MJ: **Metabolism and bioactivation of toxicants in the lung. The *in vitro* cellular approach.** *Exp Toxicol Pathol* 2005, **57:**189-204.

263. Tsuchiya S, Yamabe M, Yamaguchi Y, Kobayashi Y, Konno T, Tada K: **Establishment and characterization of a human acute monocytic leukemia cell line (THP-1).** *Int J Cancer* 1980, **26:**171-176.

264. Schwende H, Fitzke E, Ambs P, Dieter P: **Differences in the state of differentiation of THP-1 cells induced by phorbol ester and 1,25-dihydroxyvitamin D3.** *J Leukoc Biol* 1996, **59:**555-561.

265. Butterfield JH, Weiler D, Dewald G, Gleich GJ: **Establishment of an immature mast cell line from a patient with mast cell leukemia.** *LeukRes* 1988, **12:**345-355.

266. Suggs JE, Madden MC, Friedman M, Edgell CJ: **Prostacyclin expression by a continuous human cell line derived from vascular endothelium.** *Blood* 1986, **68:**825-829.

267. Henderson AJ: **Bronchoalveolar lavage.** *Arch Dis Child* 1994, **70:**167-169.

268. Blaschke E, Eklund A, Skog S, Danielsson B: **Isolation of human alveolar macrophages and lymphocytes from bronchoalveolar lavage fluid by centrifugal elutriation.** *Scand J Clin Lab Investig* 1985, **45:**691-696.

269. Fox B, Bull TB, Guz A: **Mast cells in the human alveolar wall: an electronmicroscopic study.** *J Clin Pathol* 1981, **34:**1333-1342.

270. Nemmar A, Nemery B, Hoet PH, Vermylen J, Hoylaerts MF: **Pulmonary inflammation and thrombogenicity caused by diesel particles in hamsters: role of histamine.** *Am J Respir Crit Care Med* 2003, **168:**1366-1372.

271. Alfaro-Moreno E, López-Marure R, Montiel-Dávalos A, Symonds P, Osornio-Vargas AR, Rosas I, Clifford Murray J: **E-Selectin expression in human endothelial cells exposed to PM10: The role of endotoxin and insoluble fraction.** *Environ Res* 2007, **103:**221-228.

272. Montiel-Dávalos A, Alfaro-Moreno E, López-Marure R: **PM2.5 and PM10 induce the expression of adhesion molecules and the adhesion of monocytic cells to human umbilical vein endothelial cells.** *Inhalation Toxicol* 2007, **19 Suppl 1:**91-98.

273. Mutlu GM, Green D, Bellmeyer A, Baker CM, Burgess Z, Rajamannan N, Christman JW, Foiles N, Kamp DW, Ghio AJ, et al: **Ambient particulate matter accelerates coagulation via an IL-6-dependent pathway.** *J Clin Investig* 2007, **117:**2952-2961.

274. Hermanns MI, Unger RE, Kehe K, Peters K, Kirkpatrick CJ: **Lung epithelial cell lines in coculture with human pulmonary microvascular endothelial cells: development of an alveolo-capillary barrier in vitro.** *Lab Invest* 2004, **84:**736-752.

275. Bitterle E, Karg E, Schroeppel A, Kreyling WG, Tippe A, Ferron GA, Schmid O, Heyder J, Maier KL, Hofer T: **Dose-controlled exposure of A549 epithelial cells at the air-liquid interface to airborne ultrafine carbonaceous particles.** *Chemosphere* 2006, **65:**1784-1790.

276. Geys J, Coenegrachts L, Vercammen J, Engelborghs Y, Nemmar A, Nemery B, Hoet PHM: ***In vitro* study of the pulmonary translocation of nanoparticles: A preliminary study.** *Toxicol Lett* 2006, **160:**218-226.

277. De Benedetto A, Rafaels NM, McGirt LY, Ivanov AI, Georas SN, Cheadle C, Berger AE, Zhang K, Vidyasagar S, Yoshida T, et al: **Tight junction defects in patients with atopic dermatitis.** *J Allergy Clin Immunol* 2010, **127:**773-786.

278. Brandner JM, Haftek M, Niessen CM: **Adherens Junctions, Desmosomes and Tight Junctions in Epidermal Barrier Function.** *Open Dermatol J* 2010, **4:**14-20.

279. Aufderheide M: **Direct exposure methods for testing native atmospheres.** *Exp Toxicol Pathol* 2005, **57:**213-226.

280. Tsuchiya S, Kobayashi Y, Goto Y, Okumura H, Nakae S, Konno T, Tada K: **Induction of maturation in cultured human monocytic leukemia cells by a phorbol diester.** *Cancer Res* 1982, **42:**1530-1536.

281. Carter WO, Narayanan PK, Robinson JP: **Intracellular hydrogen peroxide and superoxide anion detection in endothelial cells.** *J Leukoc Biol* 1994, **55:**253-258.

282. Vandesompele J, De Preter K, Pattyn F, Poppe B, Van Roy N, De Paepe A, Speleman F: **Accurate normalization of real-time quantitative RT-PCR data by geometric averaging of multiple internal control genes.** *Genome Biol* 2002, **3:**RESEARCH0034.

283. Pfaffl MW: **A new mathematical model for relative quantification in real-time RT-PCR.** *Nucleic Acids Res* 2001, **29:**e45.

284. Pfaffl MW, Horgan GW, Dempfle L: **Relative expression software tool (REST) for group-wise comparison and statistical analysis of relative expression results in real-time PCR.** *Nucleic Acids Res* 2002, **30:**e36.

285. Andersson Hn, Piras E, Demma J, Hellman Br, Brittebo E: **Low levels of the air pollutant 1-nitropyrene induce DNA damage, increased levels of reactive oxygen species and endoplasmic reticulum stress in human endothelial cells.** *Toxicology* 2009, **262:**57-64.

286. Mace K, Bowman ED, Vautravers P, Shields PG, Harris CC, Pfeifer AM: **Characterisation of xenobiotic-metabolising enzyme expression in human bronchial mucosa and peripheral lung tissues.** *Eur J Cancer* 1998, **34:**914-920.

287. Matsunawa M, Amano Y, Endo K, Uno S, Sakaki T, Yamada S, Makishima M: **The aryl hydrocarbon receptor activator benzo[a]pyrene enhances vitamin D3 catabolism in macrophages.** *Toxicol Sci* 2009, **109:**50-58.

288. Babina M, Krautheim M, Grützkau A, Henz BM: **Human Leukemic (HMC-1) Mast Cells Are Responsive to 1[alpha],25-Dihydroxyvitamin D3: Selective Promotion of ICAM-3 Expression and Constitutive Presence of Vitamin D3 Receptor.** *Biochem Biophys Res Commun* 2000, **273:**1104-1110.

289. Grabbe J, Welker P, Moller A, Dippel E, Ashman LK, Czarnetzki BM: **Comparative cytokine release from human monocytes, monocyte-derived immature mast cells, and a human mast cell line (HMC-1).** *J Invest Dermatol* 1994, **103:**504-508.

290. Selvan RS, Butterfield JH, Krangel MS: **Expression of multiple chemokine genes by a human mast cell leukemia.** *J Biol Chem* 1994, **269:**13893-13898.

291. Rudd CJ, Strom KA: **A spectrophotometric method for the quantitation of diesel exhaust particles in guinea pig lung.** *J Appl Toxicol* 1981, **1:**83-87.

292. Alfaro-Moreno E, Gonz√°lez-G√≥mez BE, Ramos-Godinez P, Montiel-D√°valos AI, Reyes-Maldonado E, L√≥pez-Marure R: **Urban PMs induce the adhesion of cancer cells to endothelial cells.** *Toxicol Lett* 2012, **211, Supplement:**S108-S109.

293. Szmitko PE: **New Markers of Inflammation and Endothelial Cell Activation: Part I.** *Circulation* 2003, **108:**1917-1923.

294. Kido T, Bai N, Yatera K, Suzuki H, Meredith A, Mukae H, Rosenfeld ME, van Eeden SF: **Diesel exhaust inhalation induces heat shock protein 70 expression in vivo.** *Inhal Toxicol* 2011, **23:**593-601.

295. Villeneuve NF, Lau A, Zhang DD: **Regulation of the Nrf2-Keap1 antioxidant response by the ubiquitin proteasome system: an insight into cullin-ring ubiquitin ligases.** *Antioxid Redox Signal* 2010, **13:**1699-1712.

296. Vargas MR, Johnson JA: **The Nrf2-ARE cytoprotective pathway in astrocytes.** *Expert Rev Mol Med* 2009, **11:**e17.

297. Cho H-Y, Kleeberger SR: **Nrf2 protects against airway disorders.** *Toxicol Appl Pharmacol* 2010, **244:**43-56.

298. Nelson DR, Koymans L, Kamataki T, Stegeman JJ, Feyereisen R, Waxman DJ, Waterman MR, Gotoh O, Coon MJ, Estabrook RW, et al: **P450 superfamily: update on new sequences, gene mapping, accession numbers and nomenclature.** *Pharmacogenetics* 1996, **6:**1-42.

299. Okey AB, Riddick DS, Harper PA: **The Ah receptor: mediator of the toxicity of 2,3,7,8-tetrachlorodibenzo-p-dioxin (TCDD) and related compounds.** *Toxicol Lett* 1994, **70:**1-22.

300. Ramos-Godínez MdP, González-Gómez BE, Montiel-Dávalos A, López-Marure R, Alfaro-Moreno E: **TiO2 nanoparticles induce endothelial cell activation in a pneumocyte-endothelial co-culture model.** *Toxicol In Vitro* 2013, **27:**774-781.

301. Hamoir J, Nemmar A, Halloy D, Wirth D, Vincke G, Vanderplasschen A, Nemery B, Gustin P: **Effect of polystyrene particles on lung microvascular permeability in isolated perfused rabbit lungs: role of size and surface properties.** *Toxicol Appl Pharmacol* 2003, **190:**278-285.

302. Agu RU, Jorissen M, Willems T, Augustijns P, Kinget R, Verbeke N: ***In vitro* nasal drug delivery studies: comparison of derivatised, fibrillar and polymerised collagen matrix-based human nasal primary culture systems for nasal drug delivery studies.** *J Pharm Pharmacol* 2001, **53:**1447-1456.

303. Elbert KJ, Schafer UF, Schafers HJ, Kim KJ, Lee VH, Lehr CM: **Monolayers of human alveolar epithelial cells in primary culture for pulmonary absorption and transport studies.** *Pharm Res* 1999, **16:**601-608.

304. Godfrey RWA: **Human airway epithelial tight junctions.** *Microsc Res Tech* 1997, **38:**488–499.

305. Rothen-Rutishauser B, Mühlfeld C, Blank F, Musso C, Gehr P: **Translocation of particles and inflammatory responses after exposure to fine particles and nanoparticles in an epithelial airway model.** *Part Fibre Toxicol* 2007, **4**.

306. Unfried K, Albrecht C, Klotz L-O, Von Mikecz A, Grether-Beck S, Schins RPF: **Cellular responses to nanoparticles: Target structures and mechanisms.** *Nanotoxicology* 2007, **1:**52-71.

307. Rothen-Rutishauser PDDB: **Laser scanning microscopy combined with image restoration to analyse a 3D model of the human epithelial airway barrier.** *Swiss Med Wkly* 2010, **140**.

308. Mühlfeld C, Gehr P, Rothen-Rutishauser B: **Translocation and cellular entering mechanisms of nanoparticles in the respiratory tract.** *SwissMed Wkly* 2008, **138:**387-391.

309. Fröhlich E, Bonstingl G, Höfler A, Meindl C, Leitinger G, Pieber TR, Roblegg E: **Comparison of two *in vitro* systems to assess cellular effects of nanoparticles-containing aerosols.** *Toxicol In Vitro* 2013, **27:**409-417.

310. Hemminki K, Pershagen G: **Cancer risk of air pollution: epidemiological evidence.** *Environ Health Perspect* 1994, **102 Suppl 4:**187-192.

311. Kunzli N, Jerrett M, Mack WJ, Beckerman B, LaBree L, Gilliland F, Thomas D, Peters J, Hodis HN: **Ambient air pollution and atherosclerosis in Los Angeles.** *Environ Health Perspect* 2005, **113:**201-206.

312. Peters A, Dockery DW, Muller JE, Mittleman MA: **Increased particulate air pollution and the triggering of myocardial infarction.** *Circulation* 2001, **103:**2810-2815.

313. Kim JH, Sherman ME, Curriero FC, Guengerich FP, Strickland PT, Sutter TR: **Expression of cytochromes P450 1A1 and 1B1 in human lung from smokers, non-smokers, and ex-smokers.** *Toxicol Appl Pharmacol* 2004, **199:**210-219.

314. Newland N, Baxter A, Hewitt K, Minet E: **CYP1A1/1B1 and CYP2A6/2A13 activity is conserved in cultures of differentiated primary human tracheobronchial epithelial cells.** *Toxicol In Vitro* 2011, **25:**922-929.

315. Hukkanen J, Lassila A, Paivarinta K, Valanne S, Sarpo S, Hakkola J, Pelkonen O, Raunio H: **Induction and regulation of xenobiotic-metabolizing cytochrome P450s in the human A549 lung adenocarcinoma cell line.** *Am J Respir Cell Mol Biol* 2000, **22:**360-366.

316. Hukkanen J, Pelkonen O, Hakkola J, Raunio H: **Expression and regulation of xenobiotic-metabolizing cytochrome P450 (CYP) enzymes in human lung.** *Crit Rev Toxicol* 2002, **32:**391-411.

317. Shimada T, Gillam EM, Sutter TR, Strickland PT, Guengerich FP, Yamazaki H: **Oxidation of xenobiotics by recombinant human cytochrome P450 1B1.** *Drug Metab Dispos* 1997, **25:**617-622.

318. Lekas P, Tin KL, Lee C, Prokipcak RD: **The human cytochrome P450 1A1 mRNA is rapidly degraded in HepG2 cells.** *Arch Biochem Biophys* 2000, **384:**311-318.

319. Shehin SE, Stephenson RO, Greenlee WF: **Transcriptional regulation of the human CYP1B1 gene. Evidence for involvement of an aryl hydrocarbon receptor response element in constitutive expression.** *J Biol Chem* 2000, **275:**6770-6776.

320. Schwarz D, Kisselev P, Cascorbi I, Schunck WH, Roots I: **Differential metabolism of benzo[a]pyrene and benzo[a]pyrene-7,8-dihydrodiol by human CYP1A1 variants.** *Carcinogenesis* 2001, **22:**453-459.

321. Gerde P, Muggenburg BA, Lundborg M, Dahl AR: **The rapid alveolar absorption of diesel soot-adsorbed benzo[a]pyrene: bioavailability, metabolism and dosimetry of an inhaled particle-borne carcinogen.** *Carcinogenesis* 2001, **22:**741-749.

322. World Health Organization: **Tumours of the Lung, Pleura, Thymus and Heart.** In *Pathology & Genetics* (Travis WD, Brambilla EH, Müller-Hermelink K, Harris CC eds.). Albany, USA: WHO Publications Center; 2004.

323. Matsunawa M, Akagi D, Uno S, Endo-Umeda K, Yamada S, Ikeda K, Makishima M: **Vitamin D Receptor Activation Enhances Benzo[a]pyrene Metabolism via CYP1A1 Expression in Macrophages.** *Drug Metab Dispos* 2012, **40:**2059-2066.

324. Conway DE, Sakurai Y, Weiss D, Vega JD, Taylor WR, Jo H, Eskin SG, Marcus CB, McIntire LV: **Expression of CYP1A1 and CYP1B1 in human endothelial cells: regulation by fluid shear stress.** *Cardiovasc Res* 2009, **81:**669-677.

325. McCormick SM, Eskin SG, McIntire LV, Teng CL, Lu CM, Russell CG, Chittur KK: **DNA microarray reveals changes in gene expression of shear stressed human umbilical vein endothelial cells.** *Proc Natl Acad Sci U S A* 2001, **98:**8955-8960.

326. Hashimoto SHU, Gon Y, Takeshita I, Matsumoto KEN, Jibiki I, Takizawa H, Kudoh S, Horie T: **Diesel exhaust particles activate p38 MAP kinase to produce interleukin 8 and RANTES by human bronchial epithelial cells and N-acetylcysteine attenuates p38 MAP kinase activation.** *Am J Respir Crit Care Med* 2000, **161:**280-285.

327. Takizawa H, Abe S, Ohtoshi T, Kawasaki S, Takami K, Desaki M, Sugawara I, Hashimoto S, Azuma A, Nakahara K: **Diesel exhaust particles up-regulate expression of intercellular adhesion molecule-1 (ICAM-1) in human bronchial epithelial cells.** *Clin Exp Immunol* 2000, **120:**356-362.

328. Landsiedel R, Sauer UG, Ma-Hock L, Schnekenburger J, Wiemann M: **Pulmonary toxicity of nanomaterials: a critical comparison of published in vitro assays and in vivo inhalation or instillation studies.** *Nanomedicine (Lond)* 2014, **9:**2557-2585.

329. Aufderheide M: **An efficient approach to study the toxicological effects of complex mixtures.** *Exp Toxicol Pathol* 2008, **60:**163-180.

330. Paur H-R, Cassee FR, Teeguarden J, Fissan H, Diabate S, Aufderheide M, Kreyling WG, Hänninen O, Kasper G, Riediker M: **In-vitro cell exposure studies for the assessment of nanoparticle toxicity in the lung - A dialog between aerosol science and biology.** *J Aerosol Sci* 2011, **42:**668-692.

331. Motohashi H, O'Connor T, Katsuoka F, Engel JD, Yamamoto M: **Integration and diversity of the regulatory network composed of Maf and CNC families of transcription factors.** *Gene* 2002, **294:**1-12.

332. Itoh K, Chiba T, Takahashi S, Ishii T, Igarashi K, Katoh Y, Oyake T, Hayashi N, Satoh K, Hatayama I, et al: **An Nrf2/small Maf heterodimer mediates the induction of phase II detoxifying enzyme genes through antioxidant response elements.** *Biochem Biophys Res Commun* 1997, **236:**313-322.

333. Carter EP: **Continual emerging roles of HO-1: protection against airway inflammation.** *AJP: Lung Cellular and Molecular Physiology* 2004, **287:**L24-L25.

334. Baird L, Dinkova-Kostova AT: **The cytoprotective role of the Keap1-Nrf2 pathway.** *Arch Toxicol* 2011, **85:**241-272.

335. Fredenburgh LE, Perrella MA, Mitsialis SA: **The Role of Heme Oxygenase-1 in Pulmonary Disease.** *Am J Respir Cell Mol Biol* 2007, **36:**158-165.

336. Amakawa K, Terashima T, Matsuzaki T, Matsumaru A, Sagai M, Yamaguchi K: **Supressive effects of diesel exhaust particles on cytokine release from human and murine alveolar macrophages.** *Exp Lung Res* 2003, **29:**149-164.

337. D'Acquisto F, May MJ, Ghosh S: **Inhibition of nuclear factor kappa B (NF-B): an emerging theme in anti-inflammatory therapies.** *Mol Interv* 2002, **2:**22-35.

338. Baldwin AS, Jr.: **The NF-kappa B and I kappa B proteins: new discoveries and insights.** *Annu Rev Immunol* 1996, **14:**649-683.

339. Gu H, Tang C, Peng K, Sun H, Yang Y: **Effects of chronic mild stress on the development of atherosclerosis and expression of toll-like receptor 4 signaling pathway in adolescent apolipoprotein E knockout mice.** *J Biomed Biotechnol* 2009, **2009:**613879.

340. Bukau B, Horwich AL: **The Hsp70 and Hsp60 chaperone machines.** *Cell* 1998, **92:**351-366.

341. Mambula SS, Stevenson MA, Ogawa K, Calderwood SK: **Mechanisms for Hsp70 secretion: crossing membranes without a leader.** *Methods* 2007, **43:**168-175.

342. Gualtieri M, Mantecca P, Cetta F, Camatini M: **Organic compounds in tire particle induce reactive oxygen species and heat-shock proteins in the human alveolar cell line A549.** *Environ Int* 2008, **34:**437-442.

343. Jin Y, Miao W, Lin X, Pan X, Ye Y, Xu M, Fu Z: **Acute exposure to 3-methylcholanthrene induces hepatic oxidative stress via activation of the Nrf2/ARE signaling pathway in mice: 3-Methylcholanthrene Increases Oxidative Stress in Mice Liver.** *Environ Toxicol* 2013**:**n/a-n/a.

344. Baulig A, Garlatti M, Bonvallot V, Marchand A, Barouki R, Marano F, Baeza-Squiban A: **Involvement of reactive oxygen species in the metabolic pathways triggered by diesel exhaust particles in human airway epithelial cells.** *Am J Physiol Lung Cell Mol Physiol* 2003, **285:**L671-679.

345. McMahon M, Itoh K, Yamamoto M, Hayes JD: **Keap1-dependent proteasomal degradation of transcription factor Nrf2 contributes to the negative regulation of antioxidant response element-driven gene expression.** *J Biol Chem* 2003, **278:**21592-21600.

346. Furukawa M, Xiong Y: **BTB protein Keap1 targets antioxidant transcription factor Nrf2 for ubiquitination by the Cullin 3-Roc1 ligase.** *Mol Cell Biol* 2005, **25:**162-171.

347. Jeyapaul J, Jaiswal AK: **Nrf2 and c-Jun regulation of antioxidant response element (ARE)-mediated expression and induction of gamma-glutamylcysteine synthetase heavy subunit gene.** *Biochem Pharmacol* 2000, **59:**1433-1439.

348. He CH, Gong P, Hu B, Stewart D, Choi ME, Choi AM, Alam J: **Identification of activating transcription factor 4 (ATF4) as an Nrf2-interacting protein. Implication for heme oxygenase-1 gene regulation.** *J Biol Chem* 2001, **276:**20858-20865.

349. Venugopal R, Jaiswal AK: **Nrf1 and Nrf2 positively and c-Fos and Fra1 negatively regulate the human antioxidant response element-mediated expression of NAD(P)H:quinone oxidoreductase1 gene.** *Proc Natl Acad Sci U S A* 1996, **93:**14960-14965.

350. Frohlich E, Meindl C, Wagner K, Leitinger G, Roblegg E: **Use of whole genome expression analysis in the toxicity screening of nanoparticles.** *Toxicol Appl Pharmacol* 2014, **280:**272-284.

351. Pecorelli A, Bocci V, Acquaviva A, Belmonte G, Gardi C, Virgili F, Ciccoli L, Valacchi G: **NRF2 activation is involved in ozonated human serum upregulation of HO-1 in endothelial cells.** *Toxicol Appl Pharmacol* 2013, **267:**30-40.

352. Moller W, Brown DM, Kreyling WG, Stone V: **Ultrafine particles cause cytoskeletal dysfunctions in macrophages: role of intracellular calcium.** *Part Fibre Toxicol* 2005, **2:**7.

353. Moller W, Hofer T, Ziesenis A, Karg E, Heyder J: **Ultrafine particles cause cytoskeletal dysfunctions in macrophages.** *Toxicol Appl Pharmacol* 2002, **182:**197-207.

354. Mazzarella G, Ferraraccio F, Prati MV, Annunziata S, Bianco A, Mezzogiorno A, Liguori G, Angelillo IF, Cazzola M: **Effects of diesel exhaust particles on human lung epithelial cells: an in vitro study.** *Respir Med* 2007, **101:**1155-1162.

355. Gomez-Mendikute A, Etxeberria A, Olabarrieta I, Cajaraville MP: **Oxygen radicals production and actin filament disruption in bivalve haemocytes treated with benzo(a)pyrene.** *Mar Environ Res* 2002, **54:**431-436.

356. Kang MI, Kobayashi A, Wakabayashi N, Kim SG, Yamamoto M: **Scaffolding of Keap1 to the actin cytoskeleton controls the function of Nrf2 as key regulator of cytoprotective phase 2 genes.** *Proc Natl Acad Sci U S A* 2004, **101:**2046-2051.

357. Nguyen T, Sherratt PJ, Nioi P, Yang CS, Pickett CB: **Nrf2 controls constitutive and inducible expression of ARE-driven genes through a dynamic pathway involving nucleocytoplasmic shuttling by Keap1.** *J Biol Chem* 2005, **280:**32485-32492.

358. Velichkova M, Hasson T: **Keap1 regulates the oxidation-sensitive shuttling of Nrf2 into and out of the nucleus via a Crm1-dependent nuclear export mechanism.** *Mol Cell Biol* 2005, **25:**4501-4513.

359. Schwartz AG, Prysak GM, Bock CH, Cote ML: **The molecular epidemiology of lung cancer.** *Carcinogenesis* 2007, **28:**507-518.

360. Tompkins LM, Wallace AD: **Mechanisms of cytochrome P450 induction.** *J Biochem Mol Toxicol* 2007, **21:**176-181.

361. L'Azou B, Fernandez P, Bareille R, Beneteau M, Bourget C, Cambar J, Bordenave L: **In vitro endothelial cell susceptibility to xenobiotics: comparison of three cell types.** *Cell Biol Toxicol* 2005, **21:**127-137.

362. Zeldin DC, Foley J, Ma J, Boyle JE, Pascual JM, Moomaw CR, Tomer KB, Steenbergen C, Wu S: **CYP2J subfamily P450s in the lung: expression, localization, and potential functional significance.** *Mol Pharmacol* 1996, **50:**1111-1117.

363. Scarborough PE, Ma J, Qu W, Zeldin DC: **P450 subfamily CYP2J and their role in the bioactivation of arachidonic acid in extrahepatic tissues.** *Drug Metab Rev* 1999, **31:**205-234.

364. Anttila S, Hietanen E, Vainio H, Camus AM, Gelboin HV, Park SS, Heikkila L, Karjalainen A, Bartsch H: **Smoking and peripheral type of cancer are related to high levels of pulmonary cytochrome P450IA in lung cancer patients.** *Int J Cancer* 1991, **47:**681-685.

365. Ahn EK, Yoon HK, Jee BK, Ko HJ, Lee KH, Kim HJ, Lim Y: **COX-2 expression and inflammatory effects by diesel exhaust particles in vitro and in vivo.** *Toxicol Lett* 2008, **176:**178-187.

366. Dorger M, Krombach F: **Response of alveolar macrophages to inhaled particulates.** *Eur Surg Res* 2002, **34:**47-52.

367. Fritsch-Decker S, Both T, Mülhopt S, Paur HR, Weiss C, Diabate S: **Regulation of the arachidonic acid mobilization in macrophages by combustion-derived particles.** *Part Fibre Toxicol* 2011, **8:**23.

368. Schneider JC, Card GL, Pfau JC, Holian A: **Air pollution particulate SRM 1648 causes oxidative stress in RAW 264.7 macrophages leading to production of prostaglandin E2, a potential Th2 mediator.** *Inhal Toxicol* 2005, **17:**871-877.

369. Seidel SD, Winters GM, Rogers WJ, Ziccardi MH, Li V, Keser B, Denison MS: **Activation of the Ah receptor signaling pathway by prostaglandins.** *J Biochem Mol Toxicol* 2001, **15:**187-196.

ACKNOWLEDGEMENTS/DANKSAGUNG

First of all I would like to express my gratitude to my supervisors Prof. Dr. Brunhilde Blömeke and Dr. Arno Gutleb: Thank you for the very interesting and challenging subject. Moreover I would like to thank both for all the helpful discussions and the inspiring meetings. I always felt guided in a professional and warm-hearted way. Your competent advices contributed a lot to the success of this work!

Frau Prof. Dr. Brunhilde Blömeke und Dr. Arno Gutleb möchte ich für die freundliche Überlassung des hochinteressanten Themas und die Bereitstellung des Arbeitsplatzes herzlich danken. Ich verdanke Ihnen darüber hinaus jede erdenkliche, hilfreiche Unterstützung und viele anregende Diskussionen. Jede Phase dieser Arbeit wurde von Ihnen intensiv, professionell und warmherzig begleitet. Besonders bedanken will ich mich auch für die Freiheit, die Sie mir während des gesamten Forschungsprojektes gewährten, was maßgeblich zum Gelingen dieser Arbeit beitrug. Ihr kompetenter Rat und ihre Hilfe kam mir in zahlreichen Angelegenheiten sehr zugute!

Special thanks go to Dr. Tommaso Serchi. He was always ready to listen to my problems and to discuss planning, execution and evaluation of experiments. Thanks a lot for your game-changing and creative ideas that contributed crucially to this work. I also would like to acknowledge his friendly attitude and patient willingness to share his broad toxicological and molecular biological knowledge.

Mein besonderer Dank gilt auch Dr. Tommaso Serchi. Jederzeit gewährte er mir bei der Planung, Durchführung und Auswertung der vorliegenden Arbeit außerordentlich sachkundige, erfahrene und wertvolle Unterstützung. Seine wegweisenden und kreativen Ideen haben wesentlich zum Erstellen der Arbeit beigetragen. Dankbar anerkennen will ich auch seine immer freundliche, uneingeschränkte und geduldige Bereitschaft mir sein großes toxikologisches und molekularbiologisches Wissen weiterzugeben.

Dr. Sebastién Cambier and Sylvain Legay were very patient when introducing me into the world of molecular biology. Thanks for all your great ideas that led to excellent results!

Für die unermüdliche und professionelle Einführung in sämtliche molekularbiologischen Arbeiten danke ich Dr. Sebastién Cambier und Sylvain Legay ganz herzlich. Für ihre konstruktiven Ideen, die zu hervorragenden Ergebnissen führten, gebührt ihnen ganz besonderer Dank.

A very big amount of my gratitude goes to Servane Contal. I would like to thank her for her unresting help in the cell culture lab and for all the other assistance. Without her efforts a big part of the experiments could not have been realised. Moreover I would like to thank her for her warm-hearted friendship and for her patience while teaching me the fabulous french language.

Servane Contal möchte ich für ihre unermüdliche Hilfe in der Zellkultur und bei allen anfallenden Arbeiten danken. Ohne ihren Fleiß und ihre Hilfe wäre ein Großteil der Experimente so nicht umsetzbar und realisierbar gewesen. Außerdem möchte ich mich für ihre warmherzige Art, ihre Freundschaft und ihre Geduld bei meinen „Vokabelfragen“ bedanken!

I would like to thank Dr. Gea Guerriero for countless enjoyable lunch brakes and for her useful advices in the field of qRT-PCR. It was a pleasure to have spent the lunch brakes with you!

Ich möchte mich auch besonders bei Dr. Gea Guerriero für die immer amüsanten und abwechslungsreichen Mittagspausen bedanken! Es war mir eine große Freude! Außerdem möchte ich ihr für die zahlreichen guten Ratschläge bezüglich qRT-PCR danken.

Dr. Mauricio Montaño und Anastasia Georgantzopoulou are acknowledged for countless stimulating discussions about cell culture, experimental planning, evaluation of results and statistics as well as for their friendship!

Dr. Mauricio Montaño und Dr. Anastasia Georgantzopoulou möchte ich für zahlreiche anregende Diskussionen rund um Zellkultur, experimentelle Planung, Auswertung und insbesondere Statistik. Außerdem möchte ich den zwei für ihre Freundschaft danken.

I would like to thank Dr. Jenny Hennen for several constructive discussions regarding the planning and evaluation of experiments.

Ich möchte mich recht herzlich bei Dr. Jenny Hennen für die zahlreichen konstruktiven Gespräche bei der Planung der Experimente und der Auswertung bedanken.

Special thanks go to Dr. Inge Nelissen for the multiplex analysis of the cell culture supernatants.

Ein herzliches Dankeschön an Dr. Inge Nelissen für die Durchführung der Multiplex Experimente mit den Kulturüberständen.

I would like to thank my master students Aline Chary and Audrey Jehanno. Thanks for your efforts to contribute to this PhD work. Best of luck for all your future plans!

Großer Dank gebührt meinen beiden Master Studentinnen Aline Chary und Audrey Jehanno. Danke für eure Anstrengungen und Mühen um zum Erfolg dieser Arbeit beizutragen. Ich wünsche euch viel Erfolg auf euren weiteren Wegen.

At this point I would like to acknowledge Hanna Lokys for her countless advices regarding statistics that were contributing a lot for the preparation of the manuscript.

An dieser Stelle will ich mich ganz besonders bei Hanna Lokys bedanken, die mir mit zahlreichen Tipps zur statistischen Auswertung die Arbeit am Computer und damit die Fertigstellung der Dissertation unendlich erleichterte.

Special thanks go to Brüno Printz. He was the first one I met at my first day and he became a good friend. Especially when results were not as expected, he was always willing to listen to me.

Ich bedanke mich recht herzlich bei Brüno Printz. Er war der Erste den ich an meinem ersten Tag am CRP getroffen habe und er wurde zu einem guten Freund für mich. Besonders wenn die Experimente mal nicht wie erwartet liefen hatte er immer ein offenes Ohr für mich. Danke!

Thanks to all my (former) office mates: It was a pleasure to spend 4 years with you!

Allen ehemaligen Kolleginnen und Kollegen aus meinem Büro: Herzlichen Dank für ihre Freundschaft und jeden anderen wertvollen, unterstützenden Beistand.

Special thanks go to the other PhD students and all the people that are working at the CRP-Gabriel Lippmann (now LIST) for the perfect collaboration. This work would not have been possible without your help. Thanks a lot!

Ein ganz besonderer Dank geht an meine Mitdoktoranden sowie alle Mitarbeiter und Mitarbeiterinnen des Instituts für die außerordentlich gute Zusammenarbeit. Diese Arbeit wäre ohne ihre Hilfe nicht möglich gewesen, weshalb ich mich bei allen herzlich bedanken will.

To all the members of the MTB group: Thank you for the possibility to free my mind from experiments and cell culture so that I could „cool down“ whenever it was necessary.

Den Mitgliedern der „Fahrradtruppe“ danke ich aus ganzem Herzen für allseits willkommene mentale Entspannung abseits von Labor und Experimenten.

To all people that I forgot to acknowledge: Thanks for everything!!!

An alle die ich noch vergessen habe zu erwähnen: Danke für alles!!!

This goes to my family: Thanks for your patience, for your calmness and your endurance. Thanks for always being at my side and lifting me up when I was down!

Meiner Familie danke ich für die Ausdauer, Ruhe und Geduld, womit sie mir stets zur Seite standen und mich immer wieder aufgemuntert haben!

Special thanks to the Fond National de la Recherge Luxembourg for the financial support (PHD-09-170).

Dem Fond National de la Recherche Luxembourg, danke ich für die finanzielle Unterstützung dieser Arbeit (PHD-09-170).

CURRICULUM VITAE

Saarwellingerstraße 12, 66809 Nalbach, Germany

Telephone: +49 172 2348108 E-mail: sebastian.g.klein@gmail.com

PERSONAL DETAILS

Nationality	*German*
Date and place of birth	*09.08.1984, Merzig, Germany*
Marital status	*single*

PROFESSIONAL EXPERIENCE

Scientific sales representative for SANTIS on behalf of AstraZeneca *Since May 2014*

EDUCATION

Centre de Recherche Public – Gabriel Lippmann, Belvaux, Luxembourg *March 2010 –*

University of Trier, Trier, Germany *March 2014*

Doctor of Philosophy in Toxicology

Advisors: Prof. Dr. Arno Gutleb (CRP – Gabriel Lippmann)

Prof. Dr. Brunhilde Blömeke (University Trier)

Thesis title: „Model development to evaluate the effects of environmental particleson lung and immune cells“ **(Supported by the National Research Fund, Luxembourg [PhD-09-170])**

Centre for Human and Molecular Biology, *March 2009 - Jan 2010*

University of Saarland, Saarbrücken, Germany

Diploma thesis

Department for Molecular and Cell Biology

Advisor: Prof. Dr. Manfred J. Schmitt

Thesis title: Evaluation of the toxic effects and the endocytotic uptake of the A/B-Toxin K28 in mammalian cells

Center for Human and Molecular Biology, *Oct 2004 - Jan 2009*

University of Saarland, Saarbrücken, Germany

Biology studies with focus on human and molecular biology

Main subjects:

Molecular cell biology

Developmental biology

Virology and Immunology

PEER-REVIEWED PUBLICATIONS

Luyts, K., Napierska, D., Dinsdale, D., **Klein, S. G.** and Hoet, P. H. M. (2013). The role of macrophage activation in a coculture model of the lung-blood barrier. *Toxicology and Applied Pharmacology* ***(IF=3.975)***

Georgantzopoulou, A. Skoczyńska, E., van den Berg, J. H. J., Brand, W., Legay, S., **Klein, S. G.**, Rietjens, I. M. C. M and Murk, A. J. (2013). P-gp Efflux Pump Inhibition Potential of Common Environmental Contaminants Determined *in vitro. Environmental Toxicology and Chemistry* ***(IF=2.618)***

Klein, S. G., Serchi, T., Hoffmann, L., Blömeke, B., & Gutleb, A. C. (2013). An improved 3D tetraculture system mimicking the cellular organisation at the alveolar barrier to study the potential toxic effects of particles on the lung. *Particle and fibre toxicology*, *10*(1), 31. ***(IF=9.18)***

Serchi, T., **Klein, S. G.,** Jehanno, A., Legay, S., Contal, S., Hennen, J., Gutleb, A.C., Hoffmann, L. and Blömeke, B. (2013). A 4D lung multi-culture system which mimicking alveolar cellular organization to study the toxic potential of airborne particles. *Toxicology Letters*, *221*, S183. ***(IF=3.145)***

Klein, S. G., Hennen, J., Serchi, T., Blömeke, B., & Gutleb, A. C. (2011). Potential of coculture *in vitro* models to study inflammatory and sensitizing effects of particles on the lung. *Toxicology In Vitro*, 25(8), 1516-1534. [2] ***(IF=2.65)***

MANUSCRIPTS IN PREPARATION

Klein, S. G., Cambier, S., Serchi, T., Hoffmann, L., Blömeke, B., & Gutleb, A. C. (2014). Response of the endothelial part of a 3D tetraculture *in vitro* model in a dose-controlled exposure scenario to diesel exhaust particulate matter at the air-liquid-interface*. To be submitted to Particle and fibre toxicology.*

CONTRIBUTIONS TO ABSTRACTS FOR ORAL PRESENTATIONS

Serchi, T., **Klein, S. G.,** Jehanno, A., Legay, S., Contal, S., Hennen, J., Gutleb, A.C., Hoffmann, L. and Blömeke, B. (2013). A 4D lung multi-culture system which mimicking alveolar cellular organization to study the toxic potential of airborne particles. 49th congress of the European societies of toxicology, EuroTox, Interlaken, Switzerland

Serchi, T., **Klein, S. G.,** Jehanno, A., Legay, S., Contal, S., Hennen, J., Gutleb, A.C., Hoffmann, L. and Blömeke, B. (2013): *A multi-dimensional multi-cellular coculture system which mimics alveolar cellular organization for realistic risk assessment of airborne particles.* 10th International Particle Toxicology Conference, Düsseldorf, Germany

Gutleb, A. C., **Klein, S.G.** and Blömeke, B. (2012): Multi-cellular approach for the prediction of adverse effects in lung tissue. 24th Meeting of the European Research Group on Experimental Contact Dermatitis (ERGECD), Trier, Germany.

[2] Featured in the **Sciencedirect Top 25 List of Most Downloaded Articles** ranked 11th on the Top 25 for Toxicology In Vitro – January to December 2012

Gutleb, A. C., **Klein, S. G.**, Serchi, T., Hoffmann, L. and Blömeke, B. (2012): An improved co-culture system mimicking the cellular organization at the alveolar barrier to study the toxic potency of particles. 51st Annual Meeting and ToxExpo, Society of Toxicology (SOT), San Francisco, USA.

PRESENTATIONS

Klein, S.G., Serchi, T., Hoffmann, L., Blömeke, B. and Gutleb, A. C. (2012): *An improved 3D tetraculture system mimicking the cellular organization at the alveolar barrier to study the toxic potency of particles.* PhD Day University of Trier, Trier Germany.

POSTERS

Klein, S.G., Serchi, T., Hoffmann, L., Blömeke, B. and Gutleb, A. C (2013): THP-1 and HMC-1 Cell Interaction with Epithelial Cells in a 3D Tetraculture System of the Alveolar Barrier Modulates the Response to Oxidative Stress. 52nd Annual Meeting and ToxExpo, Society of Toxicology (SOT), San Antonio, USA.

Klein, S.G., Serchi, T., Hoffmann, L., Blömeke, B. and Gutleb, A. C. (2012): An improved 3D tetraculture system mimicking the cellular organisation at the alveolar barrier to study the potential toxic effects of particles on the lung. Beltox Invitrom Symposium, Edegem, Belgium.

Klein, S.G., Serchi, T., Hoffmann, L., Blömeke, B. and Gutleb, A. C. (2011): An improved coculture system mimicking the cellular organization at the alveolar barrier to study the toxic potency of particles. BelTox - Annual Meeting 2011, Mechelen, Belgium.

Klein, S.G., Serchi, T., Hoffmann, L., Blömeke, B. and Gutleb, A. C. (2011): An improved coculture system mimicking the cellular organization at the alveolar barrier to study the potential toxic effects of particles. CellTox – Twenty years of in vitro toxicology: achievements and future challenges, Rome, Italy.

Klein, S.G., Serchi, T., Hoffmann, L., Blömeke, B. and Gutleb, A. C. (2010): Model Development to Evaluate Inflammatory and Sensitizing Effects of Engineered Nanoparticles on Lung and Immune Cells (NanSENS). BelTox - Annual Meeting, Louvain-La-Neuve, Belgium, 2010.

CONFERENCES

Member of the organizing committee of the PhD-Day 2014 and at the CRP – Gabriel Lippmann, Belvaux, Luxembourg

Member of the organizing committee of the PhD-Day 2012 and at the University of Trier, Trier, Germany

AWARDS

1st price for "the best poster of a young scientist" at the Beltox Invitrom Symposium 2012 for the poster: An improved 3D tetraculture system mimicking the cellular organization at the alveolar barrier to study the toxic potency of particles. Edegem, Belgium.

TRAINING COURSES

Hands-On Light Microscopy Workshop, Basic & Advanced Techniques. Organized by the University of Luxembourg City, Luxembourg (January 2013)

Training on improving scientific presentation skills. Organized by Birgit Michel-Dittgen, CEB Merzig, Germany (April 2011)

Image processing in Microscopy and Biomedical Imaging. Organized by Lucilinx, Luxembourg City, Luxembourg (September 2010)

TEACHING AND SUPERVISORY EXPERIENCE

Responsibility for the Microbiology lectures at the University of Trier, Trier, Germany (2013/2014)

Supervision of one master student's research project in the framework of the NanSENS PhD project, CRP – Gabriel Lippmann (2013)

Responsibility for the Microbiology lectures at the University of Trier, Trier, Germany (2012/2013)

Supervision of one master student's research project in the framework of the NanSENS PhD project, CRP – Gabriel Lippmann (2012)

Microbiology and Virology lectures as guest speaker at the University of Trier, Trier, Germany (2011/2012)

PUBLIC RELATION ACTIVITIES

Presentation of the possibilities to evaluate the potential toxic effects of airborne materials using *in vitro* systems at the CRP Open Day *(September 2013)*

Participation in the *"chercheurs à l'ecole"* activity, organised by the FNR (2012 and 2011)

Participation in *"the FNR Researchers' night"* (2011)

MEMBERSHIP SCIENTIFIC SOCIETY

Belgian Society of Toxicology (BelTox)

LANGUAGES

German:	mother tongue
English:	Fluent
French:	Fluent
Luxembourgish:	very good listening comprehension

Hiermit versichere ich an Eides Statt, dass ich die Arbeit selbstständig verfasst und keine anderen als die angegebenen Quellen und Hilfsmittel benutzt habe.
Ergebnisse oder Beiträge anderer wurden als solche explizit gekennzeichnet.

Sebastian Georg Klein